AD-A110 863 GEORGIA INST OF TECH ATLANTA ENGINEERING EXPERIMENT --ETC F/G 17/7
MARINE AIR TRAFFIC CONTROL AND LANDING SYSTEM (MATCALS INVESTIG--ETC(U)
SEP 81 E R GRAF, C L PHILLIPS, S A STARKS N00039-80-C-0032
UNCLASSIFIED GIT/EES-1-A-2550-VOL-2 NL

1 OF 2

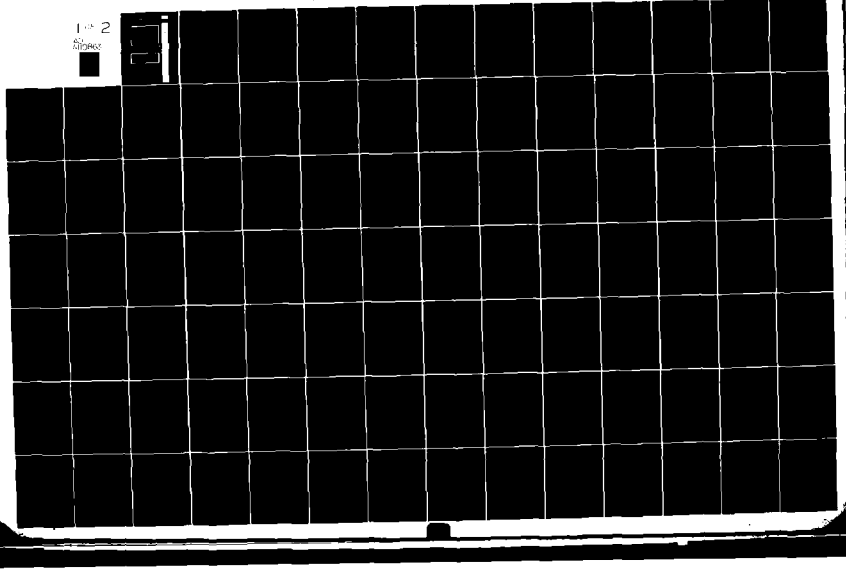

LEVEL II

ELECTRICAL

AD A110863

DTIC
ELECTE
FEB 1 1 1982
S
H

DTIC FILE COPY

ENGINEERING EXPERIMENT STATION

AUBURN UNIVERSITY

AUBURN, ALABAMA

81 11 26 070

This document has been approved for public release and sale; its distribution is unlimited

TECHNICAL REPORT
CONTRACT 1-A-2550
(SUBCONTRACTED FROM N-00039-80-C-0032)
MARINE AIR TRAFFIC CONTROL
AND LANDING SYSTEM
(MATCALS INVESTIGATION)
VOLUME II

E. R. Graf, C. L. Phillips, and S. A. Starks
CO-PROJECT LEADERS

September, 1981

DTIC
ELECTE
FEB 1 1 1982

Prepared for

The Engineering Experiment Station
Georgia Institute of Technology
Atlanta, Georgia

Prepared by

The Electrical Engineering Department
Auburn University
Auburn University, Alabama

DISTRIBUTION STATEMENT A
Approved for public release;
Distribution Unlimited

PART THREE

THE DESIGN OF OBSERVERS FOR THE MATCALS SYSTEM

Prepared for

Georgia Institute of Technology
ATLANTA, GEORGIA

Under

Contract 1-A-2550

by

Electrical Engineering Department
Auburn University
Auburn, Alabama

Prepared by: Charles L. Phillips

THE DESIGN OF OBSERVERS

FOR THE MATCALS SYSTEM

ABSTRACT

Three observers are designed for a reduced order system that represents the lateral system of the F4J aircraft in an automatic landing configuration. The observers are to be used in the aircraft's lateral control system to estimate its lateral position and lateral velocity, in place of the α-β filter that is currently used to estimate position and velocity. Results that are obtained from simulations of the F4J aircraft lateral control system indicate that an observer may be used to improve the system's response.

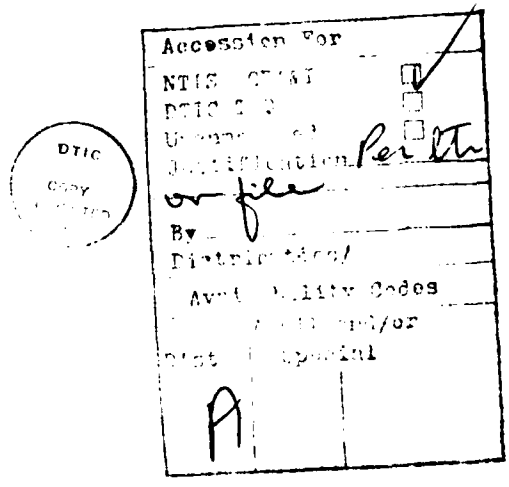

TABLE OF CONTENTS

I.	INTRODUCTION	1-1
II.	MATCALS SYSTEM	2-1
III.	OBSERVER CONTROL SYSTEM	3-1
IV.	COMPARISON OF SYSTEMS	4-1
V.	MODEL 2 SYSTEM	5-1
VI.	CONCLUSIONS	6-1
	REFERENCES	

I. INTRODUCTION

This report gives the results of the continuation of the studies described in the interim report of this contract [1]. The interim report described the design of a observer to replace the α-β filter in the flight dynamics and control module of the F4J aircraft lateral control system. This system is a part of the Marine Air Traffic Control and Landing System (MATCALS).

The observer systems are compared to four different α-β systems. The first system is the SPN-42 system [3], which is called the α-β system in this report. The second system is the SPN-42 system with the controller gains reduced by 50% to reduce the system noise response. The third system is called the ydot system, and is described in Chapter II. The fourth system is called the model 2 system, and has been used in mode 1 (automatic) landings [3]. The criteria of comparison for the systems are the radar-noise response and the wind response.

II. MATCALS SYSTEM

This chapter first contains a brief description of the lateral control system of the F4J aircraft in an automatic landing configuration (MATCALS). Next various system design criteria are developed. Finally, two variations of this control system are presented. For the first variation, the loop gain is reduced by 50 percent. In the second variation, it is assumed that the aircraft lateral velocity is available as a feedback signal.

F4J Lateral Control System

A complete description of the F4J aircraft in the MATCALS configuration is given in [2]. A brief description of this system will be given here.

A block diagram of the F4J lateral control system is given in Figure 2-1. The block labeled "aircraft system" is the aircraft with autopilots. The signal $\phi(t)$ is the command input to the bank autopilot, and $y(t)$ is the lateral distance of the aircraft from the extended centerline of the runway. The signal $w(t)$ models the wind input to the aircraft. The signal "radar noise" represents the measurement inaccuracies in the determination of the aircraft position by the radar, and $y_R(k)$ is the aircraft position as measured by the radar. The α-β filter-controller combination is basically a proportional-integral-derivative (PID)

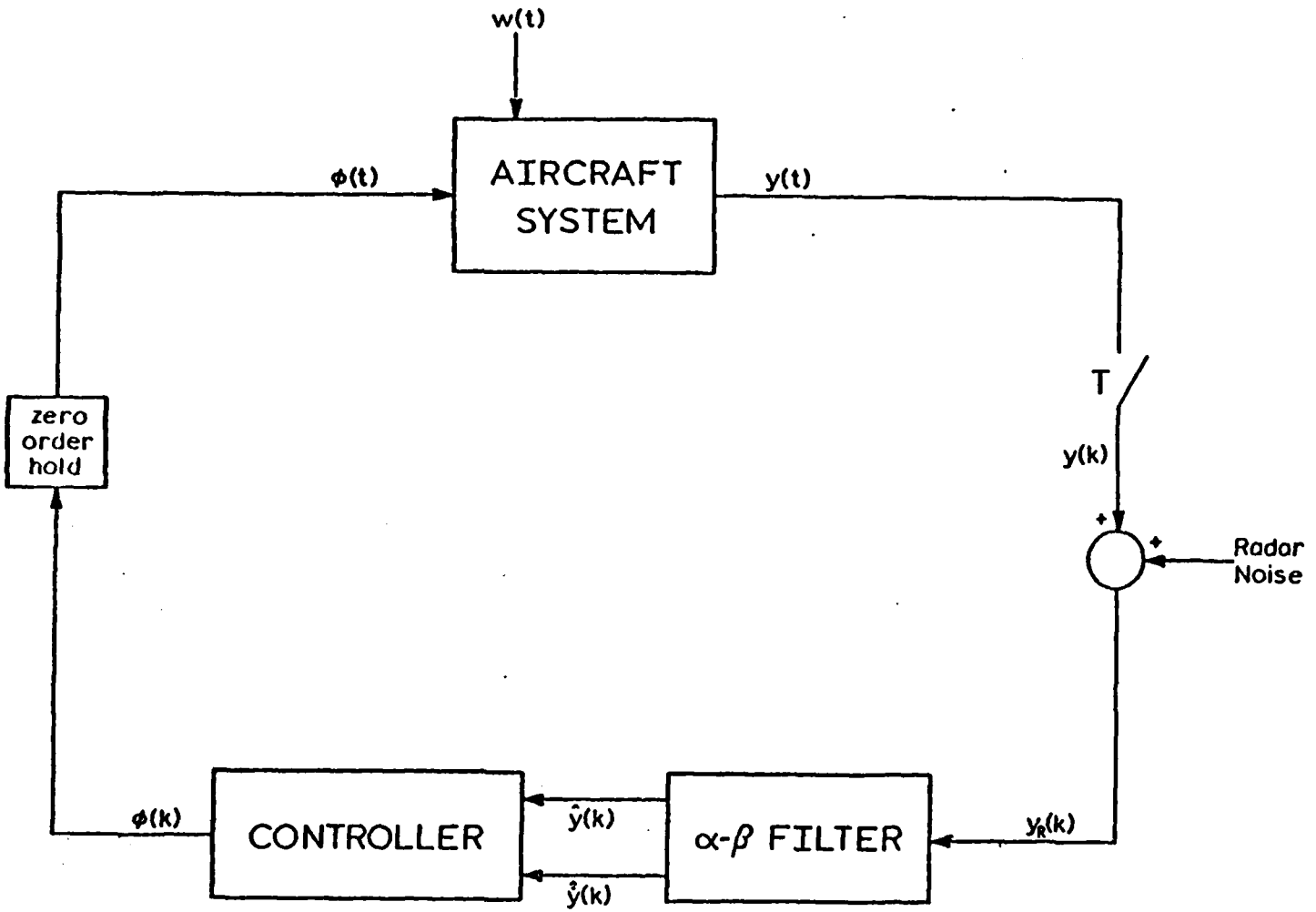

Figure 2-1. Block Diagram of the F4J Aircraft Lateral Control System with the α-β Filter.

controller used to compensate the closed-loop system. This combination also contains filtering to reduce the effects of the radar noise signal.

System Design Criteria

Even though the MATCALS control systems are discrete in nature, the important design criteria can be developed and understood by considering the equivalent analog system. The equivalent analog system is considered here because the derivations are much simpler.

The analog equivalent of the lateral control system of Figure 2-1 is given in Figure 2-2. In the controller, K_I is the gain in the integral path, K_P is the gain in the proportional path, and K_D is the gain in the derivative path. For the F4J lateral control system, $K_P = K_D = 0.75$, and $K_I = .00333$ at close range. The noise-filtering transfer function has been omitted, since it does not affect the following derivations. The transfer function from bank command input to position output for the aircraft is $G_1(s)$, and from wind input to position output is $G_2(s)$. The aircraft velocity $\dot{y}(t)$ is needed for later derivations. $Y_{rn}(s)$ is the radar noise signal, and $Y_{com}(s)$ is the system command signal.

Two transfer functions of critical importance to system operation are the transfer function from the radar noise signal to the position output and the one from the wind to the position output. From Figure 2-2, we see that

$$\frac{Y(s)}{Y_{rn}(s)} = \frac{(K_P+K_I/s+K_Ds)G_1(s)}{1 + (K_P+K_I/s+K_Ds)G_1(s)} \qquad (2\text{-}1)$$

and

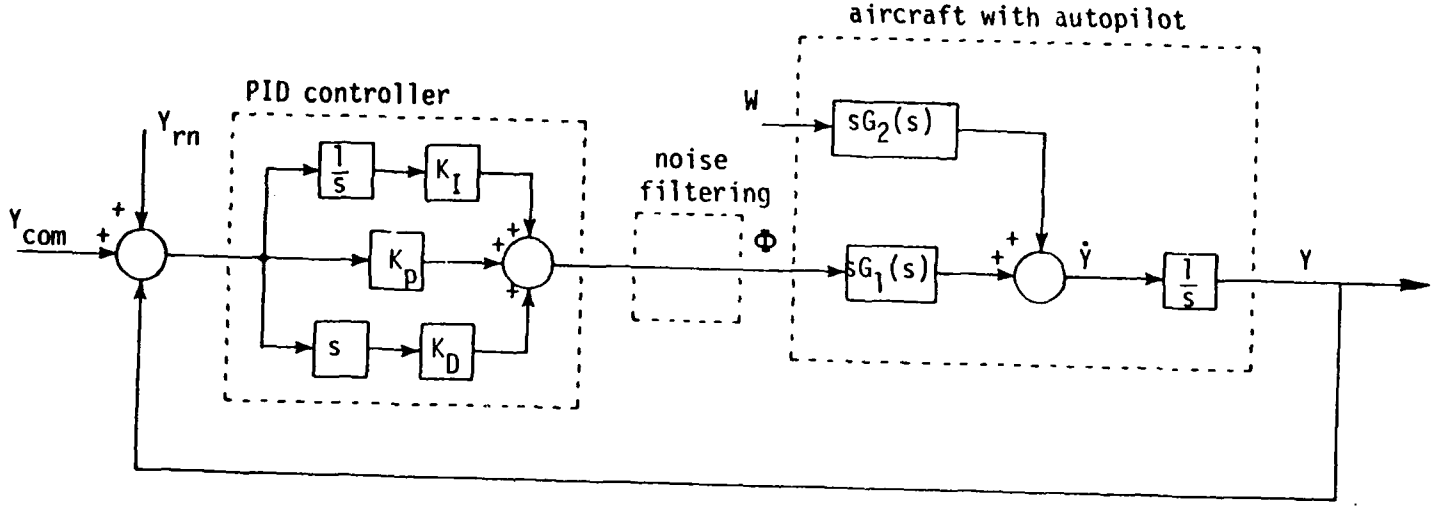

Figure 2-2. Analog Equivalent of the Lateral Control System.

$$\frac{Y(s)}{W(s)} = \frac{G_2(s)}{1 + (K_p+K_I/s+K_Ds)G_1(s)} \tag{2-2}$$

It is necessary that the plane response very little to the radar noise. However, the transfer function for the command input, Y_{com}, to position output is, from Figure 2-2,

$$\frac{Y(s)}{Y_{com}(s)} = \frac{(K_p+K_I/s+K_Ds)G_1(s)}{1 + (K_p+K_I/s+K_Ds)G_1(s)} \tag{2-3}$$

This transfer function is identical to that of $Y(s)/Y_{rn}(s)$. Thus, if system response to the radar noise is reduced, the system response to the system command is also reduced. For low frequencies;

$$(K_p+K_I/s+K_Ds)G_1(s)\Big|_{s=j\omega} >> 1 \tag{2-4}$$

Then, from (2-1) and (2-3),

$$\frac{Y(s)}{Y_{com}(s)}\Big|_{s=j\omega} = \frac{Y(s)}{Y_{rn}(s)}\Big|_{s=j\omega} \approx 1 \tag{2-5}$$

Hence, to reduce noise response, we must effectively reduce system bandwidth; i.e., we must reduce the frequency range over which (2-4) is satisfied.

However, reducing the frequency range over which (2-4) is satisfied increases the system response to wind. If (2-4) is satisfied, then for this frequency range (2-2) becomes

$$\frac{Y(s)}{W(s)}\Big|_{s=j\omega} \approx \frac{G_2(s)}{(K_p+K_I/s+K_Ds)G_1(s)}\Big|_{s=j\omega} \tag{2-6}$$

This gain is small, since the denominator is large. But, if the denominator is decreased in order to reduce the response to radar noise, the response to wind is increased.

In summary, the lateral control system must be redesigned in such a manner that the system response to radar noise is reduced, while the open-loop gain as given in (2-4) remains large such that system wind response is not degraded.

System with Reduced Gain

The first attempt to satisfy the above design specification is simply to reduce the controller gains, K_P, K_I, and K_D in Figure 2-2, by 50 percent. This is obviously not a complete solution, since the system wind response is increased. It has been suggested that this gain reduction will give an acceptable radar noise response, and for this reason this system will be used here for comparison purposes. However, the wind response for this case will probably be excessive, and thus is not acceptable. It is then assumed that this system does give an acceptable radar noise response, and an unacceptable wind response. The study of the system with full gains, i.e., the SPN-42 system, gives an unacceptable radar noise response and an acceptable wind response.

The system with full gains will be referred to as the α-β system, and the system with the gains reduced by 50 percent will be referred to as the half-gain system. Thus the redesign problem is to design a system that approaches the noise response of the half-gain system while approaching the wind response of the α-β system. Of course, adequate stability margins must also be maintained in the redesign.

YDOT System

A second variation on the α-β system that is useful to study, but cannot be implemented because of hardware constraints, is the system of Figure 2-3. This system will be referred to as the ydot system. In this system it is assumed that the aircraft velocity $\dot{y}(t)$ is measured directly on the aircraft, and is then transmitted to the ground-based controller. Thus the differentiation of a noisy signal in the PID controller is no longer required, and this leads to a reduced noise response.

For the ydot system of Figure 2-3, it is seen that the following transfer functions apply.

$$\frac{Y(s)}{Y_{com}(s)} = \frac{Y(s)}{Y_{rn}(s)} = \frac{(K_p+K_I/s)G_1(s)}{1 + (K_p+K_I/s+K_Ds)G_1(s)} \tag{2-7}$$

$$\frac{Y(s)}{W(s)} = \frac{G_2(s)}{1 + (K_p+K_I/s+K_Ds)G_1(s)} \tag{2-8}$$

A comparison of (2-7) for this system to (2-1) for the α-β system indicates that the bandwidth of the system from the radar noise input to position output has been reduced. Furthermore, comparing (2-8) to (2-2) for the α-β system shows that the wind response is the same for the two systems. Thus the ydot system appears to achieve the design objectives, and as will be shown later, does in fact achieve the design objectives.

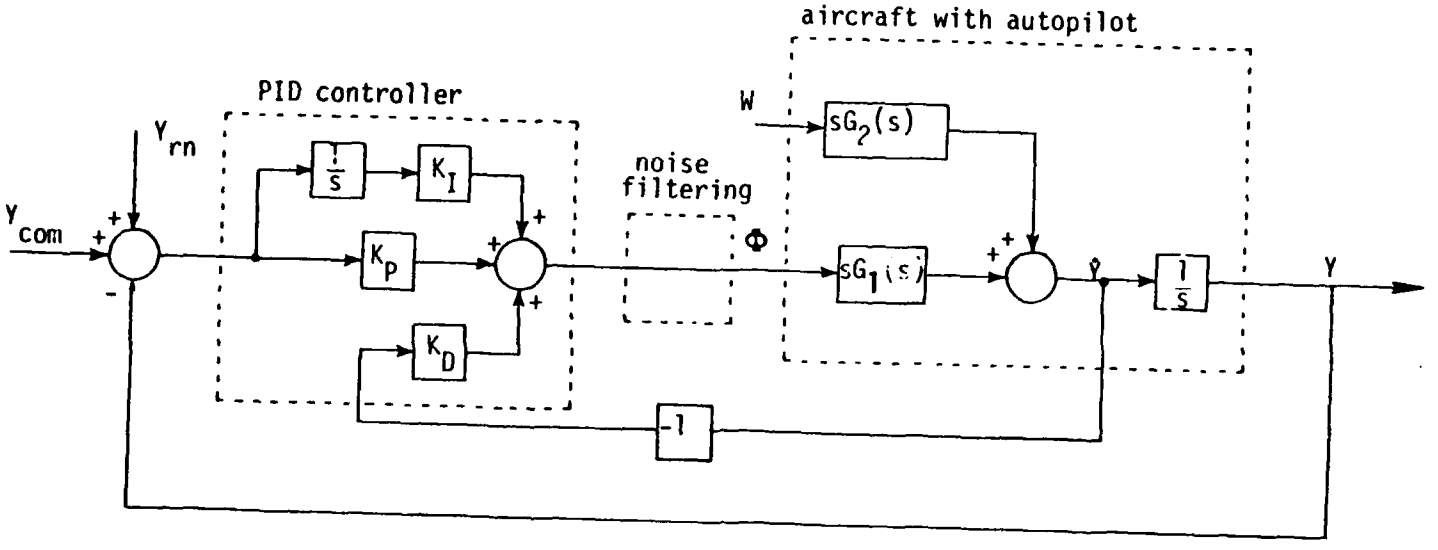

Figure 2-3. YDOT Control System.

III. OBSERVER CONTROL SYSTEM

A possible improvement in the MATCALS closed-loop system is to replace the α-β filter in Figure 2-1 with a different filter. The purpose of the α-β filter is to produce a filtered aircraft position and velocity signal, $\hat{y}(k)$ and $\dot{\hat{y}}$ respectively, based on the radar data. An observer, or state estimator, is a different type of filter that can be used to produce estimates of the states of the aircraft. Observer theory is covered in detail in [1], and will not be presented here. The observer-based MATCALS lateral control system is shown in Figure 3-1. This system will be referred to as the observer system.

Note in Figure 3-1 that the observer has as inputs the radar data $y_R(k)$ and the controller output $\phi(k)$. The observer outputs are the estimated aircraft position $\hat{y}(k)$ [$\hat{x}_1(k)$ in the observer equations below] and estimated aircraft velocity [$\hat{x}_2(k)$]. Thus there is an additional loop in the observer system that does not appear in the α-β system, which should lead to increased flexibility. The observer designed for the F4J lateral control system will now be presented.

Observer Design

The observer designed for the F4J lateral control system is based on a third-order approximation to the ninth-order model for the aircraft system in Figure 3-1 [1]. This discrete model is given by

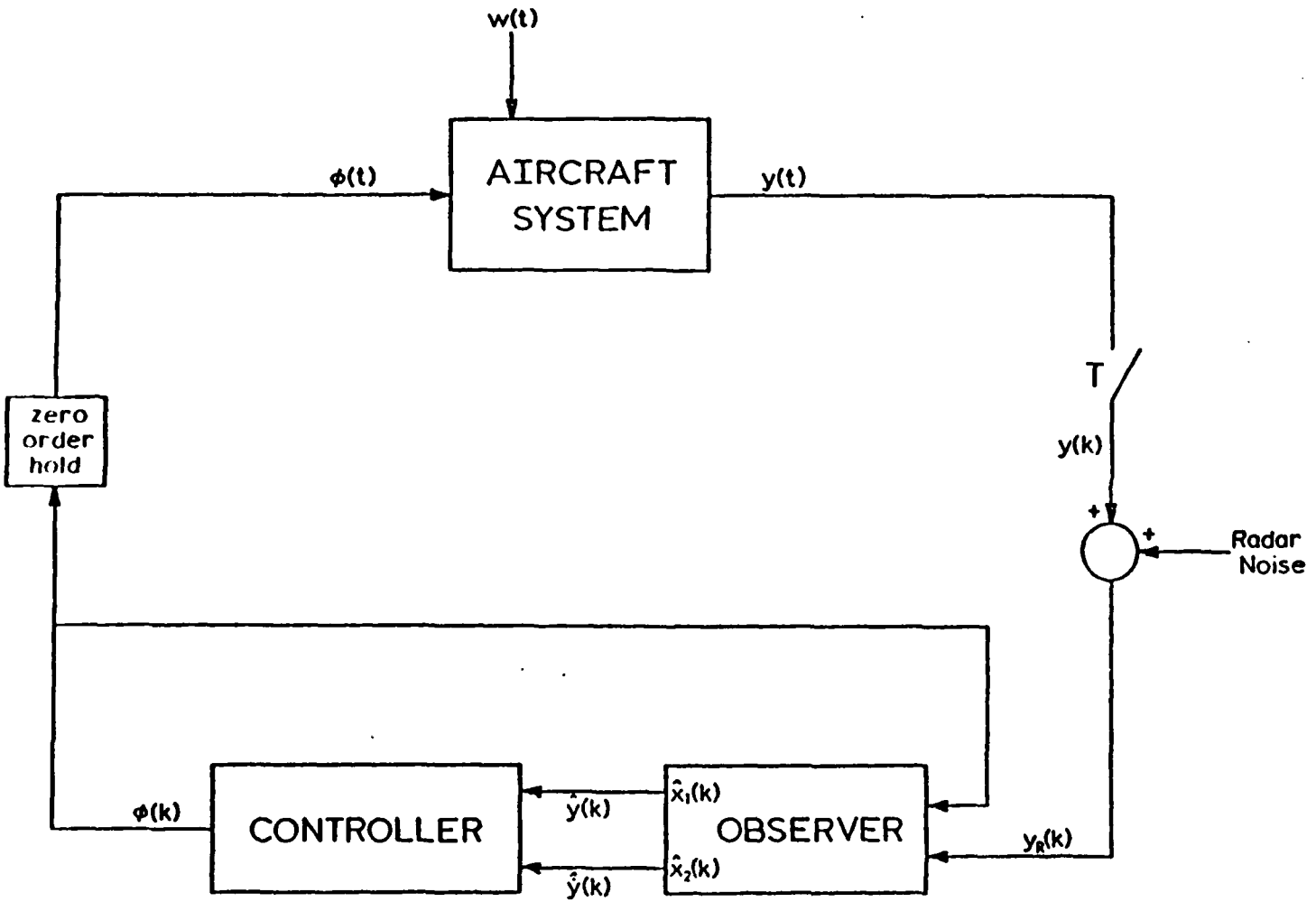

Figure 3-1. Block Diagram of the F4J Aircraft Lateral Control System with the Observer.

$$\begin{bmatrix} x_1(k+1) \\ x_2(k+1) \\ x_3(k+1) \end{bmatrix} = \begin{bmatrix} 1.0 & 0.1 & 0.00477116 \\ 0.0 & 1.0 & 0.0932144 \\ 0.0 & 0.0 & 0.867429 \end{bmatrix} \begin{bmatrix} x_1(k) \\ x_2(k) \\ x_3(k) \end{bmatrix} + \begin{bmatrix} 0.000114237 \\ 0.00338736 \\ 0.0661790 \end{bmatrix} \phi(k) \quad (3\text{-}1)$$

$$y(k) = [1.0 \quad 0.0 \quad 0.0] \begin{bmatrix} x_1(k) \\ x_2(k) \\ x_3(k) \end{bmatrix} \quad (3\text{-}2)$$

In these equations, $x_1(k) = y(k)$ [aircraft position], $x_2(k) = \dot{y}(k)$ [aircraft velocity], and $x_3(k) = \ddot{y}(k)$ [aircraft acceleration]. These equations are of the general form

$$\begin{aligned} \underline{x}(k+1) &= A\underline{x}(k) + B\phi(k) \\ y(k) &= C\underline{x}(k) \end{aligned} \quad (3\text{-}3)$$

The equations of the observer are given by

$$\hat{\underline{x}}(k+1) = (A\text{-}LC)\hat{\underline{x}}(k) + B\phi(k) + Ly(k) \quad (3\text{-}4)$$

where the matrices A, B, and C are given in (3-3), (3-1), and (3-2). The matrix L is determined by the design procedure. To determine L, the characteristic equation of the observer, denoted by $\alpha(z)$, must be chosen. Then, from (3-4),

$$\alpha(z) = |zI - (A\text{-}LC)| = 0 \quad (3\text{-}5)$$

The only unknown in (3-5) is L, and Ackermann's Formula [1] may be used to solve (3-5) for L.

For the observer designed in [1], $\alpha(z)$ was chosen as

$$\alpha(z) = (z\text{-}0.8)^3 \quad (3\text{-}6)$$

which resulted in

$$L = \begin{bmatrix} 0.467428 \\ 0.57863 \\ 0.0353145 \end{bmatrix} \tag{3-7}$$

Since $z = \epsilon^{sT} = \epsilon^{-T/\tau}$, where τ is the root time constant, then roots at $z = 0.8$ in (3-6) result in a time constant for the observer of

$$\epsilon^{-0.1/\tau} = 0.8$$

or

$$\tau = 0.448 \text{ seconds}$$

since T is 0.1 seconds.

In order to determine the effects of the choice of $\alpha(z)$ on the lateral control system of Figure 3-1, observers were also designed for

$$\alpha(z) = (z-0.85)^3 \tag{3-8}$$

and

$$\alpha(z) = (z-0.75)^3 \tag{3-9}$$

The observer time constant for (3-8) is then 0.615 seconds, and for (3-9), 0.348 seconds. The results of this design are tabulated in Table 3-1. A comparison of the responses of these three observer systems to the three systems described in Chapter II will be given in the next chapter.

TABLE 3-1

Observer Matrices

$\alpha(z)$	$(z-.85)^3$	$(z-.8)^3$	$(z-.75)^3$
L	$\begin{bmatrix} 0.317429 \\ 0.254144 \\ 0.00060367 \end{bmatrix}$	$\begin{bmatrix} 0.467428 \\ 0.57863 \\ 0.0353145 \end{bmatrix}$	$\begin{bmatrix} 0.617429 \\ 1.04757 \\ 0.186368 \end{bmatrix}$

IV. COMPARISON OF SYSTEMS

In this chapter a comparison is made of the radar noise responses and the wind responses of the F4J lateral control system for the six different control configurations described in Chapters II and III. The configurations are:

1. α-β system.
2. half-gain system.
3. ydot system.
4. $(z-0.85)^3$ observer system (characteristic equation).
5. $(z-0.8)^3$ observer system.
6. $(z-0.75)^3$ observer system.

Recall that the $(z-0.85)^3$ observer is the slowest one (i.e., narrowest bandwidth) and the $(z-0.75)^3$ observer is the fastest one (broadest bandwidth).

Initial Condition Response

The first comparison of the systems is between the initial condition responses. All responses discussed in this report were obtained from the simulation given in [1].

For the initial condition responses, the radar noise signal and the wind input were set to zero. The initial aircraft displacement y(0) was set to twenty feet at a range of 13,223 feet, which required a flight time to touchdown of sixty seconds. The results are given in Figures 4-1 and 4-2.

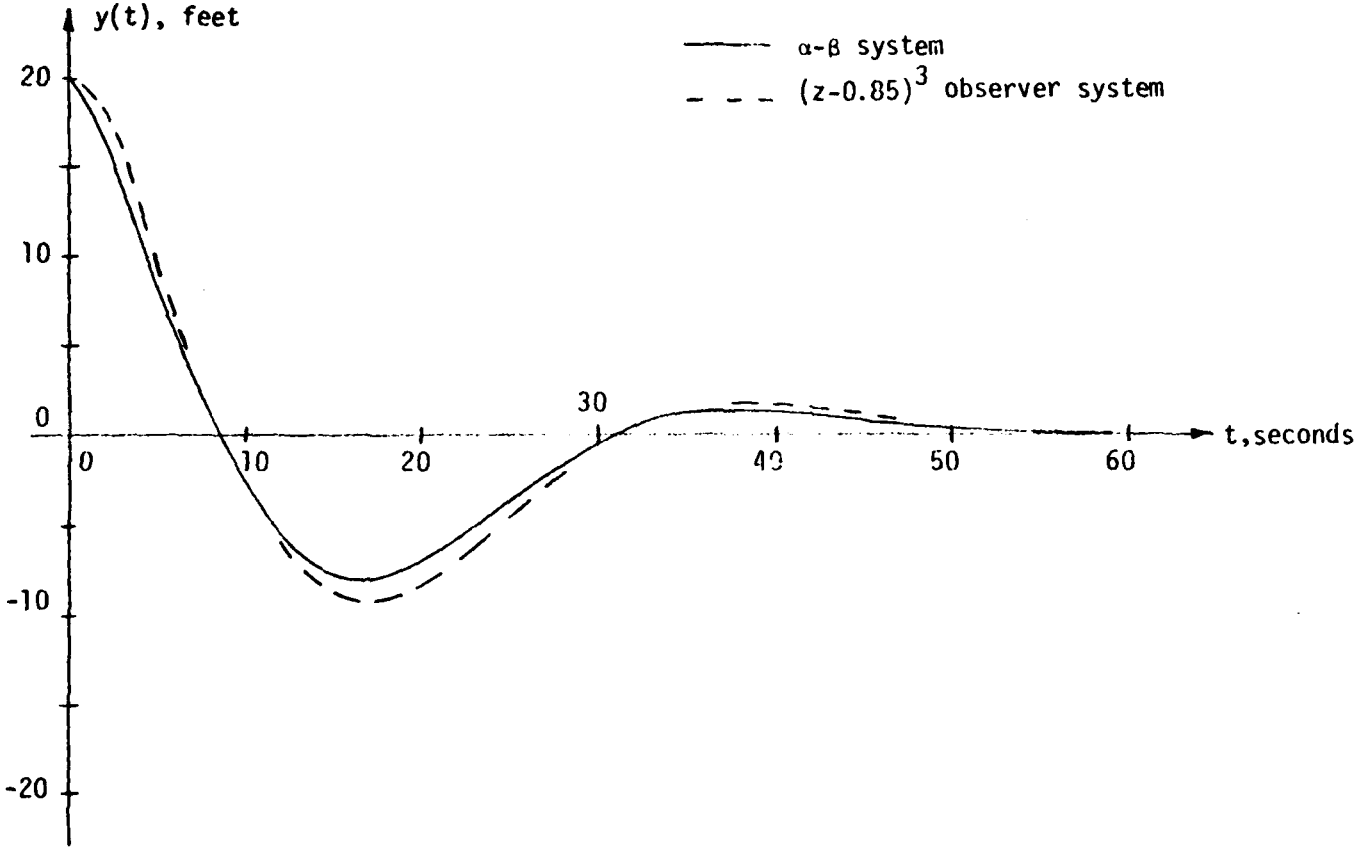

Figure 4-1. Initial Condition Response of MATCALS Systems.

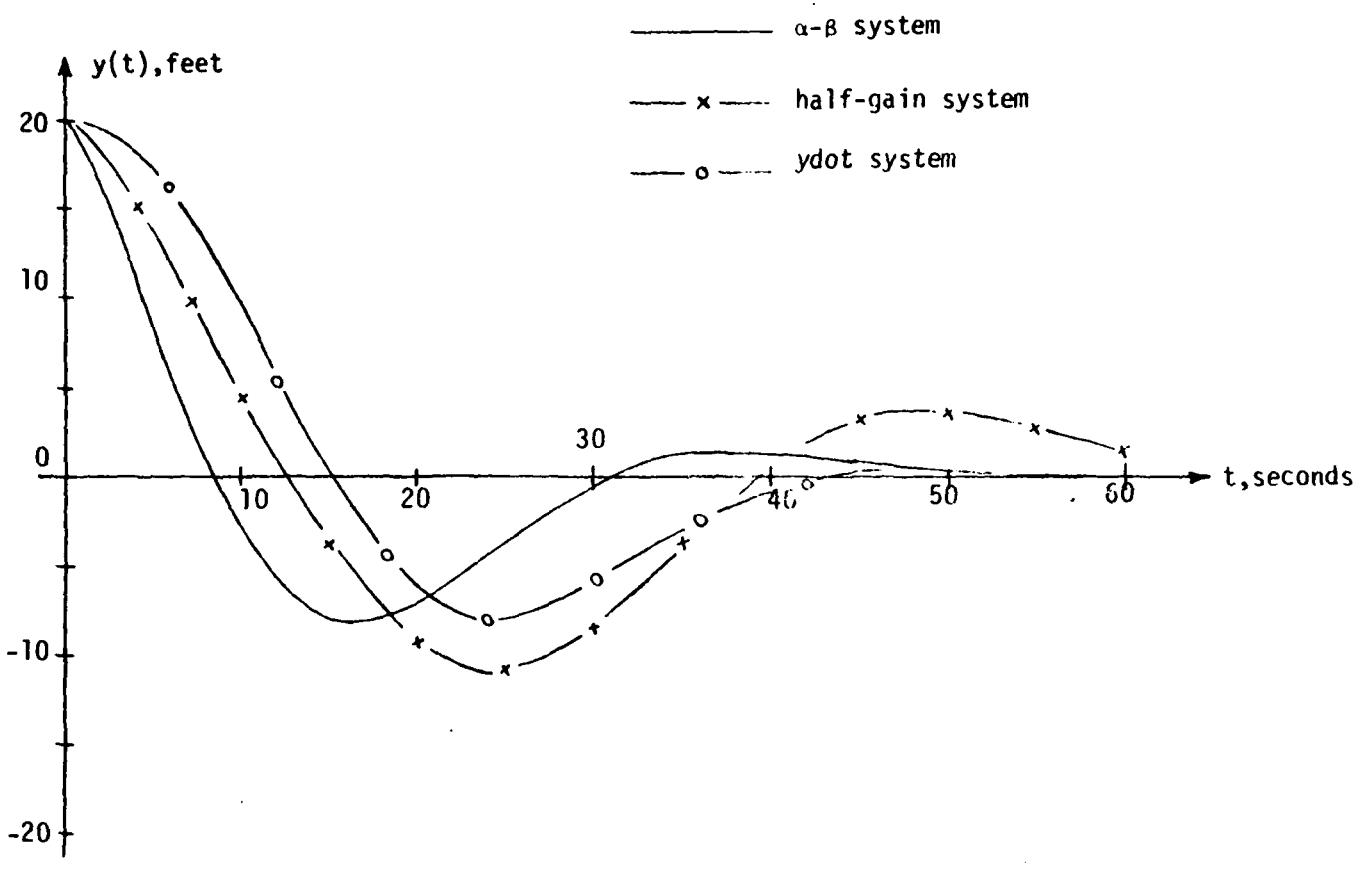

Figure 4-2. Initial Condition Response of MATCALS Systems.

In Figure 4-1 only the $(z-.85)^3$ observer system response is plotted; the responses of the other two observer systems lie between the $(z-.85)^3$ observer system response and the α-β system response. The ydot system response is much slower than the α-β system response, since the ydot system bandwidth is reduced as shown by (2-7). The half-gain system response is also slower than the α-β system response, because of the reduced system bandwidth.

Conclusions: the observer systems do not degrade the system time response to the extent of those of the ydot and half-gain systems. However, the time response of the half-gain system may be adequate; this is not known.

Stability Margins

An important measurement of the relative stability of a closed-loop system is the stability margins, i.e., the gain margin and the phase margin.

The gain margins and the phase margins of the six systems are given in Table 4-1. Recall from Figure 3-1 that the observer system contains two loops; thus the stability margins must be calculated for the system opened in each loop. A property of observer systems is that stability margins do not change in the primary loop, which in Figure 3-1 is the system opened at $\phi(k)$. However, stability margins may degrade when opened at the input to the plant, which in Figure 3-1 is the signal $\phi(t)$.

Note in Table 4-1 that stability margins for the observer systems opened at $\phi(k)$ are different from those of the α-β system. This difference originates in the use of a third-order model of the aircraft system to design the observers.

TABLE 4-1

Stability Margins-Opened at $\phi(k)$

system	phase margin	gain margin
α-β	49°	15 dB
half-gain	42°	21 dB
ydot	49°	15 dB
$(z-0.85)^3$	55°	11.2 dB
$(z-0.8)^3$	55°	11.7 dB
$(z-0.75)^3$	55°	12.0 dB
	Opened at $\phi(t)$	
$(z-0.85)^3$	43°	10.5 dB
$(z-0.8)^3$	45°	12 dB
$(z-0.75)^3$	48°	13.4 dB

Conclusions: it appears that the stability margins of all systems are adequate, since the half-gain system has the smallest phase margin. Note that the stability margins improve as the observe speed-of-response increases.

Closed-loop Noise Frequency Response

Shown in Figure 4-3 are the closed-loop frequency responses Y/Y_{rn} for the six systems. The signal Y is the aircraft position, and Y_{rn} is the radar noise signal. Note that the bandwidth of the α-β system is the broadest, and the ydot system has the narrowest bandwidth.

Conclusions: The bandwidths of the observer systems are somewhat smaller than that of the α-β system, with the $(z-.85)^3$ observer (the slowest one) having the narrowest bandwidth. Thus this observer system should have the least response to radar noise, when compared to the other two observer systems and the α-β system. The bandwidth of the ydot system is approximately one-third that of the α-β system. The bandwidth of the half-gain system is approximately one-half that of the α-β system.

Closed-loop Wind Frequency Response

Given in Figure 4-4 is the closed-loop frequency response Y/W, where Y is the aircraft position and W is the wind input. The frequency response for the ydot system is approximately the same as that of the α-β system and could not be plotted as a separate curve. This result is expected, as explained in Chapter 2.

Conclusions: The α-β system frequency response is acceptable, and that of the half-gain system is not. The observer systems frequency response falls between these two, with the $(z-.75)^3$ observer system

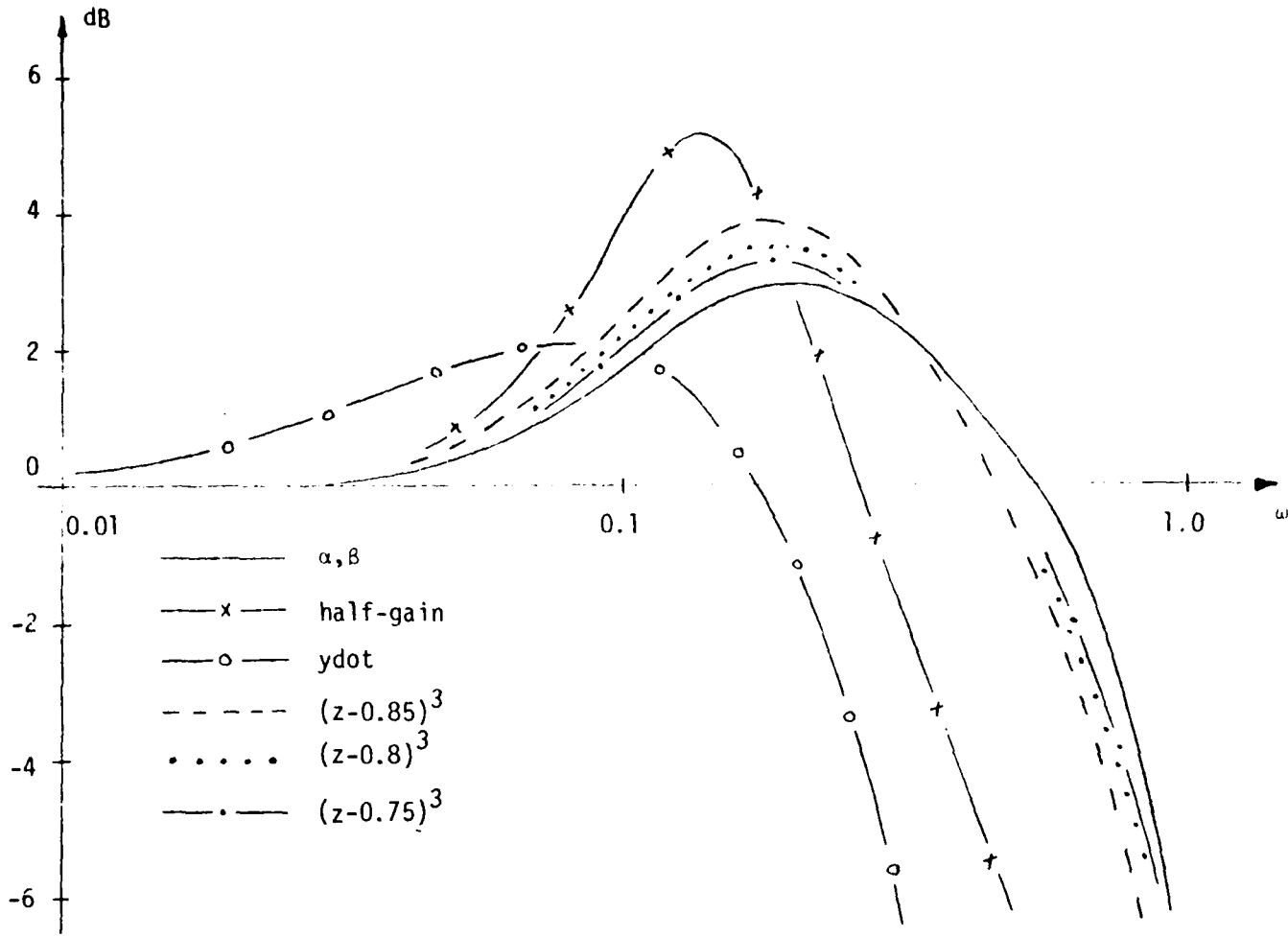

Figure 4.3. Y/Y_{rn} Closed-loop Frequency Response

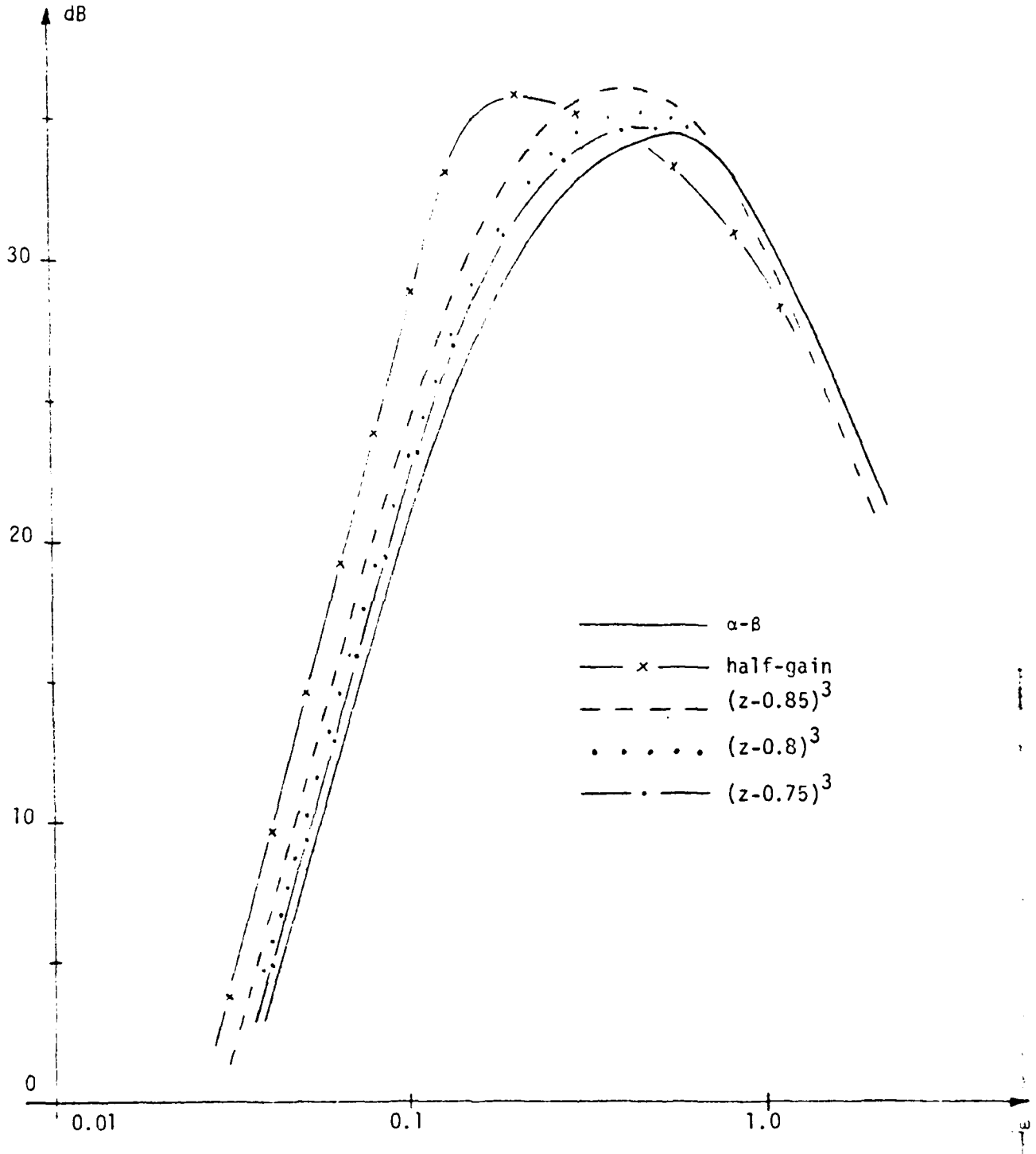

Figure 4-4. Y/W Closed-loop Frequency Response

(the fastest) closest to the acceptable α-β system response. This result is expected, since the fastest observer system has the broadest open-loop bandwidth, and this is the requirement for the least response to wind.

Closed-loop Bank Command Frequency Response

The frequency responses Y/Y_{rn} given in Figure 4-3 would be an accurate indication of system radar noise response if the system were linear. However, the effects of the nonlinearities in the aircraft do not appear on the frequency-response plots. Perhaps a better indication of the effects of radar noise on the system response is given in the frequency response Φ/Y_{rn}, where Φ is the bank command and Y_{rn} is the radar noise signal. The high frequency signals in Φ are filtered out before reaching Y, the aircraft position. However, these signals can cause both the rudder and the ailerons servos to reach the mechanical limits of travel. This limiting is a nonlinear effect.

Shown in Figure 4-5 are the frequency responses for five of the six systems. The ydot system is not included here. Note that the frequency responses of the observer systems are considerably less than that of the α-β system, but much greater than that of the half-gain system.

Conclusions: If the mechanical limiting of the travel of the rudder and the ailerons is a problem, then the observer systems should perform better than the α-β system with respect to radar noise response.

Monte Carlo Simulation Results

The Monte Carlo simulation discussed in [1] was used to determine actual time responses to radar noise and to wind. The wind model used was simply white noise; thus the use of a more realistic wind model may

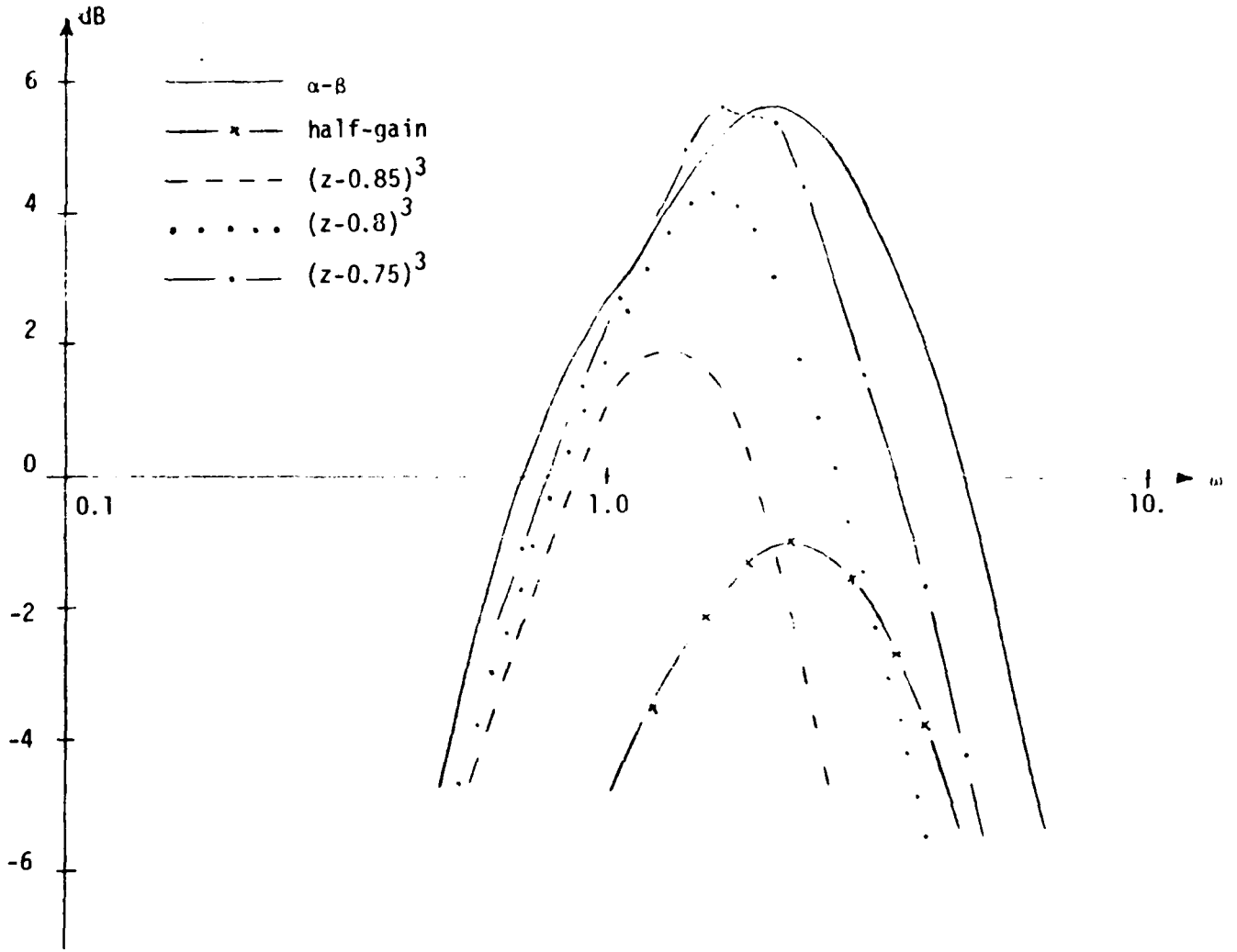

Figure 4-5. ϕ/Y_{rn} Closed-loop Frequency Response

change the results somewhat. The radar noise model used was that given in [3]. Twenty simulations were run for each Monte Carlo test, and the results given are the statistical averages of these twenty runs.

Given in Table 4-2 is the root-mean-square values of aircraft position in feet, with radar noise and no wind. The aircraft flight began at a range of 13,223 feet (60 seconds flight time to touchdown) with the aircraft on the extended centerline of the runway; i.e., $y(0) = 0$. Thus all motion of the aircraft is due to the radar noise, and hence is undesirable. The α-β system exhibits the largest motion, the ydot system the smallest. The observer systems' motions are greater than that of the half-gain system, but considerably less than that of the α-β system.

Table 4-3 gives the root-mean-square values of the bank command for the same simulations. Note that the data follows the same trends as that in Table 4-2.

Table 4-4 gives additional data from the same Monte Carlo simulation. This table gives the percentage of time that the rudder and the ailerons are limited. Note that limiting does not occur for the ydot system, and very little for the $(z-0.85)^3$ observer system. The limiting is practically the same for the half-gain system and the $(z-0.8)^3$ observer system. Extensive limiting occurs in the α-β system.

Table 4-5 gives results for the same initial conditions on the aircraft, except for this simulation the radar noise signal is set to zero and the wind input is white noise as given in [1]. Note that the α-β system exhibits the smallest motion to wind, while the half-gain system exhibits the largest. The observer systems' motion falls between these values.

TABLE 4-2

Radar Noise Response-Position Y

system	rms aircraft position, feet	% above half-gain system
α-β	2.52	77
half-gain	1.42	0
ydot	1.09	-
$(z-0.85)^3$	1.61	13
$(z-0.8)^3$	1.68	18
$(z-0.75)^3$	1.97	39

TABLE 4-3

Radar Noise Response-Bank Command ϕ

system	rms bank command-degrees	% above half-gain system
α-β	3.00	104
half-gain	1.47	0
ydot	0.17	-
$(z-0.85)^3$	1.60	9%
$(z-0.8)^3$	2.23	52%
$(z-0.75)^3$	2.70	84%

TABLE 4-4

Per Cent Time Limited

system	aileron limiting, %	rudder limiting, %
α-β	23	42
half-gain	2	16
ydot	0	0
$(z-0.85)^3$	0	1
$(z-0.8)^3$	2	15
$(z-0.75)^3$	9	30

TABLE 4-5

Wind Response-Position Y

system	rms aircraft position-feet	% above α-β system
α-β	1.90	0
half-gain	3.35	82
ydot	2.02	6
$(z-0.85)^3$	2.36	24
$(z-0.8)^3$	2.16	14
$(z-0.75)^3$	2.05	8

Conclusions: The $(z-0.75)^3$ observer system exhibits excessive motion to radar noise, and the $(z-0.85)^3$ observer system exhibits excessive motion to wind. The radar-noise motion of the $(z-0.8)^3$ observer system approaches that of the half-gain system; the wind motion of this observer system approaches that of the α-β system. In addition, the initial-condition response of the $(z-0.8)^3$ observer system approaches that of the α-β system.

V. MODEL 2 SYSTEM

In Chapter 4 an extensive comparison was made between six different systems. A different system was used to make the actual closed-loop landings, and this system is called the model 2 system in [3]. This system differs significantly from the α-β system and the half-gain system given in Chapter 2, and will now be described.

The block diagram of the α-β filter-controller of the α-β system is shown in Figure 5-1. The gains G_1, G_2, G_3 and G_4 have the standard terminology given in Table 5-1. The differences in the α-β system parameters and the model 2 system parameters are given in Table 5-2. Note that setting the parameter α_1 to unity gives that α filter in Figure 5-1 a gain of unity; i.e., that α filter is removed. Note that the model 2 gains in the derivative path and in the acceleration path have been reduced from those of the α-β system. Thus we expect the model 2 system to have a better radar noise response, but a degraded wind response, when compared to the α-β system. However, the low-frequency gain of the model 2 system is unchanged from that of the α-β system.

In the following developments, the model 2 system will be compared to an observer system. However, in this chapter, the observer system will have the same controller parameters as the model 2 system; i.e., the observer system is the same as the model 2 system, except that the α-β filter in the model 2 system is replaced with an observer. Three observers will once again be considered, with characteristic equations of either $(z-0.85)^3$, or $(z-0.8)^3$,

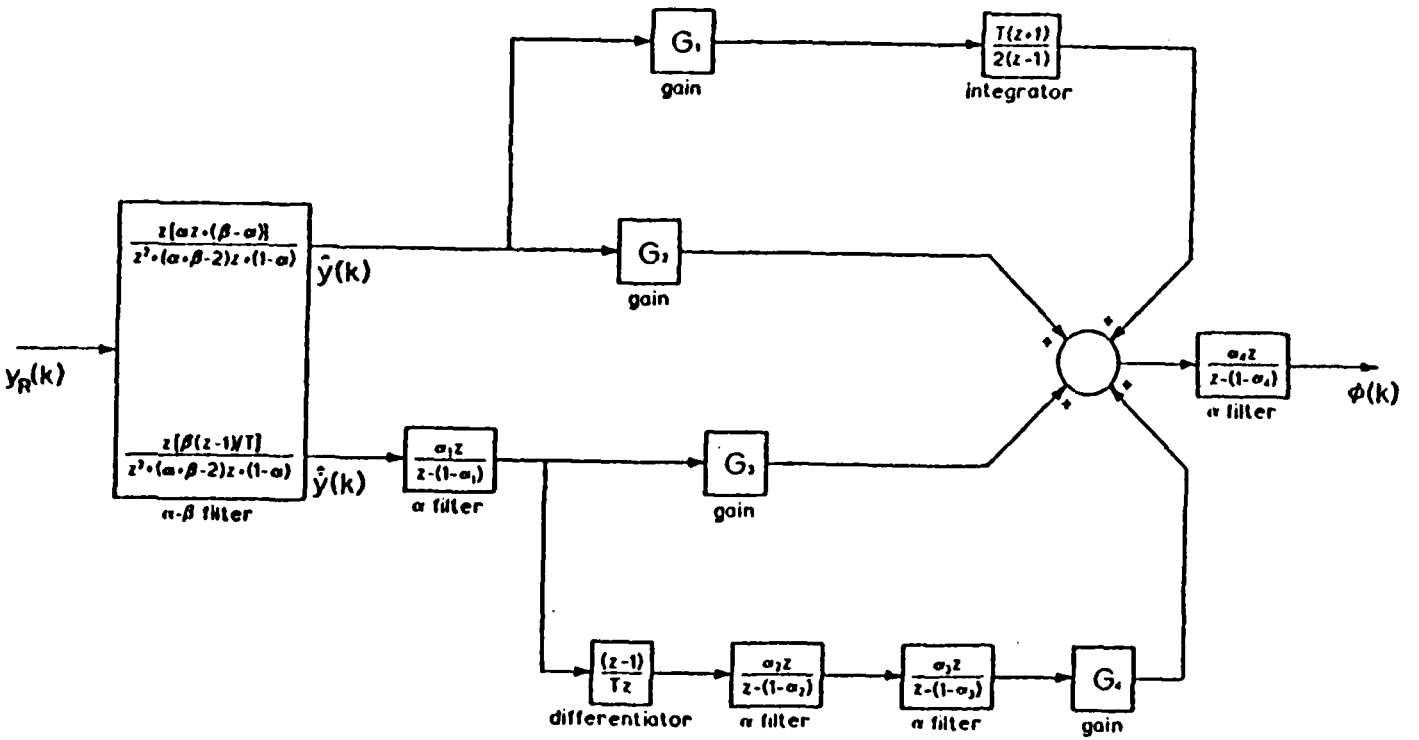

Figure 5-1. Block Diagram of Linearized SPN-42 Digital Controller with Transfer Functions.

TABLE 5-1

Gains of Figure 5-1

$$G_1 = \frac{K_{4L} * K_{CL}}{TIL}$$

$$G_2 = K_{1L} * K_{CL}$$

$$G_3 = K_{2L} * TRL$$

$$G_4 = K_{3L} * TAL$$

TABLE 5-2

Controller Parameters
(T = 0.1 seconds)

parameter	α-β system of Chapter 2	α-β system model 2
K_{CL}	0.1	0.1
TIL	30.0	30.0
TRL	7.5	6.0
TAL	7.5	2.5
α_1	0.3174	1.0
α_2	0.234	0.234
α_3	0.234	0.234
α_4	0.1211	0.1211
α	0.51	0.51
β	0.1746	0.1746

or $(z-0.75)^3$.

Initial Condition Response

First the initial condition responses will be compared. For the comparison, both the radar noise input and the wind input have been set to zero.

The initial condition responses are given in Figure 5-2. The initial aircraft displacement y(0) was set to twenty feet at a range of 13,223 feet, which required a flight time to touchdown of sixty seconds. The response of the $(z-0.75)^3$ observer is not plotted, since it is very close to that of the model 2 system.

Conclusions: The $(z-0.75)^3$ and the $(z-0.8)^3$ observer systems degrade the initial-condition response only slightly. Noticeable degradation occurs in the $(z-0.85)^3$ observer system. Recall that the $(z-0.85)^3$ observer is the slowest one.

Stability Margins

The gain margins and the phase margins of the four systems are given in Table 5-3. The description of the system opened at different points is given in Chapter 4.

Conclusions: The phase margins of the observer systems opened at $\phi(t)$ are somewhat small, but those of the $(z-0.8)^3$ and the $(z-0.75)^3$ observer are close to that of the model 2 system opened at $\phi(k)$.

Closed-loop Noise Frequency Response

Shown in Figure 5-3 are the closed-loop frequency responses Y/Y_{rn},

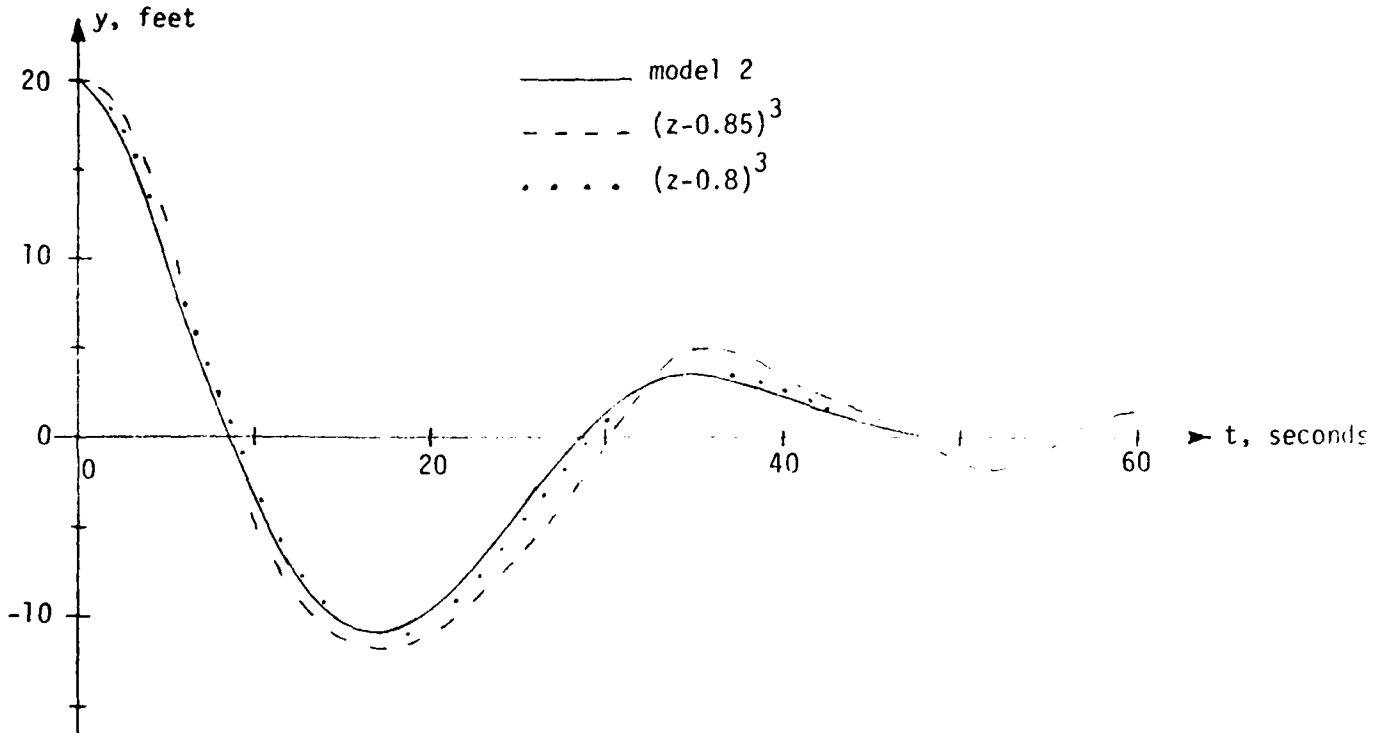

Figure 5-2. Initial Condition Response of MATCALS Systems.

TABLE 5-3

Stability Margins

Opened at $\phi(k)$

system	phase margin	gain margin
model 2	37°	20 dB
$(z-0.85)^3$	41°	17 dB
$(z-0.8)^3$	41°	17 dB
$(z-0.75)^3$	41°	18 dB

Opened at $\phi(t)$

$(z-0.85)^3$	32°	12 dB
$(z-0.8)^3$	35°	15 dB
$(z-0.75)^3$	37°	18 dB

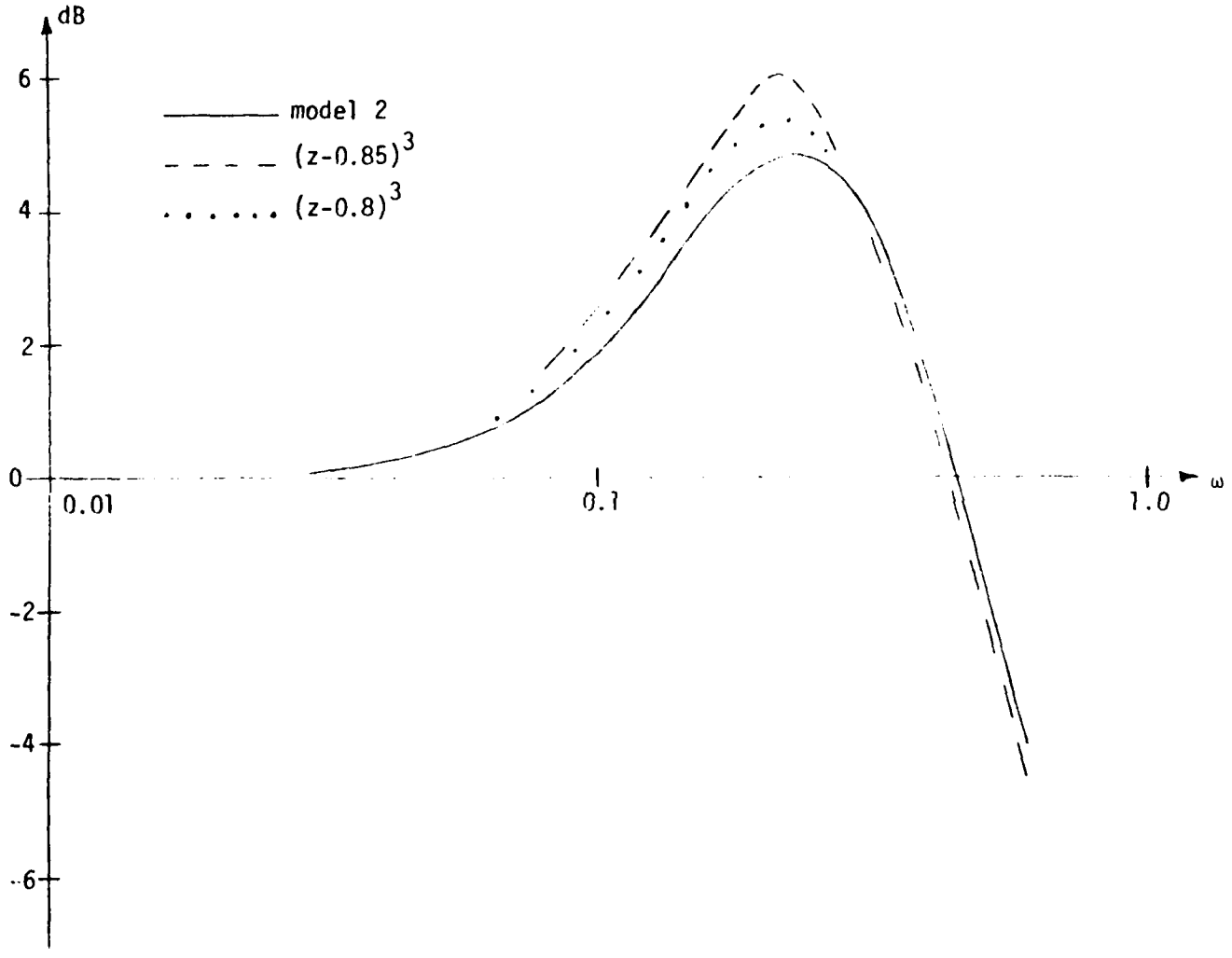

Figure 5-3. Y/Y_{rn} Closed-loop Frequency Response.

where Y is the aircraft position and Y_{rn} is the radar noise signal (see Figure 2-2). The frequency response of the $(z-0.75)^3$ observer system is not plotted, since it is quite close to that of the model 2 system.

Conclusions: The observer systems' noise responses degrade from that of the model 2 system, with the slowest observer having the narrowest bandwidth.

Closed-loop Wind Frequency Response

Given in Figure 5-4 is the closed-loop frequency response Y/W, where Y is the aircraft position and W is the wind input.

Conclusions: Since low wind response depends on a wide open-loop bandwidth, we expect the $(z-0.85)^3$ observer (slowest) to have the greatest wind response. This is seen to be true. The $(z-0.75)^3$ wind response is very close to that of the model 2 system, and is not plotted.

Closed-loop Bank Command Frequency Response

Given in Figure 5-5 are the frequency responses ϕ/Y_{rn}, where ϕ is the bank command and Y_{rn} is the radar noise signal. The importance of this frequency response is discussed in Chapter 4.

Conclusions: The observer systems show significant improvement in the system gain from radar noise to bank command. Thus the ailerons and rudder should exhibit less motion in the observer systems.

Monte Carlo Simulation Results

The Monte Carlo simulation is discussed in [1] and in Chapter 4. Given in Table 5-4 are the root-mean-square values of several signals obtained

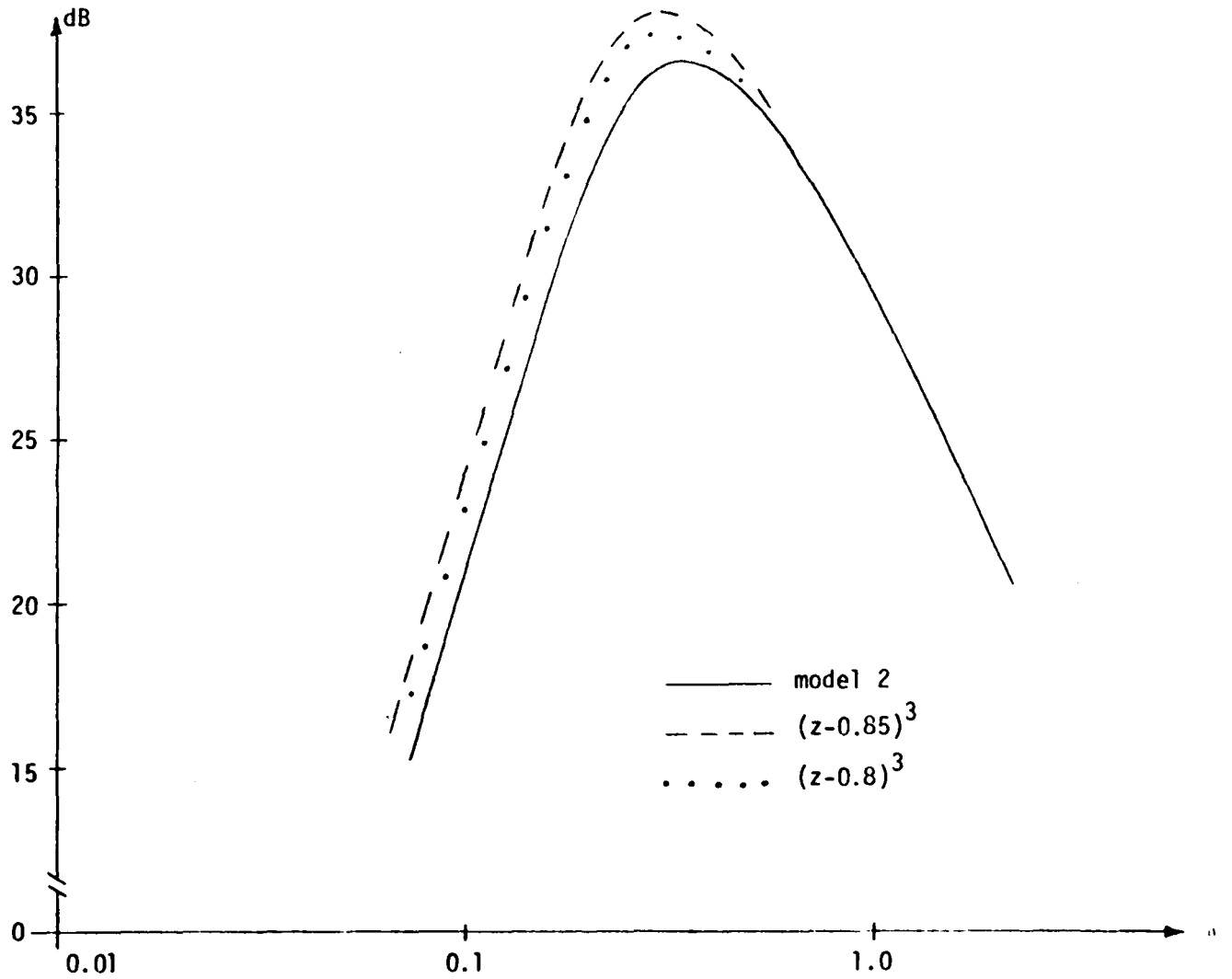

Figure 5-4. Y/W Closed-loop Frequency Response.

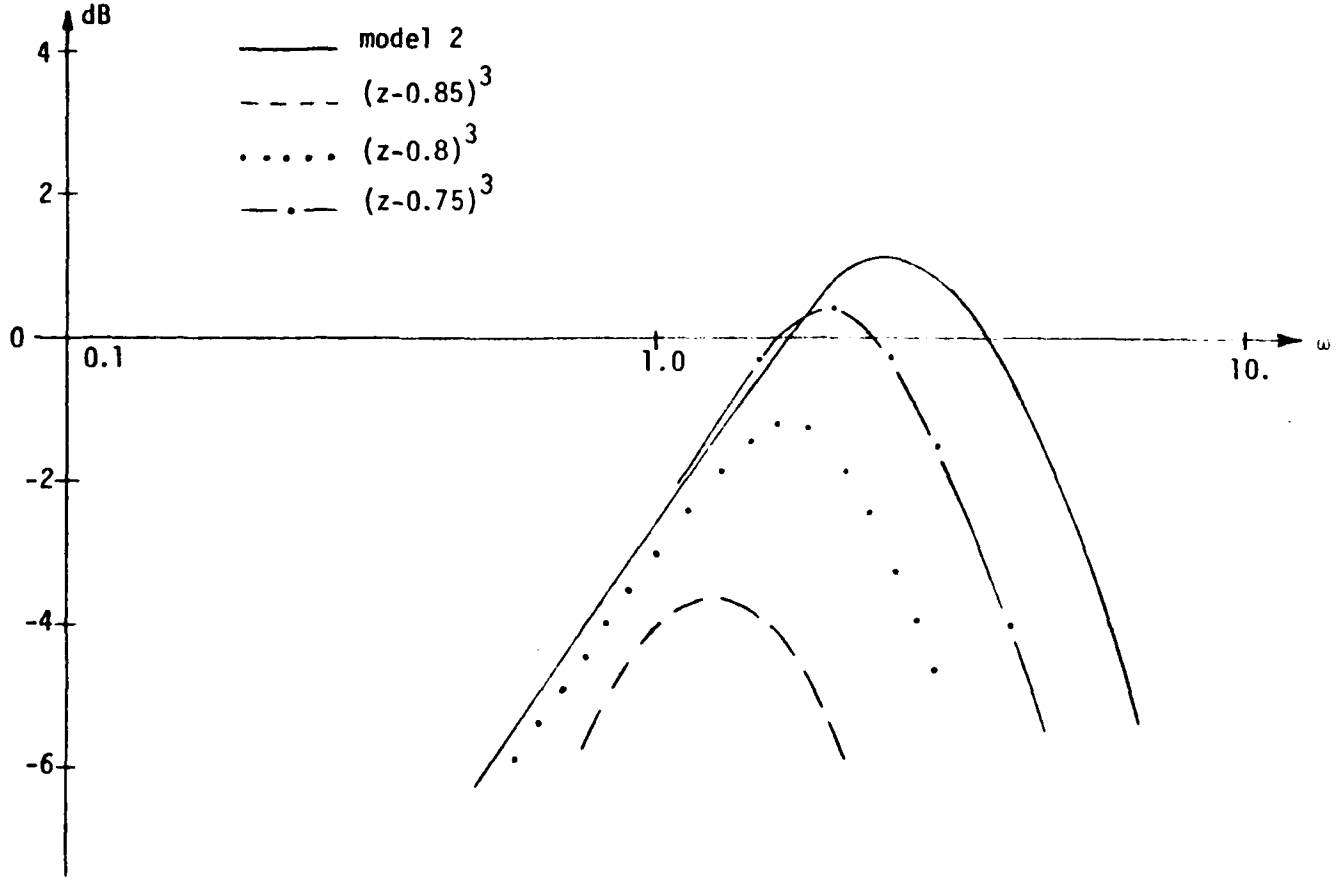

Figure 5-5. ϕ/Y_{rn} Closed-loop Frequency Response.

TABLE 5-4

Monte Carlo Simulation Results-

Radar Noise Response

system	y feet	ϕ degrees	δ_a degrees	$\dot{\delta}_a$ degrees/sec	δ_r degrees	$\dot{\delta}_r$ degrees/sec	% limit ailerons	% limit rudder
model 2	1.95	2.03	3.73	13.2	3.35	17.3	13.3%	33.8%
$(z-0.85)^3$	1.69	1.03	1.00	3.31	1.28	6.19	0%	0.1%
$(z-0.8)^3$	1.70	1.43	1.78	6.27	2.22	11.2	0.2%	5.6%
$(z-0.75)^3$	1.77	1.79	2.69	9.55	2.89	15.0	2.8%	19.3%

from Monte Carlo simulations with radar-noise input. The column labeled y is the rms value of position, ϕ is the rms value of bank command, δ_a is the rms aileron angle, $\dot{\delta}_a$ is the rms aileron velocity, δ_r is the rms rudder angle, and $\dot{\delta}_r$ the rms rudder velocity. Also given are the per cent of time that the aileron servo and the rudder servo are limited. Note that the observer systems show significantly less response to radar noise than does the model 2 system.

In terms of radar-noise response, replacing the α-β filter with an observer significantly improves response. For example, the $(z-0.8)^3$ observer has less than one-half the aileron displacement and velocity as does the model 2 system. In addition, the aileron servo limiting for this observer system is almost zero, compared to 13.3% of the time for the model 2 system. Figure 5-6 shows a typical aileron response to radar noise for the model 2 system and for the $(z-0.8)^3$ observer system. The flight time runs from 30 to 46 seconds, or for a range from approximately 6600 feet to 3000 feet. Note that the aileron motion for the observer system is significantly less than that for the model 2 system.

Table 5-5 gives results from Monte Carlo simulations with the radar noise removed and the wind input as given in [1]. Note that the model 2 system exhibits the least response to wind, but that the observer systems' responses are not significantly greater. Also given is a comparison to the wind response of the α-β system of Chapter 4.

Conclusions: The observer systems exhibit a significantly improved radar-noise response when compared to the model 2 systems, but the wind response is somewhat degraded. Thus, if an observer is employed in the system, probably the controller gains can be increased to reduce wind response while maintaining a reasonable radar-noise response.

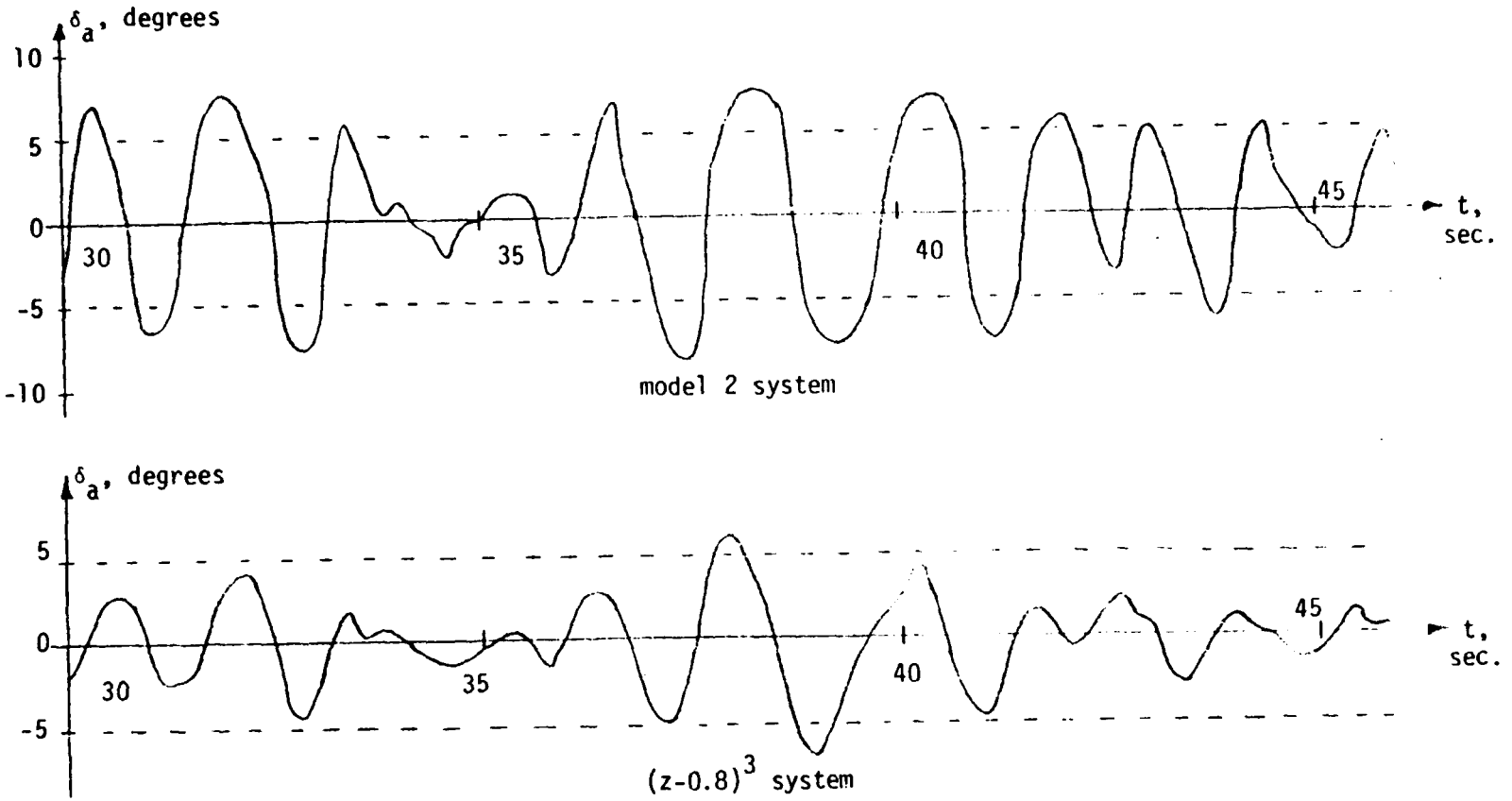

Figure 5-6. Typical Aileron Responses.

TABLE 5-5

Wind Response-Position Y

System	rms aircraft position-feet	% above model 2 system	% above z-3 system
model 2	2.24	0%	18%
$(z-0.85)^3$	2.64	18%	39%
$(z-0.8)^3$	2.46	10%	29%
$(z-0.75)^3$	2.38	6%	25%

VI. CONCLUSIONS

The F4J aircraft lateral control system in a MATCALS configuration is investigated in this report. Several different controllers are utilized in these studies to determine which yield the best radar-noise response and which yield the best wind response.

The proposed MATCALS systems contain an α-β filter in the controller. Alternative systems are constructed by replacing the α-β filter with an observer.

In general the observer control systems exhibit significantly less radar-noise response than do the α-β systems, but exhibit somewhat more wind response. These studies indicate that the observer controllers improve the MATCALS system's operation when compared to the α-β controllers, and that the observer systems should be considered further.

REFERENCES

[1] E. R. Graf, C. L. Phillips, and S. A. Starks, "Marine Air Traffic Control and Landing System (MATCALS) Investigation", Contract 1-A-2550 (subcontracted from N-00039-80-C-0032), Auburn University, Auburn University, AL, April, 1981.

[2] Charles L. Phillips, Edward R. Graf, and H. Troy Nagle, Jr., "Marine Air Traffic Control and Landing System Error and Stability Analysis", Vol. 1 and 2, Contract N00228-75-C-7080, Auburn University, Auburn University, AL, 1975.

[3] "MATCALS-AN/TPN-22 Mode 1 Final Report" ITT Gilfillan Technical Report, prepared for Naval Electronics Systems Command, Contract N0003-75-C-0021, August, 1979.

PART FOUR

THE DESIGN OF A TRI-STATE ADAPTIVE TRACKING FILTER FOR THE MATCALS SYSTEM

Prepared for

Georgia Institute of Technology
ATLANTA, GEORGIA

Under

Contract 1-A-2550

by

Electrical Engineering Department
Auburn University
Auburn, Alabama

Prepared by: Greeley M. Lee, Jr.

Reviewed by: Scott A. Starks

THE DESIGN OF A TRI-STATE ADAPTIVE TRACKING FILTER FOR THE MATCALS SYSTEM

ABSTRACT

A tri-state adaptive tracking filter is designed for use in the F4J aircraft lateral control system in an automatic landing configuration. The system presently uses an alpha-beta tracking filter to estimate the aircraft's lateral position and velocity. The tri-state adaptive filter is designed to replace the alpha-beta filter. Results from the F4J lateral control system simulation indicates that the tri-state adaptive filter improves the system's response.

TABLE OF CONTENTS

LIST OF TABLES ix

LIST OF FIGURES x

I. INTRODUCTION 1

II. THE COMPONENT FILTERS 2

Introduction
The Alpha Filter
Derivation of Alpha Filter
Alpha Filter Noise Response
Analysis of Alpha Filter in the Z-Domain
The Alpha-Beta Tracking Filter
Derivation of the Alpha-Beta Tracking Filter
Analysis of the Alpha-Beta Filter in the Z-Domain
Stability of the Alpha-Beta Filter
Alpha-Beta Filter Noise Response
Performance Measures for the Alpha-Beta Filter
The Alpha-Beta-Gamma Tracking Filter
Derivation of the Alpha-Beta-Gamma Tracking Filter
The Alpha-Beta-Gamma Filter in the Z-Domain
Stability of the Alpha-Beta-Gamma Filter
Pole Analysis for the Alpha-Beta-Gamma Tracking Filter
Alpha-Beta-Gamma Filter Noise Response
Performance Measures for the Alpha-Beta-Gamma Filter

III. THE TRI-STATE ADAPTIVE FILTER 48

Introduction
Tracking Filter Limitations
Selection of the Appropriate Filter
Alpha Filter Output Variance as a Basis for Filter Selection
Alpha-Beta Filter Output Variance as a Basis for Filter Selection
Implementation of the Tri-State Adaptive Tracking Filter

IV. SYSTEM SIMULATION 57

Introduction
The F4J Control System
The F4J Lateral Guidance System

The SPN-42 Digital Controller
AN/TPN-22 Radar

V. SIMULATION RESULTS 65

Introduction
Tracking System Comparison
Filter Parameters
Filter Frequency Response
Time Response with a Given Initial Condition
Tri-State Adaptive Control System Performance
Monte Carlo Simulation Runs
Comparison of System Responses on Identical
Simulation Runs

VI. CONCLUSIONS 91

BIBLIOGRAPHY 92

APPENDIX 94

LIST OF TABLES

5.1. Filter Parameters 68

5.2. Time Response Characteristics 77

5.3. Results of Monte Carlo Runs with Noise and Wind 80

5.4. Results of Monte Carlo Runs with Noise and Wind 83

5.5. Results of Monte Carlo Runs with Wind Only 84

5.6. Results of Monte Carlo Runs with Radar Noise Only 85

5.7. Mean Square Error of Velocity Estimates with Wind and Radar Noise 90

LIST OF FIGURES

2.1. Block Diagram Representation of Alpha Filter Transfer Function 9

2.2. Locus of Possible Pole Locations for Stable Operation of Alpha Tracking Filter 13

2.3. Sample Data Feedback System Depicting the Predictor Equation of the Alpha-Beta Tracking Filter 20

2.4. Flowchart of the Alpha-Beta Tracking Filter 30

2.5. Flowchart of the Alpha-Beta-Gamma Tracking Filter 47

3.1. Block Diagram of the Tri-State Adaptive Tracking Filter 54

3.2. Flowchart of the Tri-State Adaptive Tracking Filter 56

4.1. Block Diagram of MATCALS Automatic Landing System 58

4.2. Block Diagram of the F4J Lateral Control System 60

4.3. SPN-42 Digital Controller 62

4.4. AN/TPN-22 Radar Error Simulation 63

5.1. Block Diagram of the F4J Lateral Control System with the Alpha-Beta Tracking Filter in Operation 66

5.2. Block Diagram of the F4J Lateral Control System with the Tri-State Adaptive Tracking Filter in Operation 67

5.3. Frequency Response of the Alpha-Beta Filter used in the Alpha-Beta Control System 70

5.4. Frequency Response of the Alpha Filter used in the Tri-State Adaptive Control System 71

5.5. Frequency Response of the Alpha-Beta Filter used in the Tri-State Adaptive Control System 72

5.6. Frequency Response of the Alpha-Beta-Gamma Filter used in the Tri-State Adaptive Control System 73

5.7. Initial Condition Time Response of the Alpha-Beta Control System 74

5.8. Initial Condition Time Response of the Tri-State Adaptive Control System 75

5.9. Comparison of the Tri-State Adaptive Control System to the Alpha-Beta Control System with Identical Wind and Radar Noise 87

5.10. True Lateral Velocity of the Aircraft Compared to the Alpha-Beta Filter Velocity Estimate 88

5.11. True Lateral Velocity of the Aircraft Compared to Tri-State Adaptive Filter Velocity Estimate 89

I. INTRODUCTION

This study investigates the possible use of a tri-state adaptive tracking filter in an automatic landing system for aircraft. The automatic landing system under consideration is the Marine Air Traffic Control and Landing System (MATCALS). Presently the MATCALS control system uses an alpha-beta filter to estimate the aircraft's position and velocity. The performance of this system is greatly degraded by the amount of noise present in the system. The tri-state adaptive tracking filter is presented as a possible replacement for the alpha-beta filter. The performance of the tri-state adaptive filter was evaluated using the simulation of the F4J aircraft lateral control system.

A general discussion of the alpha filter, the alpha-beta filter, and the alpha-beta-gamma filter is given in Chapter II. This discussion includes derivations, stability analysis, and noise response evaluation for each filter. The tri-state adaptive filter, which is composed of the three filters discussed in Chapter II, is presented in Chapter III. The selection of the appropriate filter output is governed by the variance of the filters' smoothed position estimates.

A general description of the MATCALS F4J Lateral Control System Simulation is given in Chapter IV. Chapter V presents the results of the F4J lateral control system simulation using the tri-state adaptive filter in place of the alpha-beta filter.

II. THE COMPONENT FILTERS

Introduction

When using radar track-while-scan systems to track a moving aircraft, radar returns in the form of raw digitized position measurements must be processed to provide

1) a smoothed estimate of present position;
2) a smoothed estimate of present velocity;
3) a one step ahead prediction of position for track correlation or bin selection.

In the design of these tracking systems, two conflicting requirements must be met. The first requirement is that the system must have good noise smoothing properties. A system of this type is typically characterized by a sluggish system response, long time constant and narrow bandwidth. The second requirement is that the system must have fast maneuver following capabilities. This type of system is usually characterized by a fast system response, short time constant, and wide bandwidth. The first requirement is essential because of the inherent noise present in the raw unprocessed radar position measurements. On the other hand, in tracking airborne targets, the dynamics of the tracking system must be capable of tracking an object that is not stationary in space. As a result, the second requirement is necessary. Unfortunately, as one makes the tracking system more insensitive to noise, the maneuver-following capabilities suffer. Thus, some compromise is always required.

However, the smoothing equations should be structured so as to give the best compromise. That is, noise smoothing should be maximum for a given maneuver following capability and vice-versa.

The smoothing of the position and velocity estimates is usually accomplished with a digital filter. These filters can range in complexity from a simple two point extrapolator to the comparatively complex Kalman filter [1]. This section examines the alpha filter [2], alpha-beta filter [3], and the alpha-beta-gamma filter [4]. Although the Kalman filter is more sophisticated and more accurate than the filters being examined in this section, it is, computationally, the most costly to implement. The principle advantage of the alpha, alpha-beta, and alpha-beta-gamma filters versus the Kalman filter is that the computations require no matrix inversions as does the Kalman filter, which results in faster filter outputs and less data storage.

Throughout this discussion, only a single dimensional filter will be considered. The variable x may denote the aircraft's position in azimuth, elevation, or range. By assuming smoothing in any given coordinate can be handled independently, extension to multiple coordinate systems is straightforward.

The Alpha Tracking Filter

Derivation of the Alpha Filter

The first tracking filter to be examined is the alpha tracker. The alpha tracker is founded upon the fundamental theorem of exponential smoothing. The fundamental theorem states that, given a time series $\{X(t)\}$ with observations at equally spaced intervals, the first N+1 degrees of exponential smoothing can be combined, using the binomial

coefficients, to give an estimate of the values of the coefficients of an Nth degree polynomial model of the observations to date, evaluated at the time of the most recent observation [2]. The alpha tracker takes the form of the simplest first degree of exponential smoothing and can be expressed as

$$x_s(k) = \alpha\, x_m(k) + (1-\alpha)\, x_s(k-1) \quad . \tag{2-1}$$

where,

$x_s(k)$ = smoothed estimate at time kT

$x_m(k)$ = input measurement of position at time kT

α = position smoothing constant. $0 \leq \alpha \leq 1$.

Suppose that the observations of position to date give an estimate of $x_s(k-1)$ and a new observation $x_m(k)$ is received at time kT. If the new value is larger than the old estimate, the new estimate $x_s(k)$ will be larger, and conversely.

The alpha tracker is derived from the zero order "window" tracker [5]. Assume that there exists a series of regularly spaced samples of position which must be smoothed.

$$x_m(k),\ x_m(k-1),\ x_m(k-2),\ \ldots,\ x_m(1),\ x_m(0) \tag{2-2}$$

such that

$$x_m(k) = x(k) + n(k)$$

where

$x_m(k)$ = input measurement of position at time kT

$x(k)$ = actual value (constant) of position at time kT

$n(k)$ = measurement noise

At this point in the discussion, the noise is assumed to be Gaussian, zero mean, with variance = σ_n^2. The noise is also assumed to be uncorrelated from sample to sample and therefore independent from sample to sample.

If $x(k)$ equals some constant X, then the "window tracker" with a smoothing interval of L samples might be utilized to "average out" the effects of the random noise variations on $x_m(k)$ such that the estimate is approximately equal to the actual value X. This may be accomplished via equation (2-3).

$$x_s(L) = \frac{1}{L} \sum_{k=1}^{L} x_m(k) \tag{2-3}$$

Now, if the approach of minimizing mean-square error between $x_s(L)$ and $x_m(k)$ is taken, the best least squares fit of a horizontal line to the data is obtained.

$$\min_{x_s(L)} \left\{ \sum_{i=1}^{L} (x_s(L) - x_m(i))^2 \right\} = 0 \tag{2-4}$$

$$\frac{\partial}{\partial x_s(L)} \left\{ \sum_{i=1}^{L} (x_s(L) - x_m(i))^2 \right\} = \sum_{i=1}^{L} 2(x_s(L) - x_m(i)) = 0 \tag{2-5}$$

$$2 \sum_{i=1}^{L} x_s(L) - 2 \sum_{i=1}^{L} x_m(i) = 0 \tag{2-6}$$

$$\sum_{i=1}^{L} x_s(L) = \sum_{i=1}^{L} x_m(i) \tag{2-7}$$

$$L\, x_s(L) = \sum_{i=1}^{L} x_m(i) \tag{2-8}$$

$$x_s(L) = \frac{1}{L} \sum_{i=1}^{L} x_m(i) \tag{2-9}$$

Therefore, the "window" tracker provides a smoothed position estimate based upon the minimization of the mean-square error between $x_s(L)$ and $x_m(k)$.

A one step ahead prediction of position may be obtained from the "window" tracker by merely shifting the L-length window such that it spans the measured data from $x_m(2)$ to $x_m(L+1)$. Equation (2-3) now takes the form of

$$x_p(L+1) = \frac{1}{L} \sum_{i=2}^{L+1} x_m(i) \tag{2-10}$$

$$x_p(L+1) = \left(\frac{1}{L} \sum_{i=1}^{L+1} x_m(i)\right) - \frac{1}{L} x_m(1) \tag{2-11}$$

$$x_p(L+1) = \left(\frac{1}{L} \sum_{i=1}^{L} x_m(i)\right) - \frac{1}{L} x_m(1) + \frac{1}{L} x_m(L+1) \tag{2-12}$$

$$x_p(L+1) = x_s(L) + \frac{1}{L} \left(x_m(L+1) - x_m(1)\right) \tag{2-13}$$

It is safe to assume that the smoothed estimate $x_s(L)$ is a more accurate value of true position than the noise corrupted measurement $x_m(1)$. Therefore, (2-13) becomes

$$x_p(L+1) = x_s(L) + \frac{1}{L} \left(x_m(L+1) - x_s(L)\right) \tag{2-14}$$

rearranging terms

$$x_p(L+1) = \frac{1}{L} x_m(L+1) + (1 - \frac{1}{L}) x_s(L) \qquad (2\text{-}15)$$

By defining $\alpha = \frac{1}{L}$ then a familiar form of the alpha tracking filter is obtained [6].

$$x_p(k+1) = \alpha x_m(k+1) + (1-\alpha) x_s(k) \qquad (2\text{-}16)$$

where $x_p(k+1)$ is the one step ahead prediction of position. By examining (2-15), it is evident that as the length L of the smoothing window is extended, α decreases, resulting in increased smoothing since the new measurement data is not weighted as heavily as the previous estimates of position. If it were known that the initial estimates of positions were correct then there would be no point in using the measurement data as a basis for prediction and the smoothing constant α would approach the value of zero. If, on the other hand L is decreased, α increases in value (approaching unity) such that the new measurement of position is weighted more heavily, rapidly discounting the effects of the previous estimates.

When (2-16) is substituted into itself for successively earlier samples, a series emerges of the form

$$x_p(k+1) = \alpha \sum_{n=0}^{k+1} (1-\alpha)^n x_m(k+1-n) \qquad (2\text{-}17)$$

From (2-17) it is evident that the alpha tracker assigns geometrically decreasing weights to the least recent data, hence the term exponential smoothing.

Alpha-Filter Noise Response

The alpha tracker can be depicted as in Figure 2.1, where the impulse response of the digital filter is defined by

$$h(k) \triangleq \alpha\,(1-\alpha)^k \quad . \tag{2-18}$$

The output of the filter is a convolution of the input and the filter's impulse response

$$x_s(k) = h(k) * x_m(k) \quad . \tag{2-19}$$

Some idea of the noise smoothing performance of the alpha tracker may be obtained by examining the mean and variance of $x_s(k)$. The convolution of (2-19) may be written as

$$x_s(k) = \alpha \sum_{n=0}^{\infty} (1-\alpha)^n\,[X + n(k-n)]. \tag{2-20}$$

where

$\alpha(1-\alpha)^n$ = impulse response of alpha tracker

X = actual position of target

$n(k)$ = additive zero mean Gaussian noise with variance = σ_n^2

Taking the expected value of (2-20) yields the mean of the output of the alpha tracker.

$$E\{x_s(k)\} = E\{\alpha \sum_{n=0}^{\infty} (1-\alpha)^n\,[X + n(k-n)]\} \tag{2-21}$$

$$E\{x_s(k)\} = \alpha \sum_{n=0}^{\infty} (1-\alpha)^n\,E\{X + n(k-n)\} \tag{2-22}$$

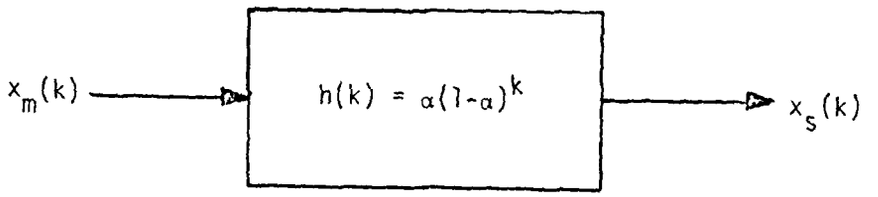

Figure 2.1. Block Diagram Representation of Alpha-Filter Transfer Function.

$$E\{x_s(k)\} = \alpha \sum_{n=0}^{\infty} (1-\alpha)^n E\{X\} + E\{n(k-n)\} \qquad (2\text{-}23)$$

Since X is a constant, $E\{X\} = X$. $n(k)$ is zero mean, therefore $E\{n(k-n)\} = 0$ and (2-23) becomes

$$E\{x_s(k)\} = \alpha \sum_{n=0}^{\infty} (1-\alpha)^n X \quad . \qquad (2\text{-}24)$$

Using the identity, for $|a| < 1$,

$$\sum_{n=0}^{\infty} a^n = \frac{1}{1-a} \quad , \qquad (2\text{-}25)$$

$$E\{x_s(k)\} = \frac{\alpha}{1-(1-\alpha)} X = X \quad . \qquad (2\text{-}26)$$

Thus the alpha tracker is capable of tracking a constant level of position, corrupted by zero mean Gaussian noise, with no bias or offset.

The variance of the output estimate $x_s(k)$ is given by

$$var\{x_s(k)\} = E\{[\alpha \sum_{n=0}^{\infty} (1-\alpha)^n [X+n(k-n)] - E\{x_s(k)\}]^2\} \; . \qquad (2\text{-}27)$$

From (2-26) $E\{x_s(k)\} = X$

so that

$$var\{x_s(k)\} = E\{[\alpha \sum_{n=0}^{\infty} (1-\alpha)^n (X+n(k-n) - X)]^2\} \qquad (2\text{-}28)$$

$$var\{x_s(k)\} = E\{[\alpha \sum_{n=0}^{\infty} (1-\alpha)^n n(k-n)]^2\} \qquad (2\text{-}29)$$

$$var\{x_s(k)\} = \alpha^2 E\{[\sum_{n=0}^{\infty} (1-\alpha)^n n(k-n)][\sum_{j=0}^{\infty} (1-\alpha)^j n(k-j)]\} \qquad (2\text{-}30)$$

$$\text{var}\{x_s(k)\} = \alpha^2 \sum_{n=0}^{\infty} \sum_{j=0}^{\infty} (1-\alpha)^n (1-\alpha)^j E\{n(k-n)\, n(k-j)\} \quad (2\text{-}31)$$

The noise n(k) is uncorrelated from sample to sample such that

$$E\{n(k-n)\, n(k-j)\} = 0 \text{ if } i \neq j$$

$$E\{n(k-n)\, n(k-j)\} = \sigma_n^2 \text{ if } i = j \quad .$$

Therefore (2-31) is reduced to only one summation.

$$\text{var}\{x_s(k)\} = \alpha^2 \sum_{n=0}^{\infty} (1-\alpha)^{2n} \sigma_n^2 \quad . \quad (2\text{-}32)$$

Using the identity $\sum_{n=0}^{\infty} a^k = \frac{1}{1-a}$ again,

$$\text{var}\{x_s(k)\} = \frac{\alpha^2}{1-(1-\alpha)^2} \quad (2\text{-}33)$$

$$\text{var}\{x_s(k)\} = \frac{\alpha}{2-\alpha} \sigma_n^2 \quad . \quad (2\text{-}34)$$

It is evident that as α decreases the noise response of the system, and thus the variance in the output estimate, decreases.

Analysis of the Alpha Filter in the Z-domain

By taking the z-transform [7] of equation (2-1) the alpha-tracker may be examined in the z-domain,

$$x_s(z) = (1-\alpha)z^{-1} x_s(z) + \alpha x_m(z) \quad . \quad (2\text{-}35)$$

Rearranging terms yields the z-transform of the alpha-tracker [6].

$$H(z) = \frac{x_s(z)}{x_m(z)} = \frac{\alpha}{1-(1-\alpha)z^{-1}} \quad . \tag{2-36}$$

The alpha-tracker is seen to have a pole located at

$$z = 1-\alpha \quad . \tag{2-37}$$

Since a tracking system with stable dynamics is required, α must be selected such that the system pole lies within the unit circle. The locus of possible pole locations within the unit circle is shown in Figure 2.2. By examining Figure 2.2 it is evident that α must fall within the range of $0 < \alpha < 1$ for stable operation. Selecting α too close to 1 causes the weighting sequence of the alpha-tracker to rapidly approach zero. Such a selection yields a system with fast response to transients. Selecting α close to 0 results in a sluggish system response (more smoothing) and a decreased response to noise. The zero of the alpha-tracker is located at

$$z = 0 \tag{2-38}$$

and thus weights the entire frequency response of the system equally.

The alpha-tracker, though simple to implement, is limited in its ability to track a moving target. The limited tracking ability of the alpha-tracker becomes evident when $x_s(k)$ is examined as a function of $x_m(k)$ for different target trajectories.

The case of constant position, zero velocity will first be examined. This case might be analogous to the azimuth or elevation tracking of an aircraft moving radially with respect to the radar.

$$x_m(k) = X \tag{2-39}$$

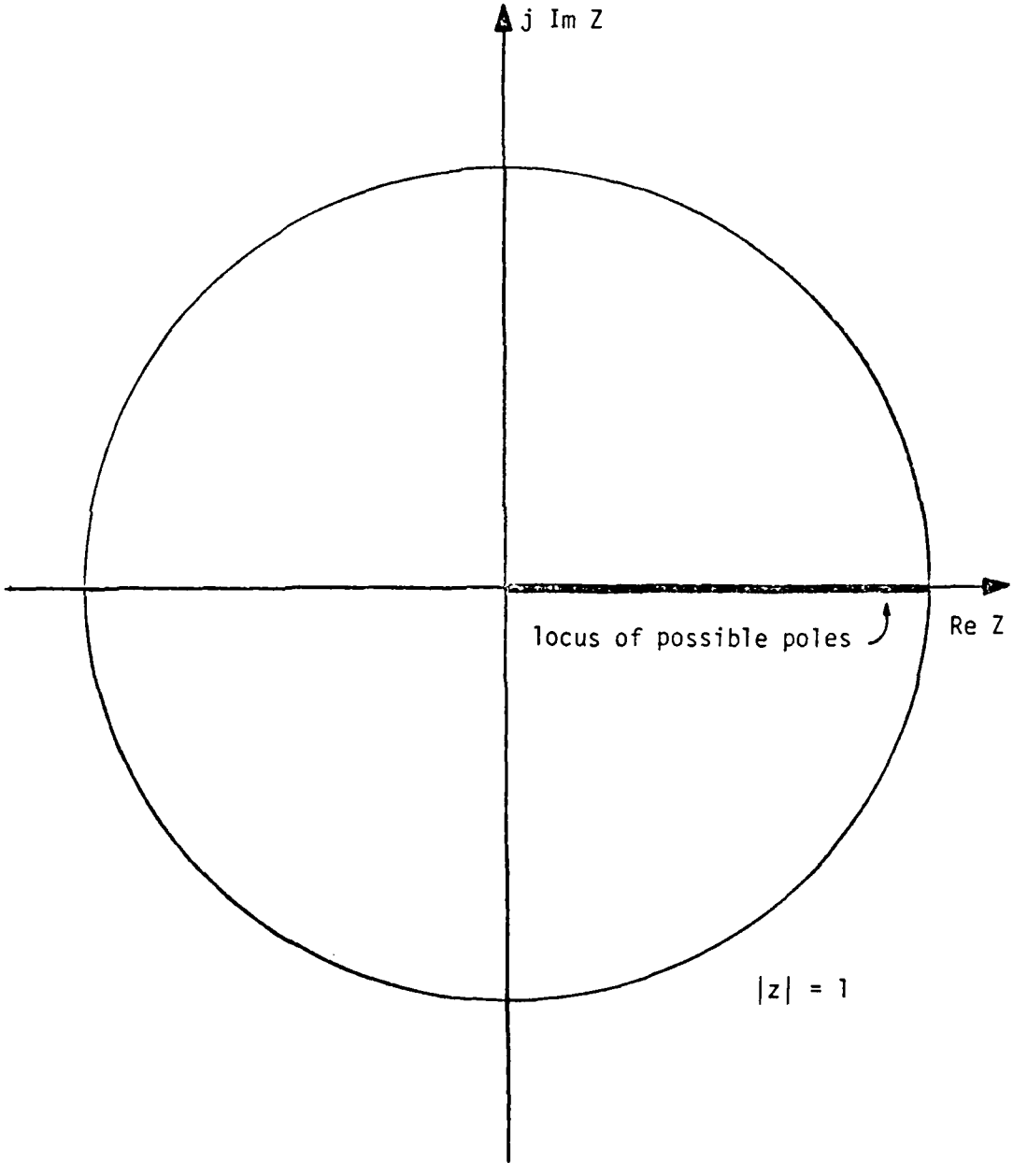

Figure 2.2. Locus of Possible Pole Locations for Stable Operation of Alpha Tracking Filter.

Applying the z transform,

$$x_m(z) = \frac{Xz}{z-1} \tag{2-40}$$

$$H(z) = \frac{\alpha z}{z-(1-\alpha)} \quad . \tag{2-41}$$

Therefore

$$x_s(z) = \frac{Xz}{z-1} \cdot \frac{\alpha z}{z-(1-\alpha)} = \frac{\alpha X z}{(z-1)(z-(1-\alpha))} \quad . \tag{2-42}$$

By utilizing the partial function expansion method,

$$x_s(z) = \frac{Xz}{z-1} - \frac{(1-\alpha)Xz}{z-(1-\alpha)} \quad . \tag{2-43}$$

Finally,

$$x_s(k) = X - (1-\alpha)(1-\alpha)^k X \tag{2-44}$$

$$x_s(k) = X - (1-\alpha)^{k+1} X \quad , \tag{2-45}$$

where

X = actual signal

$X(1-\alpha)^{k+1}$ = bias or amount of lag .

As k increases, the bias rapidly approaches zero and the output equals the constant position input X.

The alpha-tracker does not perform as well when a constant velocity input is applied to the system. This can be verified by making $X_m(k)$ a sampled ramp function.

$$x_m(k) = Vk \tag{2-46}$$

$$x_m(z) = \frac{Vz}{(z-1)^2} \tag{2-47}$$

Therefore,

$$x_s(z) = \frac{\alpha Vz^2}{(z-1)^2(z-(1-\alpha))} \tag{2-48}$$

After applying the partial fraction expansion,

$$x_s(k) = Vk - \frac{V(1-\alpha)}{\alpha}\ [1-(1-\alpha)^k] \tag{2-49}$$

where,

Vk = actual signal

$\frac{V(1-\alpha)}{\alpha}\ [1-(1-\alpha)^k]$ = bias .

Unlike before, as k increases, the bias does not approach zero such that

$$x_s(k) = Vk - \frac{V(1-\alpha)}{\alpha} \quad . \tag{2-50}$$

From (2-49) the inability of the alpha-tracker to track, with zero bias, any signal other than a constant amplitude signal with random noise variations is established.

The Alpha-Beta Tracking Filter

Derivation of the Alpha-Beta Filter

The inability of the alpha-tracker to track without bias a target whose position is changing with respect to time suggests that a more generalized model for target trajectory should be investigated. The new model should account for the target's change in position via a constant velocity term such that the new model for target trajectory is

$$x(k) = x(k-1) + vT \quad . \tag{2-51}$$

where

$x(k)$ = actual position at time kT

$x(k-1)$ = actual position at time $(k-1)T$

v = velocity (constant)

T = time between samples .

To track a target following a trajectory as prescribed in (2-51), both smoothed estimates of position and velocity are required. From [3] one method to obtain smoothed estimates of position and velocity is to define a tracking system such that

$$x_s(k) = gx(0)x_m(k) + gx(1)x_m(k-1) + \ldots \tag{2-52}$$

and

$$\dot{x}_s(k) = g\dot{x}(0)x_m(k) + g\dot{x}(1)x_m(k-1) + \ldots \tag{2-53}$$

where

$x_m(k)$ = noise corrupted position measurement at time nT
$(x_m(k) = x(k) + n)$

$x_s(k)$ = smoothed estimate of position at time kT

$\dot{x}_s(k)$ = smoothed estimate of velocity at time kT

$gx(k)$ = the input position to output position weighting sequence or unit-impulse response

$g\dot{x}(k)$ = the input position to output velocity weighting sequence or unit-impulse response

Smoothed estimates of position and velocity may also be obtained by defining a set of recursive equations of the form

$$x_s(k) = \gamma_1 x_s(k-1) + \gamma_2 x_s(k-2) + \ldots + \gamma_N x_s(k-N) + \delta_0 x_m(k) + \delta_1 x_m(k-1) + \ldots + \delta_m x_m(k-m) \quad (2\text{-}54)$$

$$\dot{x}_s(k) = \eta_1 \dot{x}_s(k-1) + \eta_2 \dot{x}_s(k-2) + \ldots + \eta_N \dot{x}_s(k-N) + \lambda_0 x_m(k) + \lambda_1 x_m(k-1) + \ldots + \lambda_m x_m(k-m) \quad . \quad (2\text{-}55)$$

Equations (2-54) and (2-55) are termed Nth order (since γ_k and $\eta_k = 0$ for $k \geq N+1$) and at least N storage locations in a computer are required to compute these estimates. Equations (2-54) and (2-55) may be combined to form a set of second order difference equations known as the alpha-beta tracking filter [8].

$$x_s(k) = x_p(k) + \alpha(x_m(k) - x_p(k)) \quad (2\text{-}56)$$

$$\dot{x}_s(k) = \dot{x}_s(k-1) + \beta/T\,(x_m(k) - x_p(k)) \quad (2\text{-}57)$$

$$x_p(k+1) = x_s(k) + T\,\dot{x}_s(k) \quad (2\text{-}58)$$

$$\dot{x}_p(k+1) = \dot{x}_s(k) \quad (2\text{-}59)$$

where

$x_m(k)$ = noise corrupted position measurement at time kT

$x_s(k)$ = smoothed estimate of position at time kT

$\dot{x}_s(k)$ = smoothed estimate of velocity at time kT

$x_p(k+1)$ = one step ahead prediction of position at time (k+1)T

$\dot{x}_p(k+1)$ = one step ahead prediction of velocity at time $(k+1)T$

α = position smoothing constant

β = velocity smoothing constant

T = time between samples .

Successive corrections are made to the smoothed values of position and velocity proportional to the differences between the measured position $x_m(k)$ and the previous predicted estimate of position $x_p(k)$. As time progresses from the interval $(k-1)T < t \leq kT$ to the next interval, $kT < t \leq (k+1)T$, $x_s(k)$ is increased by the amount $\alpha[x_m(k) - x_p(k)]$, and the velocity $\dot{x}_s(k)$ is increased by the amount $\beta[x_m(k) - x_p(k)]$. Examining (2-56) through (2-59) it is apparent that the value of α and β determine the degree of smoothing between measured and predicted values of position to yield the smoothed estimate of position. If α and β approach unity, then the measured values of position are weighted more heavily than the predicted values of position. Such a system is characterized by wide bandwidth resulting in very little smoothing of the incoming positional data. Conversely, if α and β approach zero then the predicted values of position are weighted more heavily than the measured values effectively narrowing the bandwidth of the system and resulting in increased data smoothing. The predictor equations are based upon the assumption that the target aircraft will maintain a constant velocity trajectory throughout the tracking procedure.

Analysis of the Alpha-Beta Filter in the Z-Domain

The predictor equation (2-58) can be modeled as a sampled data feedback system in which the error defined by $e_x(t) = x_{in}(t) - x_p(t)$, is converted to a train of impulses,

$$e_x^*(t) \equiv \sum_k e_x(kT)\,\delta(t-kT) \quad . \tag{2-60}$$

This train is applied to a single and double integrator combination whose impulse response is the sum of a step function of height α and a ramp of slope β/T. The block diagram is shown in Figure 2.3.

The transfer function of the single and double integrator combination may be expressed via its Laplace transform as

$$G_p(s) = \frac{\alpha}{s} + \frac{\beta}{Ts^2} \quad , \tag{2-61}$$

The transformation of the continuous error $e_x(t)$ into the impulse train $e_x^*(t)$ is indicated by the sampling switch.

In the z-domain, the transfer function of the predictor can be expressed as

$$G_p(z) = \sum_{k=0}^{\infty} [(\alpha+\beta k)z^{-k}] - \alpha \quad , \tag{2-62}$$

which sums to the following closed form [9],

$$G_p(z) = \frac{(\alpha+\beta)z^{-1} - \alpha z^{-2}}{(1-z^{-1})^2} \quad . \tag{2-63}$$

By manipulation of (2-63), the predictor transfer function can be found to be

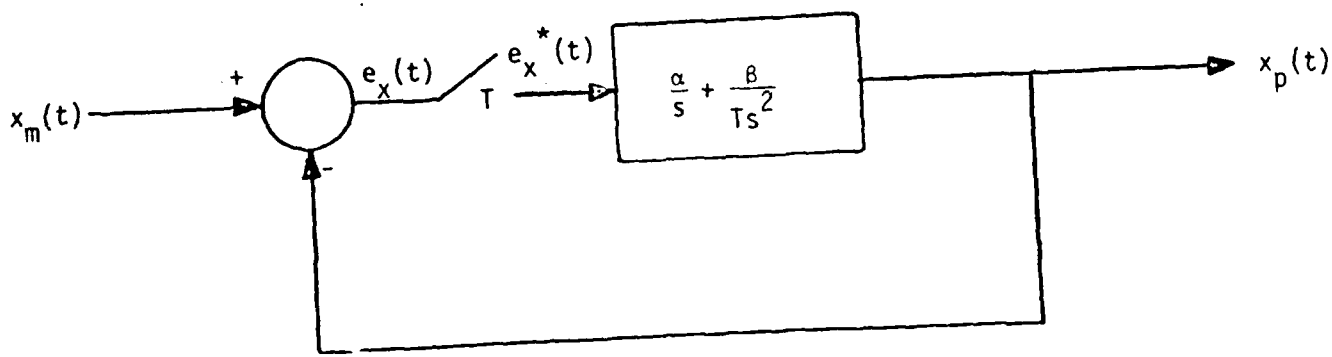

Figure 2.3. Sampled Data Feedback System Depicting the Predictor Equation of the Alpha-Beta Tracking Filter.

$$H_3(z) = \frac{x_p(z)}{x_m(z)} = \frac{(\alpha+\beta)z - \alpha}{z^2 + (\beta+\alpha-2)z + (1-\alpha)} \quad . \tag{2-64}$$

In a similar manner, the transfer functions for smoothed position and smoothed velocity may be found to be

$$H_2(z) = \frac{\dot{x}_s(z)}{x_m(z)} = \frac{\beta}{T} \frac{z(z-1)}{z^2 + (\beta+\alpha-2)z + (1-\alpha)} \tag{2-65}$$

$$H_1(z) = \frac{x_s(z)}{x_m(z)} = \frac{z[\alpha z + \beta - \alpha]}{z^2 + (\beta+\alpha-2)z + (1-\alpha)} \quad . \tag{2-66}$$

Note that the three transfer functions have the same characteristic equation and the poles of the transfer functions can be found solving for the roots of,

$$z^2 + (\beta+\alpha-2)z + (1-\alpha) = 0 \quad . \tag{2-67}$$

By applying the quadratic formula, the roots of the characteristic equation are seen to occur at

$$z = \frac{2-\alpha-\beta}{2} \pm \frac{1}{2} (\beta^2 + \alpha^2 + 2\alpha\beta - 4\beta)^{1/2} \quad . \tag{2-68}$$

Stability of the Alpha-Beta Filter

Since a stable tracking system is desired, the values for α and β must be selected such that the system poles lie within the unit circle of the z-plane. One method of determining the values of α and β for stability is to apply the Jury stability test [10]. The Jury stability test is a stability criterion for sampled data systems that is similar to the Routh-Hurwitz criterion [11]. Applying the Jury criterion to (2-67), the Jury array obtained is

$$\begin{array}{ccc} z^0 & z^1 & z^2 \\ \hline (1-\alpha) & (\alpha+\beta-2) & 1 \end{array} \quad . \tag{2-69}$$

The necessary and sufficient conditions for the second order characteristic equation (2-67) to have no roots on or outside the unit circle are as follows:

$$\begin{aligned} &\text{Condition 1:} \quad F(1) > 0 \\ &\text{Condition 2:} \quad (-1)^2 F(-1) > 0 \\ &\text{Condition 3:} \quad |a_0| < a_2 \quad . \end{aligned} \tag{2-70}$$

Condition 1: $z^2 + (\alpha+\beta-2)z + (1-\alpha)\Big|_{z=1} > 0$

$$(1)^2 + (\alpha+\beta-2)(1) + (1-\alpha) > 0$$

$$\beta > 0 \quad .$$

Condition 2: $(-1)^2 [z^2 + (\alpha+\beta-2)z + (1-\alpha)]\Big|_{z=-1} > 0$

$$1 + 2-\alpha+\beta + 1-\alpha > 0$$

$$2\alpha+\beta < 4 \quad .$$

Condition 3: $|a_0| < a_2$

where,

$$a_0 = 1-\alpha$$

$$a_2 = 1$$

$$|1-\alpha| < 1$$

therefore

$$\alpha > 0.$$

An additional stable condition exists when $\beta = 0$, since in that case the zero of the denominators of equations (2-64) through (2-66) at $z = 1$ is cancelled by one of the zeroes of the numerators. The resulting requirements for stability are

$$\alpha > 0$$

$$\beta \geq 0$$

$$2\alpha + \beta > 4 \quad . \tag{2-71}$$

Alpha-Beta Filter Noise Response

Some insight into the noise smoothing performance of the alpha-beta filter may be obtained by examining the mean and variance of the smoothed position estimate $x_s(k)$. Utilizing the partial fraction expansion method to inverse transform equation (2-66), the impulse response for the smoothed position output of the alpha-beta filter is,

$$h_1(k) = \left[\frac{\alpha}{2} + \frac{-\alpha^2-\alpha\beta+2\beta}{2(\beta^2+\alpha+2\alpha\beta-4\beta)^{1/2}}\right]\left[\frac{2-\alpha-\beta}{2} + \frac{1}{2}\,(\beta^2+\alpha^2+\alpha\beta-4\beta)^{1/2}\right]^k$$

$$+ \left[\frac{\alpha}{2} - \frac{-\alpha^2-\alpha\beta+2\beta}{2(\beta^2+\alpha^2+2\alpha\beta-4\beta)^{1/2}}\right]\left[\frac{2-\alpha-\beta}{2} - \frac{1}{2}\,(\beta^2+\alpha^2+2\alpha\beta-4\beta)^{1/2}\right]^k \quad . \tag{2-72}$$

Assuming a constant velocity target, the input to the filter is given by:

$$x_m(k) = X + vkT + n(k) \tag{2-73}$$

where,

X = actual position of target aircraft

v = actual velocity of target aircraft

$n(k)$ = additive zero mean Gaussian noise with variance = σ_n^2

T = sampling interval ,

The smoothed position estimate $x_s(k)$ is given by the convolution of the impulse response $h_1(k)$ and the input $x_m(k)$.

$$x_s(k) = \sum_{n=0}^{\infty} h_1(n)\, x_m(k-n) \tag{2-74}$$

From (2-72) the impulse response may be expressed as

$$h_1(k) = C_1[B_1]^k + C_2[B_2]^k \tag{2-75}$$

where,

$$C_1 = \frac{\alpha}{2} + \frac{-\alpha^2-\alpha\beta+2\beta}{2\,(\beta^2+\alpha^2+2\alpha\beta-4\beta)^{1/2}}$$

$$C_2 = \frac{\alpha}{2} - \frac{-\alpha^2-\alpha\beta+2\beta}{2\,(\beta^2+\alpha^2+2\alpha\beta-4\beta)^{1/2}}$$

$$B_1 = \frac{2-\alpha-\beta}{2} + \frac{1}{2}\,(\beta^2+\alpha^2+2\alpha\beta-4\beta)^{1/2}$$

$$B_2 = \frac{2-\alpha-\beta}{2} - \frac{1}{2}\,(\beta^2+\alpha^2+2\alpha\beta-4\beta)^{1/2}$$

Substituting (2-75) and (2-73) for $h_1(k)$ and $x_m(k)$ respectively, the smoothed position estimate is given by

$$x_s(k) = \sum_{n=0}^{\infty} [C_1(B_1)^n + C_2(B_2)^n][X + vkT + n(k-n)] \quad . \tag{2-76}$$

The mean of $x_s(k)$ may be found by taking the expected value of (2-76)

$$E\{x_s(k)\} = E\{\sum_{n=0}^{\infty} [C_1(B_1)^n + C_2(B_2)^n][X + vkT + n(k-n)]\} \tag{2-77}$$

$$E\{x_s(k)\} = \sum_{n=0}^{\infty} [C_1(B_1)^n + C_2(B_2)^n]\, E\{[X + vkT + n(k-n)]\} \tag{2-78}$$

$$E\{x_s(k)\} = \sum_{n=0}^{\infty} [C_1(B_1)^n + C_2(B_2)^n][E\{X\} + E\{vkT\} + E\{n(k-n)\}] \tag{2-79}$$

Since X and v are deterministic, and n(k) is zero mean,

$$E\{X\} = X$$

$$E\{vkT\} = vkT$$

$$E\{n(k-n)\} = 0 \quad .$$

such that (2-79) becomes

$$E\{x_s(k)\} = \sum_{n=0}^{\infty} [C_1(B_1)^n + C_2(B_2)^n][X + vkT] \quad . \tag{2-80}$$

$$E\{x_s(k)\} = [X + vkT] \sum_{n=0}^{\infty} [C_1(B_1)^n + C_2(B_2)^n] \quad . \tag{2-81}$$

Using the identity $\sum_{n=0}^{\infty} a^k = \frac{1}{1-a}$,

$$E\{x_s(k)\} = [X + vkT] \left[\frac{C_1}{1-B_1} + \frac{C_2}{1-B_2}\right] \tag{2-82}$$

After extensive algebraic manipulation, it can be shown that the mean of the smoothed position estimates is

$$E\{x_s(k)\} = X + vkT \quad . \tag{2-83}$$

The result shown in (2-83) implies that, given a constant velocity target trajectory, the smoothed position estimate $x_s(k)$ is unbiased.

In a similar manner, the variance of the smoothed position estimate may be calculated.

$$\text{var}\{x_s(k)\} = E\{[[\sum_{n=0}^{\infty} C_1(B_1)^n + C_2(B_2)^n][X + vkT + n(k-n) - E\{x_s(k)\}]]^2\} \quad . \tag{2-84}$$

From (2-83)

$$E\{x_s(k)\} = X + vkT \quad ,$$

so that (2-84) becomes

$$\text{var}\{x_s(k)\} = E\{[\sum_{n=0}^{\infty} (C_1(B_1)^n + C_2(B_2)^n)n(k-n)]^2\} \tag{2-85}$$

$$\text{var}\{x_s(k)\} = E\{[C_1 \sum_{n=0}^{\infty} (B_1)^n n(k-n) + C_2 \sum_{n=0}^{\infty} (B_2)^n n(k-n)] \cdot [C_1 \sum_{j=0}^{\infty} (B_1)^j n(k-j) + C_2 \sum_{j=0}^{\infty} (B_2)^j n(k-j)]\} \tag{2-86}$$

$$\text{var}\{x_s(k)\} = \sum_{n=0}^{\infty} \sum_{j=0}^{\infty} [C_1(B_1)^n + C_2(B_2)^n][C_1(B_1)^j + C_2(B_2)^j] E\{n(k-n)n(k-j)\} \quad . \tag{2-87}$$

The noise is uncorrelated from sample to sample, therefore

$$E\{n(k-n)\ n(k-j)\} = 0 \quad \text{if } i \neq j$$

$$E\{n(k-n)\ n(k-j)\} = \sigma_n^2 \quad \text{if } i=j \quad .$$

Now (2-87) is reduced to a single sum

$$\text{var}\{x_s(k)\} = \sum_{n=0}^{\infty} [C_1(B_1)^n + C_2(B_2)^n]^2 \sigma_n^2 \tag{2-88}$$

$$\text{var}\{x_s(k)\} = \sum_{n=0}^{\infty} [C_1^2(B_1)^{2n} + 2C_1C_2(B_1)^n(B_2)^n + C_2^2(B_2)^{2n}]\ \sigma_n^2 \quad . \tag{2-89}$$

Since $(B_1)^n(B_2)^n = (B_1B_2)^n$ and $\sum_{n=0}^{\infty} a^k = \frac{1}{1-a}$, (2-89) becomes

$$\text{var}\{x_s(k)\} = \left[\frac{C_1^2}{1-B_1^2} + \frac{2C_1C_2}{1-(B_1B_2)} + \frac{C_2^2}{1-B_2^2}\right]\ \sigma_n^2 \quad . \tag{2-90}$$

With considerable algebraic manipulation, it can be shown [3] that variance of the smoothed position estimate is

$$\text{var}\{x_s(k)\} = \left[\frac{2\alpha^2 + \beta(2-3\alpha)}{\alpha\ (4-\beta-2\alpha)}\right]\ \sigma_n^2 \quad . \tag{2-91}$$

If the variance in the smoothed position is expressed as

$$\text{var}\{x_s(k)\} = K_x(0)\sigma_n^2 \tag{2-92}$$

then $K_x(0)$ is known as the variance reduction ratio [9]. If $K_x(0)$ is less than one then the tracking system has reduced the effect of noise on the output signal. If $K_x(0)$ is greater than one, the system has accentuated the noise. The variance reduction ratio is superior for values of α and β approaching zero.

Performance Measures for the Alpha-Beta Filter

Benedict and Border [3] introduced two performance measures in order to assess properly the attributes of noise reduction and transient performance and derive an optimal relation between α and β.

For noise smoothing, the performance measures are the aforementioned variance reduction ratio in position output defined by:

$$K_x(0) = \frac{\text{steady-state variance in position output}}{\text{variance in raw position input}} , \tag{2-93}$$

and the variance reduction ratio in velocity output defined by:

$$K_{\dot{x}}(0) = \frac{\text{steady-state variance in velocity output}}{\text{variance in raw position input}} . \tag{2-94}$$

For transient performance the performance measures are

$$D_x^2 = \sum_{n=0}^{\infty} [(\text{unit-increment ramp}) - (\text{position ramp response})]^2 \tag{2-95}$$

and

$$D_{\dot{x}}^2 = \sum_{n=0}^{\infty} [(\text{velocity of unit-increment ramp}) - (\text{velocity ramp response})]^2 . \tag{2-96}$$

If the impulse responses of both the smoothed position output (previously derived in this paper) and the smoothed velocity output are obtained, then the performance measures for the alpha-beta tracker is found to be [3],

$$K_x(0) = \frac{2\alpha^2 + \beta(2-3\alpha)}{\alpha[4-\beta-2\alpha]} \tag{2-97}$$

$$K_{\dot{x}}(0) = \frac{1}{T^2} \frac{2\beta^2}{\alpha[4-2\alpha-\beta]} \tag{2-98}$$

$$D_x^2 = \frac{(2-\alpha)(1-\alpha)^2}{\alpha\beta[4-\beta-2\alpha]} \tag{2-99}$$

$$D_x^2 = \frac{1}{T^2} \frac{\alpha^2(2-\alpha) + 2\beta(1-\alpha)}{\alpha\beta[4-\beta-2\alpha]} . \tag{2-100}$$

Based upon these performance measures, Benedict and Bordner [3] utilized the calculus of variations to optimally select the values of α and β so as to minimize respectively D_x^2 and $D_{\dot{x}}^2$ for a given $K_x(0)$ and $K_{\dot{x}}(0)$, and vice versa. The relationship between α and β which results in the optimal tracker is given by

$$\beta = \frac{\alpha^2}{2-\alpha} \quad . \tag{2-101}$$

The recursive nature of the alpha-beta filter equations allows them to be incorporated easily into a computer algorithm which performs the filtering process. A flowchart for implementing the alpha-beta filter on a computer is given in Figure 2.4.

The Alpha-Beta-Gamma Tracking Filter

Derivation of the Alpha-Beta-Gamma Tracking Filter

The alpha-beta tracking filter previously discussed is best suited for a target under track which has constant velocity. For the case of an aircraft experiencing a great deal of maneuvering, changes in velocity between sample intervals are often significant. As a result, the ability of the alpha-beta filter to track an accelerating target is severely hindered. The degradation in performance which occurs when an alpha-beta filter tracks an accelerating target, suggests that a tracking filter which includes an acceleration estimate might be appropriate for a maneuvering aircraft. The model for the accelerating target trajectory is therefore chosen as

$$x(k) = x(k-1) + vT + \frac{aT^2}{2} \quad , \tag{2-102}$$

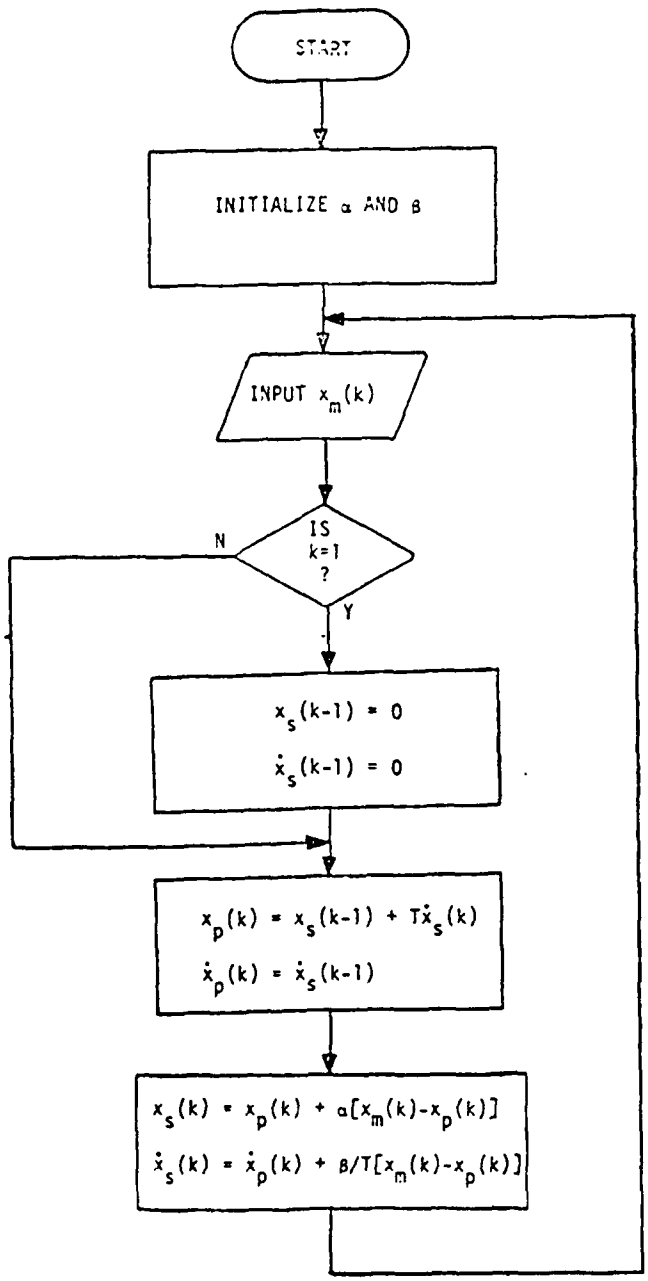

Figure 2.4. Flowchart of the Alpha-Beta Tracking Filter.

where,

$x(k)$ = actual target position at time kT

$x(k-1)$ = actual target position at time (k-1)T

v = velocity of target

a = acceleration of target (constant)

T = time between samples .

In order to accurately track a target following a trajectory such as prescribed in (2-102), smoothed estimates of position, velocity and acceleration must be available. Simpson [4] defines a system of weighting sequences in order to obtain the smoothed estimates of position, velocity, and acceleration. These are:

$$x_s(k) = \sum_{n=0}^{\infty} g_x(n)\, x_m(k-n) \tag{2-103}$$

$$\dot{x}_s(k) = \sum_{n=0}^{\infty} g_{\dot{x}}(n)\, x_m(k-n) \tag{2-104}$$

$$\ddot{x}_s(k) = \sum_{n=0}^{\infty} g_{\ddot{x}}(n)\, x_m(k-n) \quad , \tag{2-105}$$

where

$x_m(k)$ = noise corrupted position measurement at time kT

($x_m(k) = x(k) + n$).

$x_s(k)$ = smoothed estimate of position at time kT

$\dot{x}_s(k)$ = smoothed estimate of velocity at time kT

$\ddot{x}_s(k)$ = smoothed estimate of acceleration at time kT

$g_x(n)$ = the input position to output position weighting sequence, or unit-impulse response of the system

$g_{\dot{x}}(n)$ = the input position to output velocity weighting sequence, or unit-impulse response of the system

$g_{\ddot{x}}(n)$ = the input position to output acceleration weighting sequence, or unit-impulse response of the system .

Alternately, a corresponding sampled data system can be characterized by a set of recursive equations such as

$$x_s(k) = \rho_1 x_s(k-1) + \rho_2 x_s(k-2) + \ldots \rho_N x_s(k-N) + \delta_0 x_m(k) + \delta_1 x_m(k-1) + \ldots + \delta_m x_m(k-m) \quad (2\text{-}106)$$

$$\dot{x}_s(k) = \eta_1 \dot{x}_s(k-1) + \eta_2 \dot{x}_s(k-2) + \ldots + \eta_N \dot{x}_s(k-N) + \lambda_0 x_m(k) + \lambda_1 x_m(k-1) + \ldots + \lambda_m x_m(k-m) \quad (2\text{-}107)$$

$$\ddot{x}_s(k) = \Pi_1 \ddot{x}_s(k-1) + \Pi_2 \ddot{x}_s(k-2) + \ldots + \Pi_N \ddot{x}_s(k-N) + \varepsilon_0 x_m(k) + \varepsilon_1 x_m(k-1) + \ldots \varepsilon_m x_m(k-m) \quad . \quad (2\text{-}108)$$

When such recursive equations terminate (i.e., $\rho_k = \eta_k = \Pi_k = 0$ for $k \geq N+1$), the equations are termed Nth order.

Equations (2-106) through (2-108) may be combined to form a set of third order difference equations which define the alpha-beta-gamma tracking filter [4]. These are given as

$$x_s(k) = x_p(k) + \alpha(x_m(k) - x_p(k)) \quad (2\text{-}109)$$

$$\dot{x}_s(k) = \dot{x}_p(k) + (\beta/T)\,(x_m(k) - x_p(k)) \quad (2\text{-}110)$$

$$\ddot{x}_s(k) = \ddot{x}_s(k-1) + (\gamma/T^2)\,(x_m(k) - x_p(k)) \quad (2\text{-}111)$$

$$x_p(k) = x_s(k-1) + T\,\dot{x}_s(k-1) \quad (2\text{-}112)$$

$$\dot{x}_p(k) = \dot{x}_s(k-1) + T\,\ddot{x}_s(k-1) \quad , \tag{2-113}$$

where

$x_m(k)$ = noise corrupted position measurement at time kT

$x_s(k)$ = smoothed estimate of position at time kT

$\dot{x}_s(k)$ = smoothed estimate of velocity at time kT

$\ddot{x}_s(k)$ = smoothed estimate of acceleration at time kT

$x_p(k)$ = one-step ahead prediction of position at time kT

$\dot{x}_p(k)$ = one-step ahead prediction of velocity at time kT

α = position smoothing constant

β = velocity smoothing constant

γ = acceleration smoothing constant

T = time between samples

The alpha-beta-gamma tracking filter is a third order filter which can track a constant acceleration target with a trajectory as prescribed in (2-102) with zero steady-state error. The similarities between the alpha-beta filter and the alpha-beta-gamma filter are obvious when equations (2-109) through (2-113) are compared to those for the alpha-beta filter. While α and β perform the same function as they did in the alpha-beta filter, the γ term provides the much needed acceleration estimate essential for accurately tracking a maneuvering target. This more generalized tracking filter not only maintains track throughout maneuvers or turbulent conditions, but in addition, provides smoothed estimates of position, velocity, and acceleration with very little increase in computational effort.

The Alpha-Beta-Gamma Filter in the Z-Domain

The properties of the alpha-beta-gamma tracking filter may be more effectively studied in the Z-domain. Taking the Z-transform of equations (2-109) through (2-113) and using the right shifting property results in

$$x_p(z) = z^{-1} x_s(z) + T z^{-1} \dot{x}_s(z) \tag{2-114}$$

$$\dot{x}_p(z) = z^{-1} \dot{x}_s(z) + T z^{-1} \ddot{x}_s(z) \tag{2-115}$$

$$x_s(z) = (1-\alpha) x_p(z) + \alpha x_m(z) \tag{2-116}$$

$$\dot{x}_s(z) = \dot{x}_p(z) + (\beta/T) x_m(z) - (\beta/T) x_p(z) \tag{2-117}$$

$$\ddot{x}_s(z) = z^{-1} \ddot{x}_s(z) + (\gamma/T^2) x_m(z) - (\gamma/T^2) x_p(z) \quad . \tag{2-118}$$

In the alpha-beta-gamma tracker, there is one input to the system, $x_m(k)$, and five output signals $x_p(k)$, $\dot{x}_p(k)$, $x_s(k)$, $\dot{x}_s(k)$, and $\ddot{x}_s(k)$. Therefore, there must exist five separate transfer functions relating $x_m(z)$ to $x_p(z)$, $\dot{x}_p(z)$, $x_s(z)$, $\dot{x}_s(z)$, and $\ddot{x}_s$. These transfer functions may be obtained by dividing each side of equations (2-114) through (2-118) by $x_m(z)$ to yield

$$H_1(z) = \frac{x_p(z)}{x_m(z)} = z^{-1} \frac{x_s(z)}{x_m(z)} + T z^{-1} \frac{\dot{x}_s(z)}{x_m(z)} \tag{2-119}$$

$$H_2(z) = \frac{\dot{x}_p(z)}{x_m(z)} = z^{-1} \frac{\dot{x}_s(z)}{x_m(z)} + T z^{-1} \frac{\ddot{x}_s(z)}{x_m(z)} \tag{2-120}$$

$$H_3(z) = \frac{x_s(z)}{x_m(z)} = \frac{(1-\alpha) x_p(z)}{x_m(z)} + \alpha \frac{x_m(z)}{x_m(z)} \tag{2-121}$$

$$H_4(z) = \frac{\dot{x}_s(z)}{x_m(z)} = \frac{\dot{x}_p(z)}{x_m(z)} + \frac{(\beta/T)\ x_m(z)}{x_m(z)} - \frac{(\beta/T)x_p(z)}{x_m(z)} \qquad (2\text{-}122)$$

$$H_5(z) = \frac{\ddot{x}_s(z)}{x_m(z)} = z^{-1}\ \frac{\ddot{x}_s(z)}{x_m(z)} + \frac{(\gamma/T^2)\ x_m(z)}{x_m(z)} - \frac{(\gamma/T^2)\ x_p(z)}{x_m(z)} \qquad (2\text{-}123)$$

After incorporating the transfer function relationships

$$H_1(z) = \frac{x_p(z)}{x_m(z)}\ ,\ H_2(z) = \frac{\dot{x}_p(z)}{x_m(z)}\ ,\ H_3(z) = \frac{x_s(z)}{x_m(z)}\ ,$$

$$H_4(z) = \frac{\dot{x}_s(z)}{x_m(z)}\ ,\ H_5(z) = \frac{\ddot{x}_s(z)}{x_m(z)}\ ,$$

and rearranging terms, the set of five equations becomes

$$H_1(z) - z^{-1}\ H_3(z) - T\ z^{-1}\ H_4(z) = 0 \qquad (2\text{-}124)$$

$$H_2(z) - z^{-1}\ H_4(z) - T\ z^{-1}\ H_5(z) = 0 \qquad (2\text{-}125)$$

$$(1-\alpha)\ H_1(z) - H_3(z) = -\alpha \qquad (2\text{-}126)$$

$$(\beta/T)\ H_1(z) - H_2(z) + H_4(z) = \beta/T \qquad (2\text{-}127)$$

$$(\gamma/T^2)\ H_1(z) + (1-z^{-1})\ H_5(z) = \gamma/T^2\ . \qquad (2\text{-}128)$$

The transfer functions, $H_i(z)$, now have the rational form $N_i(z)/D(z)$. The general determinant $D(z)$ is given by

$$\begin{vmatrix} 1, & 0, & -z^{-1}, & -Tz^{-1}, & 0 \\ 0, & 1, & 0, & -z^{-1}, & -Tz^{-1} \\ (1-\alpha) & 0, & -1, & 0, & 0 \\ (\beta/T), & -1, & 0, & 1, & 0 \\ (\gamma/T^2), & 0, & 0, & 0, & (1-z^{-1}) \end{vmatrix} \quad . \tag{2-129}$$

which upon evaluation yields [12]

$$D(z) = (-z)^{-3}\,[z^3+(\alpha+\beta-3)z^2 + (3+\gamma-2\alpha-\beta)z + (\alpha-1)] \; . \tag{2-130}$$

By using the theory of determinants [12] and performing considerable algebra, the transfer functions for the smoothed output variables are [12],

$$H_3(z) = \frac{x_s(z)}{x_m(z)} = \frac{\alpha z^3 + (\beta-2\alpha)z^2 + (\alpha+\beta-\gamma)z}{z^3 + (\alpha+\beta-3)z^2 + (3+\gamma-2\alpha-\beta)z + (\alpha-1)} \tag{2-131}$$

$$H_4(z) = \frac{\dot{x}_s(z)}{x_m(z)} = \frac{1}{T} \quad \frac{\beta z^3 + (\gamma-2\beta)z^2 + (\beta-\gamma)}{z^3 + (\alpha+\beta-3)z^2 + (3+\gamma-2\alpha-\beta)z + (\alpha-1)} \tag{2-132}$$

$$H_5(z) = \frac{\ddot{x}_s(z)}{x_m(z)} = \frac{\gamma}{T^2} \quad \frac{z^3 - 2z^2 + z}{z^3 + (\alpha+\beta-3)z^2 + (3+\gamma-2\alpha-\beta)z + (\alpha-1)} \; . \tag{2-133}$$

These transfer functions have the same denominator polynomial and therefore have the same set of poles. Observing the transfer function solutions for the alpha-beta filter outputs $x_s(z)$ (2-56) and $\dot{x}_s(z)$ (2-57), it is interesting to note that the solutions (2-131) through (2-132) do not reduce to those of the simpler alpha-beta filter solutions for $\gamma = 0$. This can also be seen from the original difference equation statements of both systems. The alpha-beta-gamma filter can be reduced to behave as

the alpha-beta filter in practice by letting $\gamma = 0$ and requiring the boundary condition $\dot{x}_s^{\cdot\cdot}(0) = 0$. The point to be made here is that the alpha-beta-gamma filter is not merely a simple extension of the alpha-beta filter.

Stability of the Alpha-Beta-Gamma Filter

A stable tracking system requires that a bounded filter input produces a bounded filter output. In the Z plane, this strictly means that the poles of the characteristic equation lie within the unit circle. There are many tests for stability but the Jury stability criterion [10] will be applied here as it was for the alpha-beta filter. First, the denominator of the transfer function is written as

$$F(z) = (1-\alpha) + (3 -2\alpha-\beta+\gamma)z + (\alpha+\beta-3)z^2 + (1)z^3 \qquad (2\text{-}134)$$

where

$$F(z) = a_0 + a_1 z^1 + a_2 z^2 + a_3 z^3$$

From (2-134) the Jury array obtained is

$$\begin{array}{cccc} z^0 & z^1 & z^2 & z^3 \\ \hline (\alpha-1) & (3-2\alpha-\beta+\gamma) & (\alpha+\beta-3) & (1) \end{array} \qquad (2\text{-}135)$$

The requirement that F(z) has all of its roots within the unit circle is satisfied by the conditions:

Condition 1: $F(1) > 0$

Condition 2: $(-1)^3 F(-1) > 0$

Condition 3: $|a_0| < a_2$

Condition 4: $|b_0| > |b_2|$

where

$$b_k = \begin{vmatrix} a_0 & a_{m-k} \\ a_m & a_k \end{vmatrix}_{m=3} .$$

Condition 1: $z^3 + (\alpha+\beta-3)z^2 + (3+\gamma-2\alpha-\beta)z + (\alpha-1)\Big|_{z=1} > 0$

$$(1)^3 + (\alpha+\beta-3)(1)^2 + (3+\gamma-2\alpha-\beta)(1) + (\alpha-1) > 0$$

$$1 + \alpha + \beta - 3 + 3 + \alpha - 2\alpha - \beta + \alpha - 2 > 0$$

$$\alpha > 0 \quad . \tag{2-136}$$

Condition 2: $z^3 + (\alpha+\beta-3)z^2 + (3+\gamma-2\alpha-\beta)z + (\alpha-1)\Big|_{z=-1} > 0$

$$(-1)^3 + (\alpha+\beta-3)(-1)^2 + (3+\gamma-2\alpha-\beta)(-1) + (\alpha-1) > 0$$

$$-1 + \alpha + \beta - 3 - 3 - \gamma + 2\alpha + \beta + \alpha - 1 > 0$$

$$4\alpha + 2\beta - \gamma - 8 > 0$$

$$4\alpha + 2\beta - \gamma > 8$$

$$\frac{\alpha}{2} + \frac{\beta}{4} - \frac{\gamma}{8} > 1 \quad . \tag{2-137}$$

Condition 3: $|a_0| < a_2$,

where,

$$a_0 = \alpha - 1$$

$$a_2 = 1$$

$$|\alpha - 1| < 1$$

$$0 < \alpha < 2 \tag{2-138}$$

AD-A110 863 GEORGIA INST OF TECH ATLANTA ENGINEERING EXPERIMENT --ETC F/G 17/7
MARINE AIR TRAFFIC CONTROL AND LANDING SYSTEM (MATCALS INVESTIG--ETC(U)
SEP 81 E R GRAF, C L PHILLIPS, S A STARKS N00039-80-C-0032
UNCLASSIFIED GIT/EES-1-A-2550-VOL-2 NL

2 OF 2
AD
A110863

END
DATE FILMED
3 82
DTIC

Condition 4: $|b_0| > |b_2|$,

where,

$$b_0 = \begin{vmatrix} a_0 & a_3 \\ a_3 & a_0 \end{vmatrix} = (\alpha-1)^2 - 1 = \alpha^2 - 2\alpha$$

$$b_2 = \begin{vmatrix} a_0 & a_1 \\ a_3 & a_2 \end{vmatrix} = (\alpha-1)(\alpha+\beta-3) - (3-2\alpha-\beta+\gamma)(1)$$

$$b_2 = \alpha^2 + \alpha\beta - 2\alpha + \gamma \quad ,$$

therefore,

$$|\alpha^2-2\alpha| > |\alpha^2+\alpha\beta-2\alpha+\gamma|$$

$$\alpha\beta > \gamma \quad , \tag{2-139}$$

since $0 < \alpha < 2$,

$$\beta > 0 \quad . \tag{2-140}$$

The relations just presented are necessary and sufficient for the poles of the characteristic equation to lie within the unit circle. These relations are very useful when manipulating α, β, and γ in designing a filter to satisfy a particular set of specifications.

Pole Analysis for the Alpha-Beta-Gamma Tracking Filter

When one of the equations (2-116) through (2-118) are solved to obtain one of the outputs $x_{out}(z)$, the output will be of the rational form [9]

$$x_{out}(z) = \frac{N(z)}{D(z)} = \frac{\prod_{i=1}^{N_1} (z-w_i)}{\prod_{i=1}^{N_2} (z-p_i)^{m_i}}, \qquad (2\text{-}141)$$

where m_i is the multiplicity of the ith pole, w_i is the ith zero of the system and p_i is the ith pole of the system. The partial fraction expansion and inversion will yield the general form [9]

$$\begin{aligned} x_{out}(nT) = A_0(p_i,w_i) &+ \sum_{k=1}^{m_1} g_1k(k, p_i, w_i)(p_1)^k \\ &+ \sum_{k=1}^{m_2} g_2k(k, p_i, w_i)(p_2)^k \\ &+ \vdots \\ &+ \sum_{k=1}^{m_{N_2}} g_N2(k, p_i, w_i)(p_{N_2})^k \quad . \qquad (2\text{-}142) \end{aligned}$$

All the terms, except A_0 decay as the power of a given pole or root of the denominator $(p_i)^k$ where $|p_i| < 1$. The g coefficients may contain powers of k which offset this decay, but the structure of (2-142) provides an approach to alter the response of the filter by choosing the

poles and then obtaining the required α, β, and γ. Thus given the poles of the characteristic equation and defining

$$D_0(z) = z^3 + (\alpha+\beta-3)z^2 + (3+\gamma-2\alpha-\beta)z + (\alpha-1)$$
$$= (z-p_1)(z-p_2)(z-p_3) \quad , \tag{2-143}$$

it can be shown that [12],

$$P \equiv \alpha + \beta - 3 = -(p_1 + p_2 + p_3) \tag{2-144}$$

$$Q \equiv 3 + \gamma - 2\alpha - \beta = p_1p_2 + p_2p_3 + p_1p_3 \tag{2-145}$$

$$R \equiv \alpha - 1 = -p_1p_2p_3 \quad . \tag{2-146}$$

Conversely the poles may be derived by knowing α, β, γ and solving the cubic equation $D_0(z) = 0$. If

$$D_0(z) = z^3 + Pz^2 + Qz + R \quad , \tag{2-147}$$

then from [13],

$$a \equiv \frac{1}{3} \ (3Q - P^2) \tag{2-148}$$

$$b \equiv \frac{1}{27} \ (2P^3 - 9PQ + 27R) \tag{2-149}$$

$$G \equiv \left[\frac{b^2}{4} + \frac{a^3}{27}\right]^{1/2} \tag{2-150}$$

$$A \equiv \left[\frac{-b}{2} + G\right]^{1/3} \tag{2-151}$$

$$B \equiv \left[\frac{-b}{2} - G\right]^{1/3} \tag{2-152}$$

$$E_1 \equiv A + B \tag{2-153}$$

$$E_{2,3} \equiv - \left[\frac{A+B}{2}\right] \pm j\sqrt{3} \left[\frac{A-B}{2}\right] \quad , \tag{2-154}$$

and the poles are,

$$p_1 = E_1 - P/3 \tag{2-155}$$

$$p_{2,3} = E_{2,3} - P/3 \quad . \tag{2-156}$$

Alpha-Beta-Gamma Filter Noise Response

Singer and Behnke [14] have shown that an alpha-beta filter has a noise response which is less than 20% worse than that of a Kalman filter for smoothed estimates of position and velocity. The second order comparison suggests that the alpha-beta-gamma filter will perform in a similar manner when compared with a third order Kalman filter.

Once again the variance reduction ratios $K_x(0)$, $K_{\dot{x}}(0)$, and $K_{\ddot{x}}(0)$ are introduced to evaluate the noise throughput of the tracking system. Simpson [4] defines the noise performance measures as

$$K_x(0) = \sum_{k=0}^{\infty} g_x^2(k) \tag{2-157}$$

$$K_{\dot{x}}(0) = \frac{1}{T^2} \sum_{k=0}^{\infty} g_{\dot{x}}^2(k) \tag{2-158}$$

$$K_{\ddot{x}}(0) = \frac{1}{T^4} \sum_{k=0}^{\infty} g_{\ddot{x}}^2(k) \quad . \tag{2-159}$$

Wilcox [12] provides an algorithmic approach to the calculation of the noise performance of the alpha-beta-gamma filter, assuming a zero mean Gaussian measurement noise with variance = σ_n^2.

For the calculation of $K_x(0)$, let

$$b_0 = \alpha,\ b_1 = \beta-2\alpha,\ b_2 = \alpha+\gamma-\beta,\ b_3 = 0$$

$$a_0 = 1,\ a_1 = \alpha+\beta-3,\ a_2 = 3+\gamma-2\alpha-\beta,\ a_3 = \alpha-1 \quad .$$

For the calculation of $K_{\dot{x}}(0)$, let the a_i's remain the same and

$$b_0 = (\beta/T),\ b_1 = \frac{(\gamma-2\beta)}{T},\ b_2 = \frac{(\beta-\gamma)}{T},\ b_3 = 0 \quad .$$

For the calculation of $K_{\ddot{x}}(0)$, let the a_i's remain the same and

$$b_0 = b_2 = (\gamma/T^2),\ b_1 = (-2\gamma/T^2),\ b_3 = 0 \quad .$$

Now defining

$$K_x(0) = K_1(0),\ K_{\dot{x}}(0) = K_2(0),\ K_{\ddot{x}}(0) = K_3(0),$$

then the noise response for each estimate is calculated by substituting the appropriate values of a_i and b_i into

$$K_i(0) = \frac{a_0B_0Q_0 - a_0B_1Q_1 + a_0B_2Q_2 - B_3Q_3}{a_0[(a_0^2-a_3^2)Q_0 - (a_0a_1-a_2a_3)Q_1 + (a_0a_2-a_1a_3)Q_2} \quad (2\text{-}160),$$

where

$$B_0 = b_o^2 + b_1^2 + b_2^2 + b_3^2$$

$$B_1 = 2(b_0b_1 + b_1b_2 + b_2b_3)$$

$$B_2 = 2(b_0b_2 + b_1b_3)$$

$$B_3 = 2b_0b_3$$

$$E_1 = a_0 + a_2$$

$$E_2 = a_1 + a_3$$

$$Q_0 = a_0E_1 - a_3E_2$$

$$Q_1 = a_0a_1 - a_2a_3$$

$$Q_2 = a_1E_2 - a_2E_1$$

$$Q_3 = (a_1-a_3)(E_2^2-E_1^2) + a_0\,(a_0E_2-a_3E_1) \quad .$$

It can be shown that as α, β, and γ approach zero the poles of the characteristic equation approach one, which results in higher noise suppression since the bandwidth decreases and the effective data smoothing capability of the filter increases.

Performance Measures for the Alpha-Beta-Gamma Filter

Simpson [4] and Neal [15] define two transient performance measures for the transient analysis of the alpha-beta-gamma filter. The first transient performance measure is the unit-increment ramp response used earlier in the analysis of the alpha-beta tracker,

$$D_x^2 = \sum_{n=0}^{\infty} [(\text{unit-increment ramp}) - (\text{position ramp response})]^2 \qquad (2\text{-}161)$$

$$D_{\dot{x}}^2 = \sum_{n=0}^{\infty} [(\text{velocity of unit-increment ramp}) - (\text{velocity ramp response})]^2 \qquad (2\text{-}162)$$

$$D_{\ddot{x}} = \sum_{n=0}^{\infty} [(\text{acceleration of unit ramp response } (=0)) - (\text{acceleration ramp response})]^2 \quad , \tag{2-163}$$

thus,

$$D_x^2 = \sum_{n=0}^{\infty} [n - \sum_{j=0}^{n} g_x(j)(n-j)]^2 \tag{2-164}$$

$$D_{\dot{x}}^2 = \sum_{n=0}^{\infty} [1 - \sum_{j=0}^{n} g_{\dot{x}}(j)(n-j)]^2 \tag{2-165}$$

$$D_{\ddot{x}}^2 = \sum_{n=0}^{\infty} [- \sum_{j=0}^{n} g_{\ddot{x}}(j)(n-j)]^2 \quad . \tag{2-166}$$

Similarly the transient performance measure (A^2) due to a unit step input of acceleration is defined, in the same manner, as the sum of the squares of the errors arising from this input. Therefore,

$$A_x^2 = \sum_{n=0}^{\infty} [\frac{n^2}{2} - \frac{1}{2} \sum_{j=0}^{\infty} g_x(j)(n-j)^2]^2 \tag{2-167}$$

$$A_{\dot{x}}^2 = \frac{1}{T^2} \sum_{n=0}^{\infty} [n - \frac{1}{2} \sum_{n=0}^{\infty} g_{\dot{x}}(j)(n-j)^2]^2 \tag{2-168}$$

$$A_{\ddot{x}}^2 = \frac{1}{T^2} \sum_{n=0}^{\infty} [1 - \frac{1}{2} \sum_{j=0}^{n} g_{\ddot{x}}(j)(n-j)^2]^2 \quad . \tag{2-169}$$

By numerical evaluation of these performance measures, Simpson [4] derived an optimal relation between α, β, and γ such that for a given noise smoothing, the optimal transient response is achieved, and vice versa.

$$2\beta - \alpha(\alpha + \beta + \frac{1}{2}\gamma) = 0 \tag{2-170}$$

In a later paper, Neal [15] verified Simpson's relation analytically using a new approach [1] to linear estimation theory and also derived an additional relation between α, β, γ.

$$\beta^2 = 2\alpha\gamma \tag{2-171}$$

The preceding relations (2-170) and (2-171) provide a method of optimally choosing two of the parameters of the alpha-beta-gamma tracking filter thus simplifying the task of optimizing the tracker in a given tracking environment.

The recursive nature of the alpha-beta-gamma filter makes it a prime candidate for implementation on a digital computer. A flowchart of the alpha-beta-gamma filter is given in Figure 2.5.

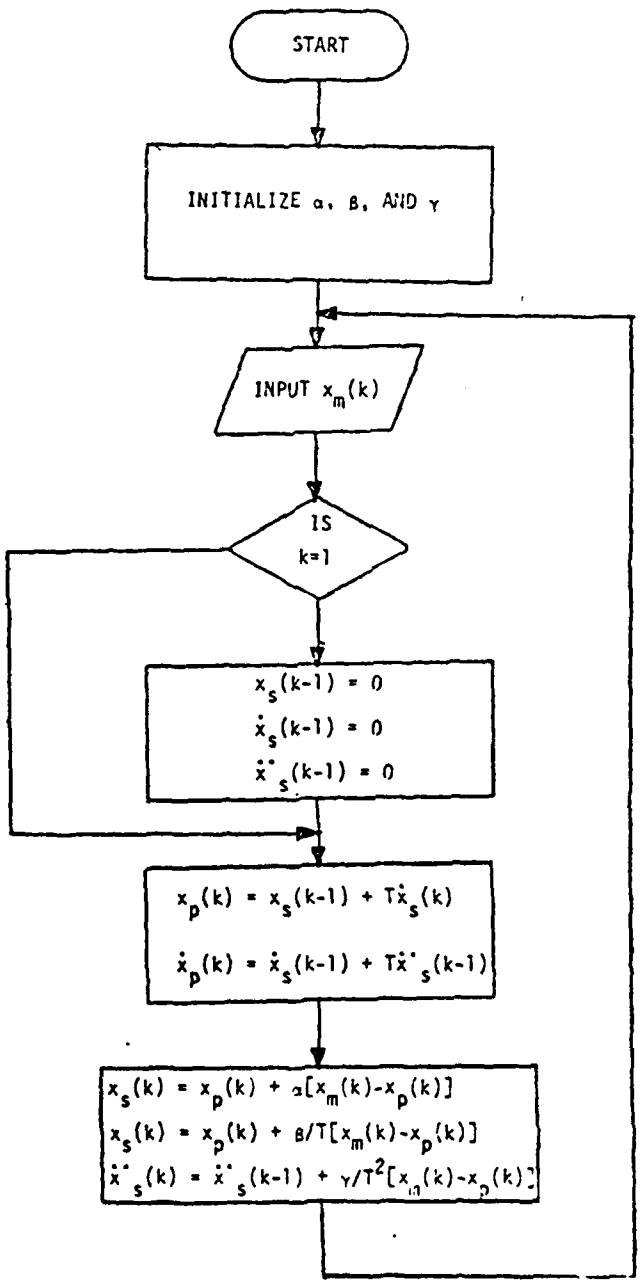

Figure 2.5. Flowchart of the Alpha-Beta-Gamma Tracking Filter.

III. THE TRI-STATE ADAPTIVE FILTER

Introduction

Three different tracking filters have been discussed in the previous chapter for implementation in a track-while-scan radar system. These trackers are capable of providing optimum estimates of an aircraft's position provided the dynamical models on which the tracking algorithm are based, are accurate assumptions of the aircraft's true trajectory. Unfortunately, due to the presence of radar measurement noise and wind turbulence, no single dynamical model for the aircraft's trajectory will be an accurate model throughout the period that the aircraft is under track.

Tracking Filter Limitations

Although the alpha filter is the simplest tracker that has been discussed, it provides the greatest noise smoothing performance. It is based upon the assumption that the aircraft's position is not changing with respect to time. The constant position model is applicable to the azimuth or elevation tracking of an aircraft whose trajectory is radial to the radar. The alpha filter is capable of tracking a constant position target with less error than either the alpha-beta filter or the alpha-beta-gamma filter, but because the alpha filter assumes a zero target velocity, its ability to track a target undergoing a change in position is impaired.

The alpha-beta tracker is a second order tracking filter which is designed to minimize the mean-square error in filtered position and velocity, assuming no velocity change between data samples. Thus the alpha-beta filter's capability to track severely maneuvering (accelerating) targets is severely limited.

If the target is assumed to be maneuvering, its trajectory may be modeled by a constant acceleration model with time varying position and and velocity. This more generalized model of the target's trajectory leads to the third order alpha-beta-gamma tracker which is capable of providing good estimates of the target's position and velocity throughout a maneuver. If, however, the target is not maneuvering, the alpha-beta-gamma filter suffers a significant degradation in noise smoothing performance compared to the simpler alpha-beta tracker (for constant velocity trajectory) or alpha tracker (for constant position trajectory).

Selection of the Appropriate Filter

Since the state of the target's trajectory may change as a function of time and range, no single filter will provide accurate estimates of the target's position and velocity throughout the tracking interval. However, if a bank of three filters consisting of the alpha filter, the alpha-beta filter, and the alpha-beta-gamma filter were operated in parallel with one another, accurate estimates of the target's position and velocity would be available regardless of the changes in the target's trajectory. Some type of adaptivity should be built into the filter bank so that if no position change is detected then the estimate from the alpha tracker, should be selected. If the target is ascertained to have a constant velocity, then the estimate from the alpha-beta tracking

filter should be selected. And if the target is undergoing a change in velocity, then the estimate from the alpha-beta-gamma tracker, should be selected.

Detection of a change in the target's trajectory and the selection of the appropriate filter output may be accomplished by monitoring the variance in the smoothed position estimates of both the alpha filter and the alpha-beta filter.

Alpha Filter Output Variance as a Basis for Filter Selection

If a constant position measurement of the form

$$x_m(k) = X + n(k) \tag{3-1}$$

where ,

$x_m(k)$ = radar position measurement at time kT

X = actual position at time kT (constant)

$n(k)$ = zero mean Gaussian noise with variance = σ_n^2 ,

is the input to an alpha tracker, then from equation (2-34) the variance in the smoothed position estimate is given by

$$\text{var}\{x_s(k)\} = \frac{\alpha}{2-\alpha}\ \sigma_n^2 \quad . \tag{3-2}$$

The input noise variance σ_n^2 is usually available, and if not, it can be easily calculated. The variance in the smoothed position estimates of the alpha filter can be approximated directly from the filter's output by

$$\text{var}\{x_s(k)\} \simeq \frac{1}{L} \sum_{i=0}^{L} [x_s(i) - E\{x_s(k)\}]^2 \quad , \tag{3-3}$$

where,

$x_s(i)$ = ith estimate of smoothed position

L = the integral number of samples over which the variance in smoothed position is being calculated

$$E\{x_s(k)\} = \frac{1}{L} \sum_{i=0}^{L} x_s(i) \quad .$$

As long as constant position measurements of the form prescribed in equation (3-1), are input to the alpha tracker, then the variance in the smoothed position estimates, approximated by equation (3-3), will remain less than or equal to the variance calculated via equation (3-2). If, however, radar measurements of a target undergoing a change in position are input to the alpha tracker, the variance in the smoothed position estimates, approximated by equation (3-3), will exceed the expected variance calculated via equation (3-2). Thus the variance in smoothed position obtained from equation (3-2) may be used as a threshold to determine if the alpha filter is capable of tracking the target. If the variance in the smoothed position estimates, approximated by equation (3-3), is less than the variance threshold calculated via equation (3-2), then the alpha tracker's smoothed estimate of position is considered the best estimate of the target's position and the velocity of the target is assumed to be zero. If the variance of the alpha tracker's smoothed position estimates, approximated by equation (3-3), exceeds the variance threshold obtained from equation (3-2), then the alpha tracker's smoothed

estimate of position is rejected and the alpha-beta filter's smoothed estimates of position and velocity are examined to determine if they yield a more accurate representation of the target's trajectory. When the variance of the alpha tracker's smoothed output (3-3) drops below the variance threshold (3-2), then the alpha filter's smoothed position estimate is once again considered a valid estimate of the target's position.

Alpha-Beta Filter Output Variance as a Basis for Filter Selection

In a similar manner, if the radar measurement of a constant velocity target is input to an alpha-beta filter it has the form of

$$x_m(k) = x(k) + vkT + n(k) \quad , \tag{3-4}$$

where,

$x_m(k)$ = radar position measurement at time kT

$x(k)$ = actual position at time kT

v = velocity of target (constant)

T = sampling interval .

Assuming an input as prescribed in (3-4), the variance expected in the smoothed position estimate is

$$\text{var}\{x_s(k)\} = \left[\frac{2\alpha^2 + \beta(2-3\alpha)}{\alpha(4-\beta-2\alpha)} \right] \sigma_n^2 \quad . \tag{3-5}$$

Equation (3-5) is of course, based upon the previous relation given by equation (2-91).

As with the alpha filter, the variance in the smoothed position estimates of the alpha-beta filter can be approximated from the filter's smoothed output by equation (3-3).

As long as the target maintains a constant-velocity straight-line trajectory, the variance in the alpha-beta filter's smoothed estimates of position (3-3) will remain less than or equal to the expected variance in smoothed position calculated via equation (3-5). Since the alpha-filter's estimate of position has been previously examined and found to be inaccurate for a constant-velocity target trajectory, it is assumed that the alpha-beta filter's smoothed estimates of position and velocity best represent the true trajectory of the target.

If the target undergoes an acceleration, the variance in the alpha-beta filter's smoothed position estimates, approximated by equation (3-3), will exceed the variance threshold calculated in equation (3-6). Under this condition, the alpha-beta filter's smoothed estimates of position and velocity are deemed inaccurate and tracking control is transferred to the higher order alpha-beta-gamma filter. Estimates of smoothed position and smoothed velocity from the alpha-beta-gamma filter are used only as long as the variances in the smoothed position estimates of the alpha filter or alpha-beta filter exceed their variance thresholds, calculated via equations (3-2) and (3-5), respectively. If the variances in the smoothed position estimates of both the alpha filter and the alpha-beta filter drop below their respective variance thresholds during the same sample interval, then track control is transferred to the alpha filter since it provides a greater degree of noise smoothing than the other two filters. A block diagram depicting the tracking system discussed in the previous paragraphs is shown in Figure 3.1.

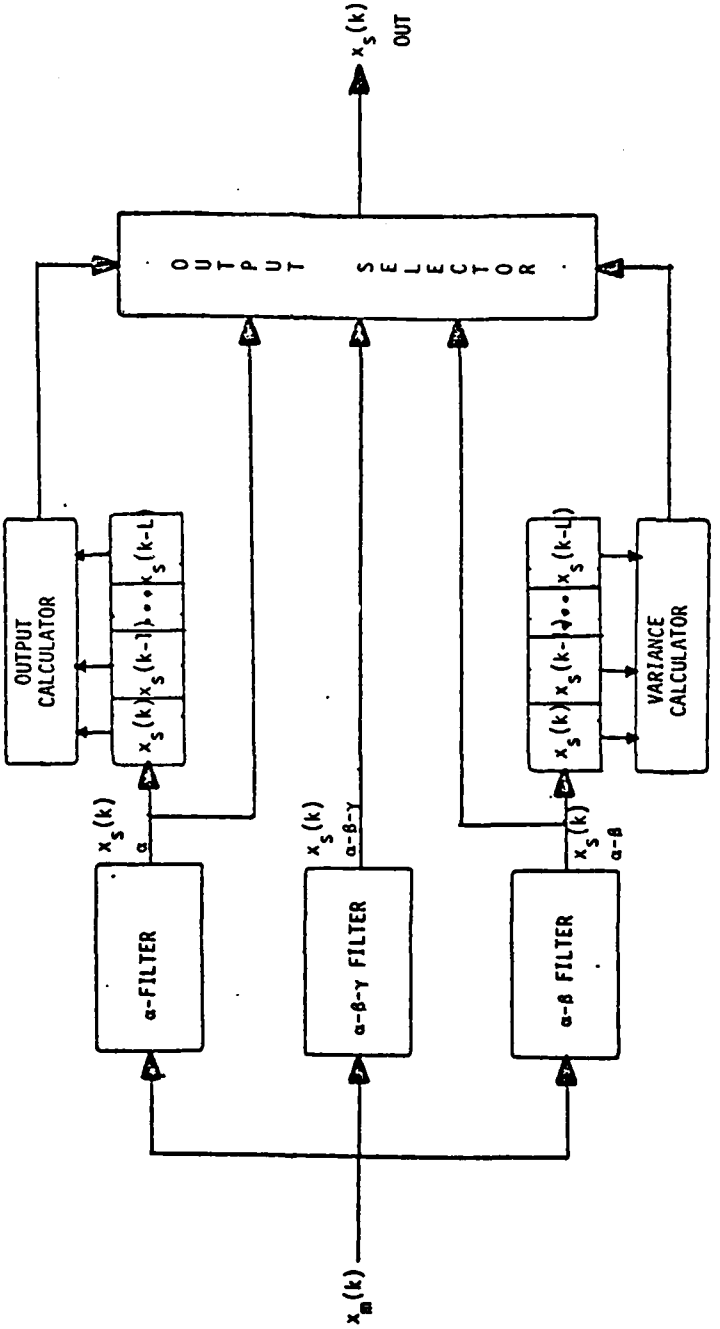

Figure 3.1. Block Diagram of the Tri-State Adaptive Tracking Filter.

Implementation of the Tri-State Adaptive Tracking Filter

Examination of Figure 3.1 shows that the alpha, alpha-beta, and alpha-beta-gamma tracking filters operate in parallel. Each filter generates its own estimates of smoothed position and smoothed velocity based upon its implicit model of the target's trajectory. The smoothed position estimates from the alpha filter and the alpha-beta filter are stored in separate L-length shift registers. From the stored values of the alpha filter's smoothed position estimates, the variance in the alpha filter's smoothed position estimates is calculated via equation (3-3). In a similar manner the variance in the alpha-beta filter's smoothed position is calculated using the stored values of the alpha-beta filter's smoothed position estimates. The calculated variances in the alpha filter and alpha-beta filter smoothed position estimates are then compared to their respective variance thresholds (calculated via (3-2) and (3-5)). The appropriate filter output is then selected based upon the criteria previously discussed. At the next sample interval, the new smoothed position estimates are shifted into the shift registers and the variance in smoothed position is recalculated for each of the two filters.

A flowchart depicting the operation of the tri-state adaptive tracking algorithm is presented in Figure 3.2.

The implementation of the tri-state adaptive tracking filter, as a FORTRAN IV subroutine, is given in the Appendix. The subroutine performs azimuth tracking on an incoming aircraft. The inputs to the subroutine are the sampling interval T, the azimuth noise variance, the range of the aircraft at each sample interval, and the radar's measurement of lateral position in feet.

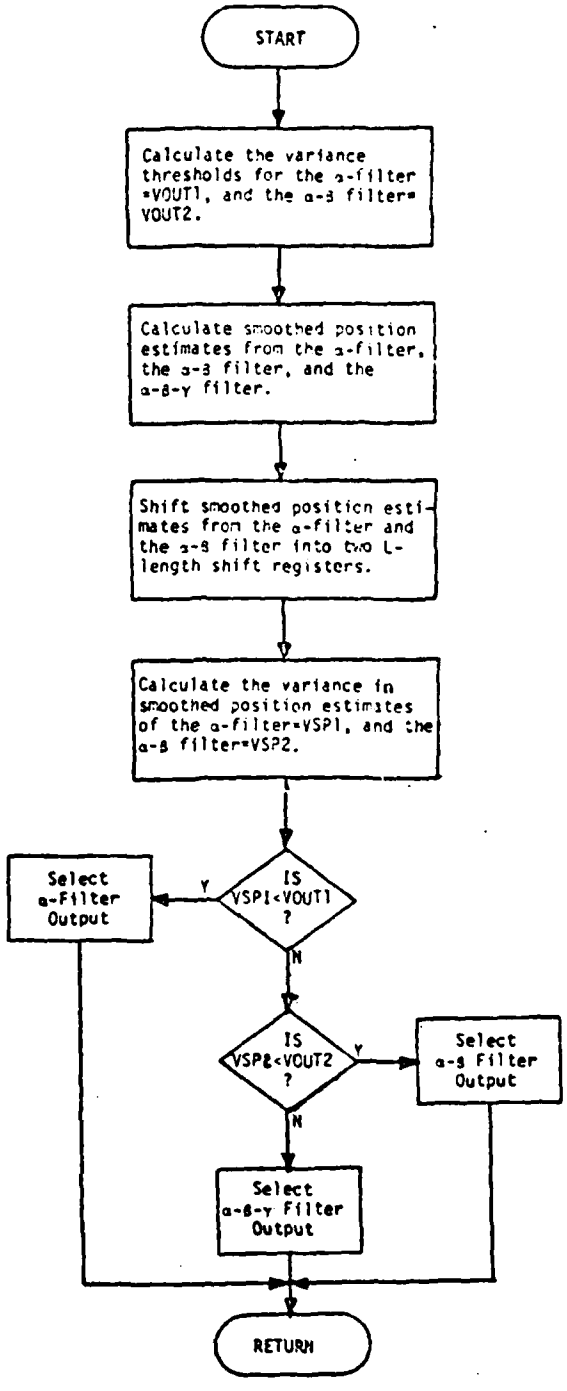

Figure 3.2. Flowchart of the Tri-State Adaptive Tracking Filter.

IV. SYSTEM SIMULATION

Introduction

This study investigates the application of a tri-state adaptive filter in an automatic landing system for aircraft. The automatic landing system under consideration is the Marine Air Traffic Control and Landing System (MATCALS). The MATCALS utilizes an AN/TPN-22 track-while-scan, electronically steerable microwave radar to produce raw digitized measurements of the aircraft's vertical and lateral positions. This positional information is filtered and processed by a groundbased controller which calculates the appropriate bank and pitch commands to correct the aircraft's trajectory. The commands are then transmitted via a communication link to the aircraft's autopilot to automatically land the aircraft. This configuration is presented in Figure 4.1. A more detailed discussion of the MATCALS is available in [16].

FORTRAN IV programs have been written to simulate the F4J and A7E aircraft dynamics, the F4J and A7E autopilots, the landing system controller, and the AN/TPN-22 radar. The FORTRAN IV program listings are given in [16]. Each of the aircraft simulations consists of two parts - the lateral control system simulation and the longitudinal control system simulation. The two control systems are uncoupled and are structurally identical. The lateral control system of the F4J will be used to study

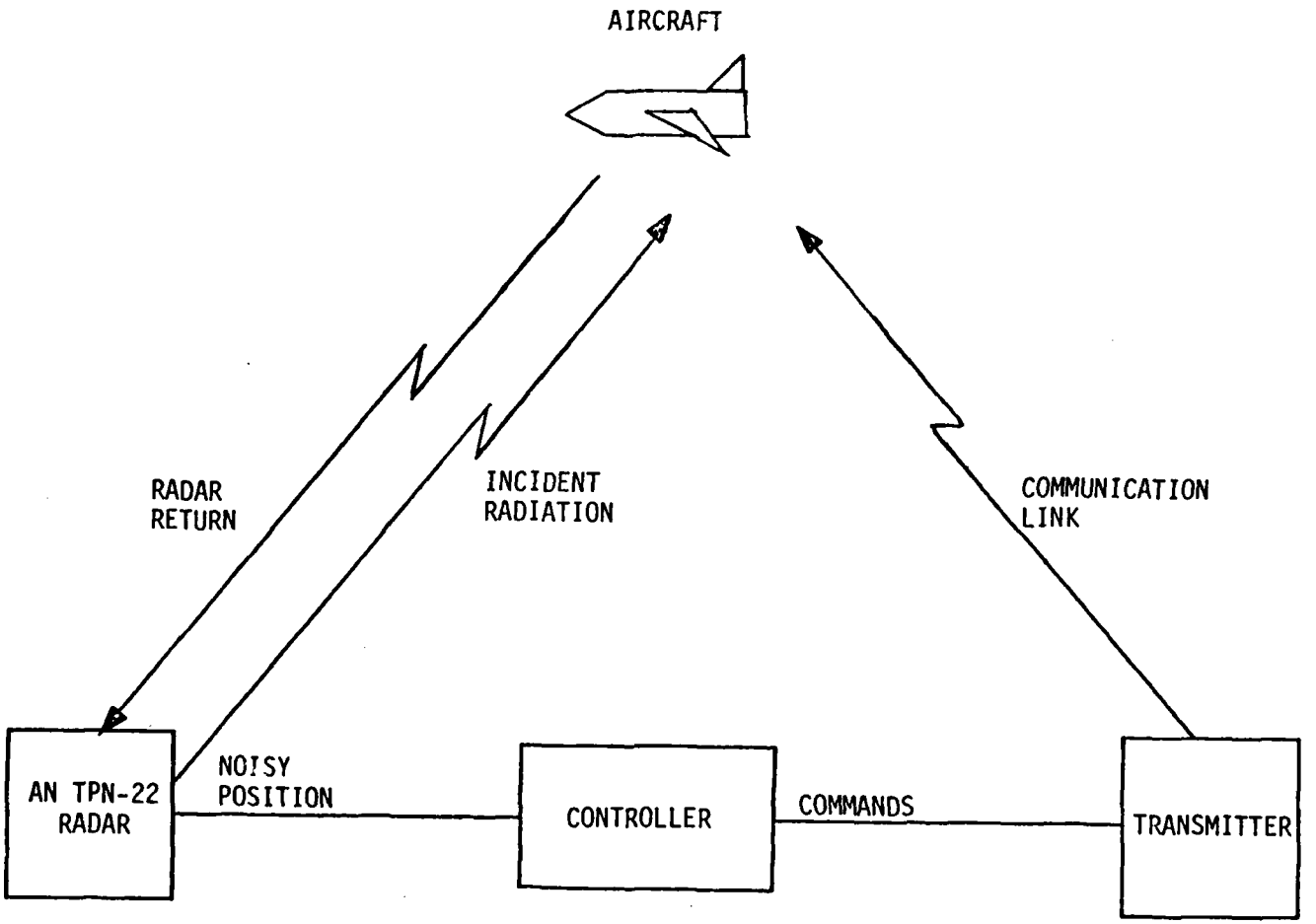

Figure 4.1. Block Diagram of MATCALS Automatic Landing System.

the performance of the tri-state adaptive filter, since stability is more difficult to obtain in this system than in the longitudinal control system [17].

The F4J Control System

The lateral control system of the F4J automatic landing system is modeled as a sampled data control system. The aircraft's lateral dynamics and autopilot generate the analog signal $y(t)$ (lateral position). The AN/TPN-22 radar is modeled as an A/D converter, which converts the continuous process $y(t)$ into discrete measurements of position every T seconds, where T, the sampling period, is selected to be 0.1 seconds. The groundbased controller is modeled as a digital transfer function which generates discrete bank commands, $\phi(k)$, and a zero order hold which restructures the discrete bank commands into the continuous signals $\phi(t)$. A block diagram of the lateral control system for the F4J aircraft is given in Figure 4.2.

The F4J Lateral Guidance System

The F4J aircraft lateral dynamics are described by a set of sixth order linear differential equations. The autopilot dynamics are given by a set of third order differential equations. Thus, the lateral control system is ninth order. In addition the lateral control system includes three nonlinearities. The system equations are of the form

$$\dot{\underline{x}}(t) = A\underline{x}(t) + B\underline{u}(t) + E\underline{f}(t) \qquad (4\text{-}1)$$

$$\underline{y}(t) = C\underline{x}(t) + D\underline{u}(t) \qquad (4\text{-}2)$$

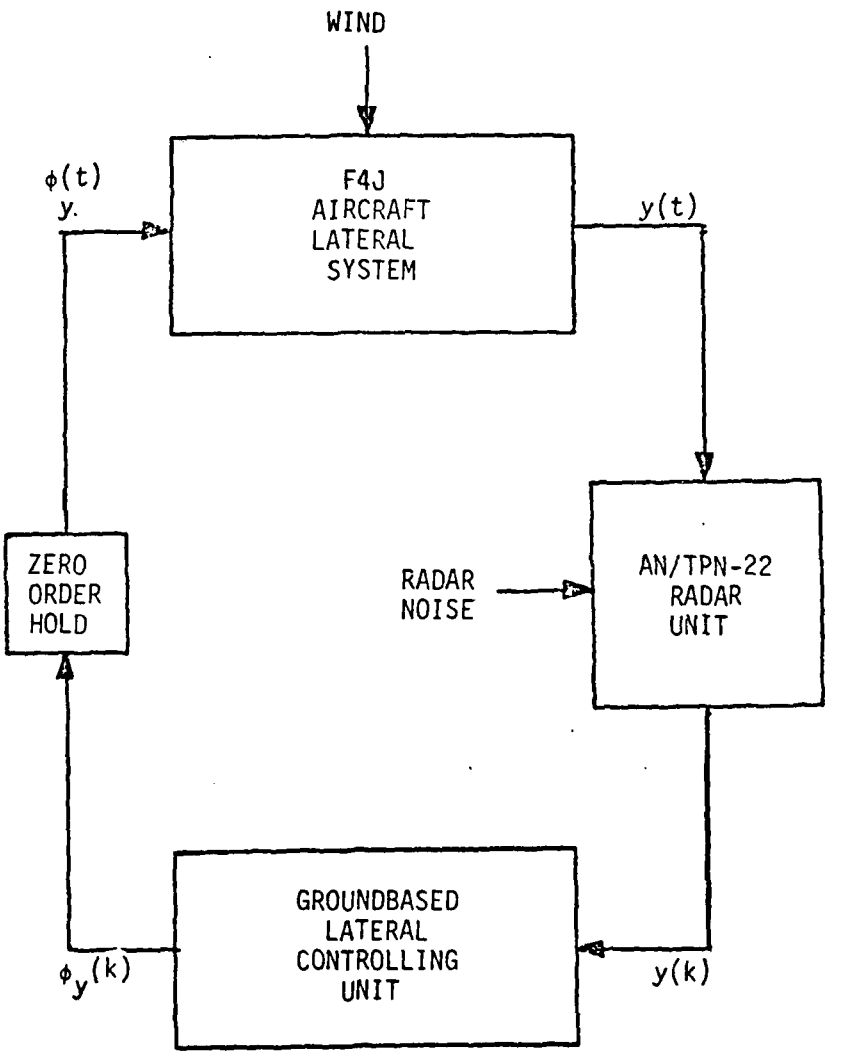

Figure 4.2. Block Diagram of the F4J Lateral Control System.

where the nonlinearities are simulated by the term Ef. The simulation of the F4J aircraft's lateral dynamics and the dynamics of the autopilot is discussed in detail in Reference [16].

The SPN-42 Digital Controller

The groundbased control unit for the F4J lateral control system is the SPN-42 digital controller. The SPN-42 is described as a PID controller. In this notation, P indicates proportional, I indicates integral, and D indicates derivative. The SPN-42 digital controller is composed of an α-β tracking filter, a differentiator, an integrator, four α filters, and a floating limiter. A block diagram of the SPN-42 lateral control system digital controller is presented in Figure 4.3, with all nonlinearities omitted. A detailed description of the SPN-42 digital controller is available in [17].

AN/TPN-22 Radar

The AN/TPN-22 phased array radar is utilized in the lateral control system of the F4J aircraft to measure the lateral position of the aircraft. In the measurement process a significant amount of noise is introduced into the system such that the reported lateral position of the aircraft is degraded. A model for simulating the noise associated with the AN/TPN-22 radar is the ITT-Gilfillan AN/TPN-22 radar noise model [18]. A block diagram of the radar noise simulation is given in Figure 4.4. The difference equation describing the AN/TPN-22 azimuth radar noise is given by [17],

$$\Delta\phi(n) = 0.382\ \Delta\phi(n-1) + 0.15\ \Delta\phi(n-2) + 0.122\ \Delta\phi(n-3) + 0.0045\ \Delta\ (n-4) + v(n) \qquad (4\text{-}3)$$

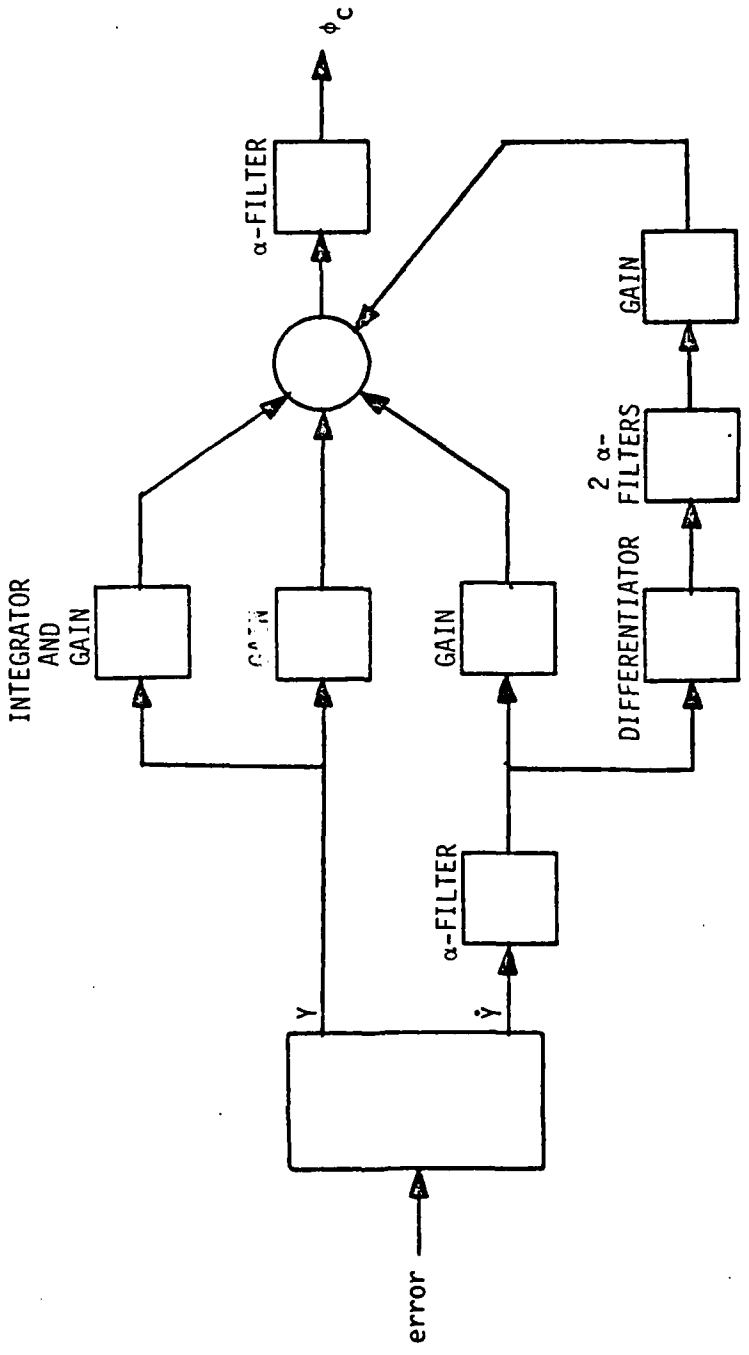

Figure 4.3. SPN-42 Digital Controller.

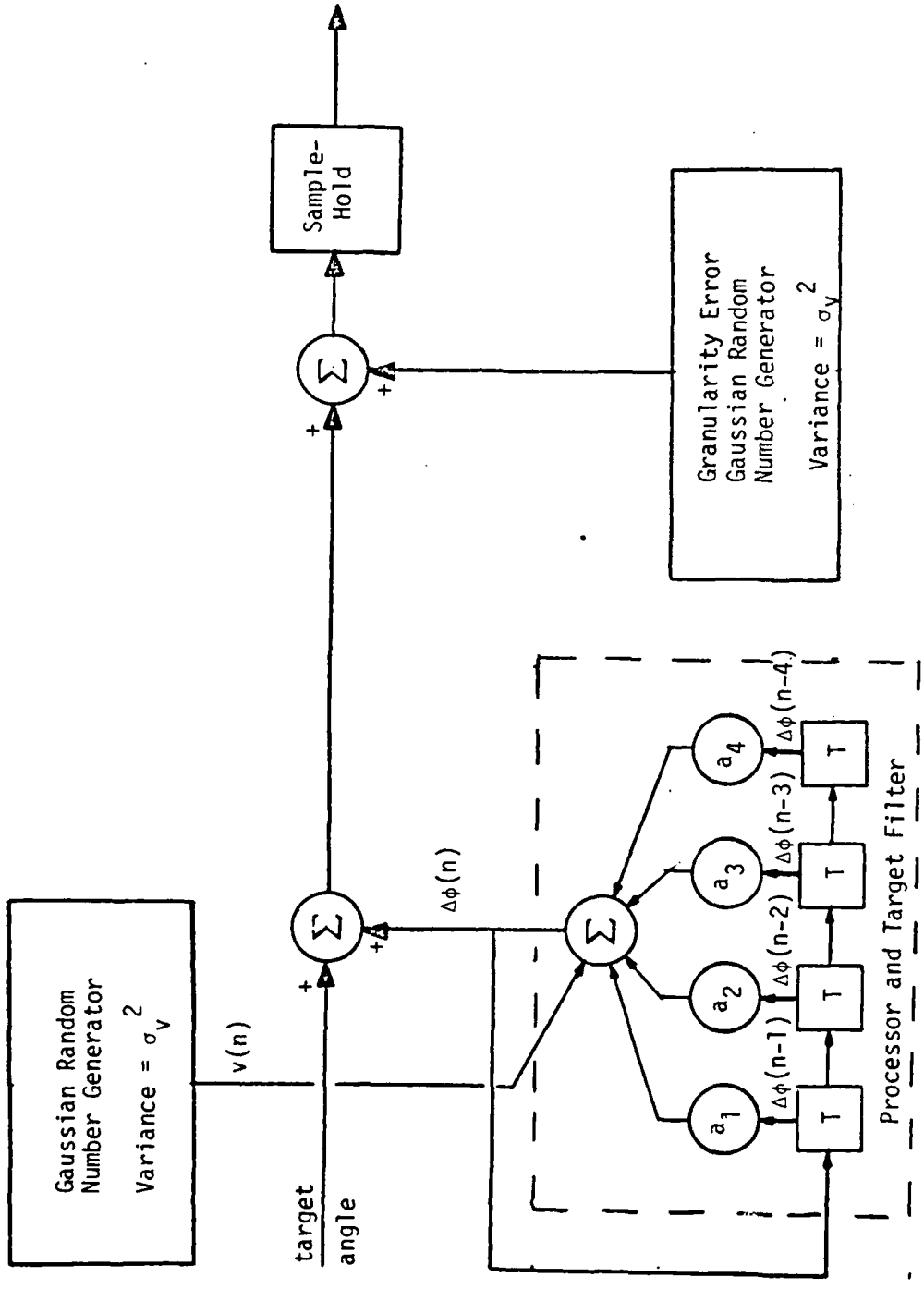

Figure 4.4. AN/TPN-22 Radar Error Simulation.

and,

$$\text{measured angle } (n) = \Delta\phi(n) + g(n) + \text{target angle} \quad , \qquad (4\text{-}4)$$

where,

$\Delta\phi(n)$ = azimuth noise at the nth sample

$g(n)$ = azimuth granularity error sequence with standard deviation, $\sigma_g = 0.148$ mr

$v(n)$ = white noise sequence with mean = 0.0 and variance, $\sigma_v^2 = 0.320\ \text{mr}^2$

The aircraft's normal touchdown point on the runway is offset from the radar center by:

Longitudinal	X offset = 762.9 feet
Lateral	Y offset = -178.1 feet

The target angle is given by:

$$\text{target angle} = \tan^{-1}\left[\frac{Y + 178.1}{X + 762.9}\right] . \qquad (4\text{-}5)$$

The lateral position of the aircraft, measured by the radar, is given by

$$Y_R(n) = (X + 762.9)\ \tan[\text{measured angle } (n)] - 178.1 \qquad (4\text{-}6)$$

V. SIMULATION RESULTS

Introduction

The feasibility of using the tri-state adaptive tracking filter in the MATCALS may be studied by incorporating the tri-state adaptive filter and the alpha-beta filter into the F4J lateral control system simulation discussed in Chapter IV. The response of the F4J lateral control system, using the alpha-beta filter to estimate the aircraft's position and velocity, may then be compared to the control system's response using the tri-state adaptive filter to estimate the aircraft's position and velocity. Block diagrams depicting the implementation of the alpha-beta filter and the tri-state adaptive filter in the F4J lateral control system are given in Figure 5-1 and 5-2, respectively.

For ease of reference, the lateral control system using the alpha-beta filter to estimate the aircraft's position and velocity shall be called the alpha-beta control system. Likewise, the lateral control system using the tri-state adaptive filter to estimate the aircraft's position and velocity shall be called the tri-state adaptive control system.

Tracking System Comparison

Filter Parameters

The filter coefficients used to obtain the simulation results for the alpha-beta control system and the tri-state adaptive control system are given in Table 5-1. The filter coefficients for the alpha-beta

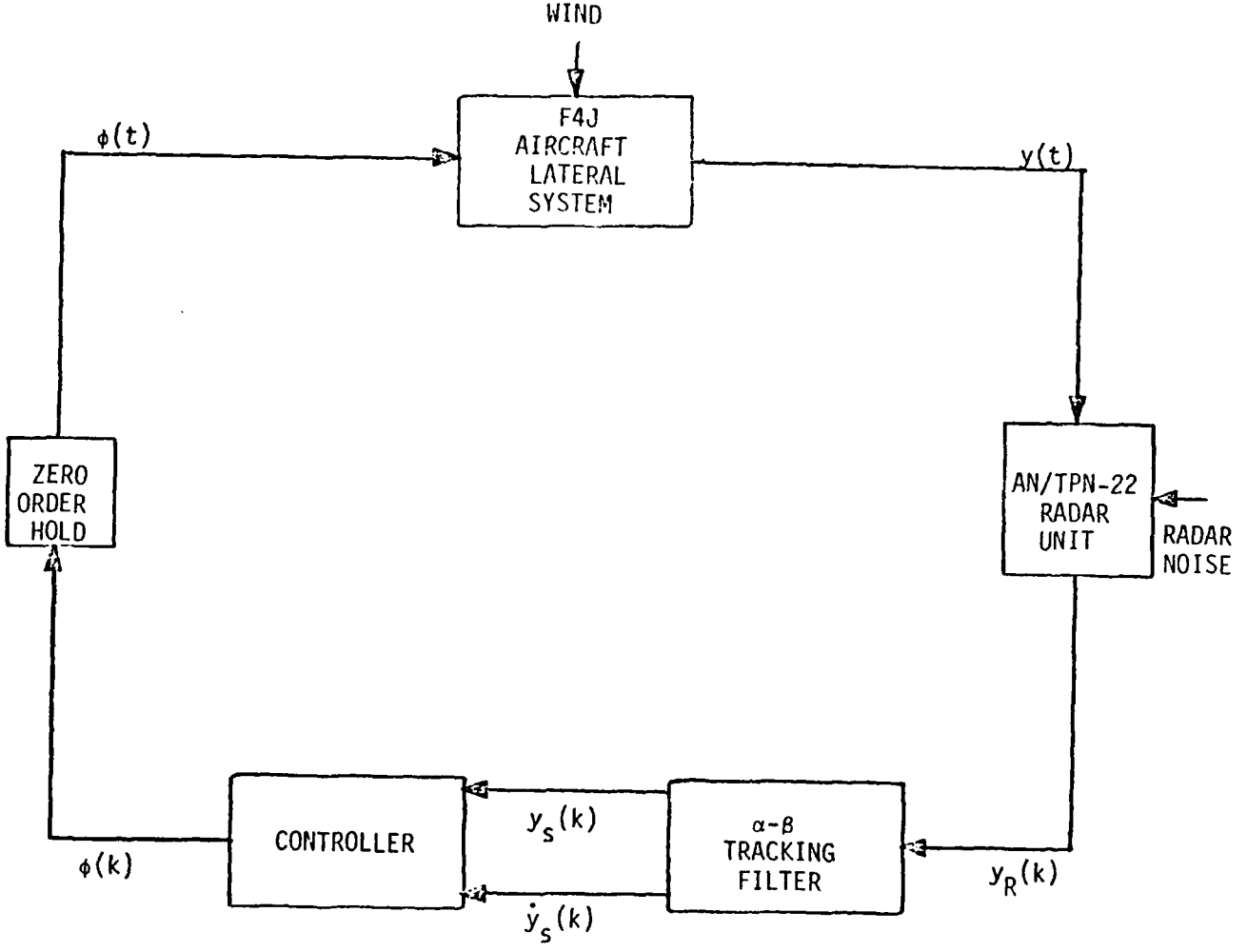

Figure 5.1. Block Diagram of the F4J Lateral Control System with the Alpha-Beta Tracking Filter in Operation.

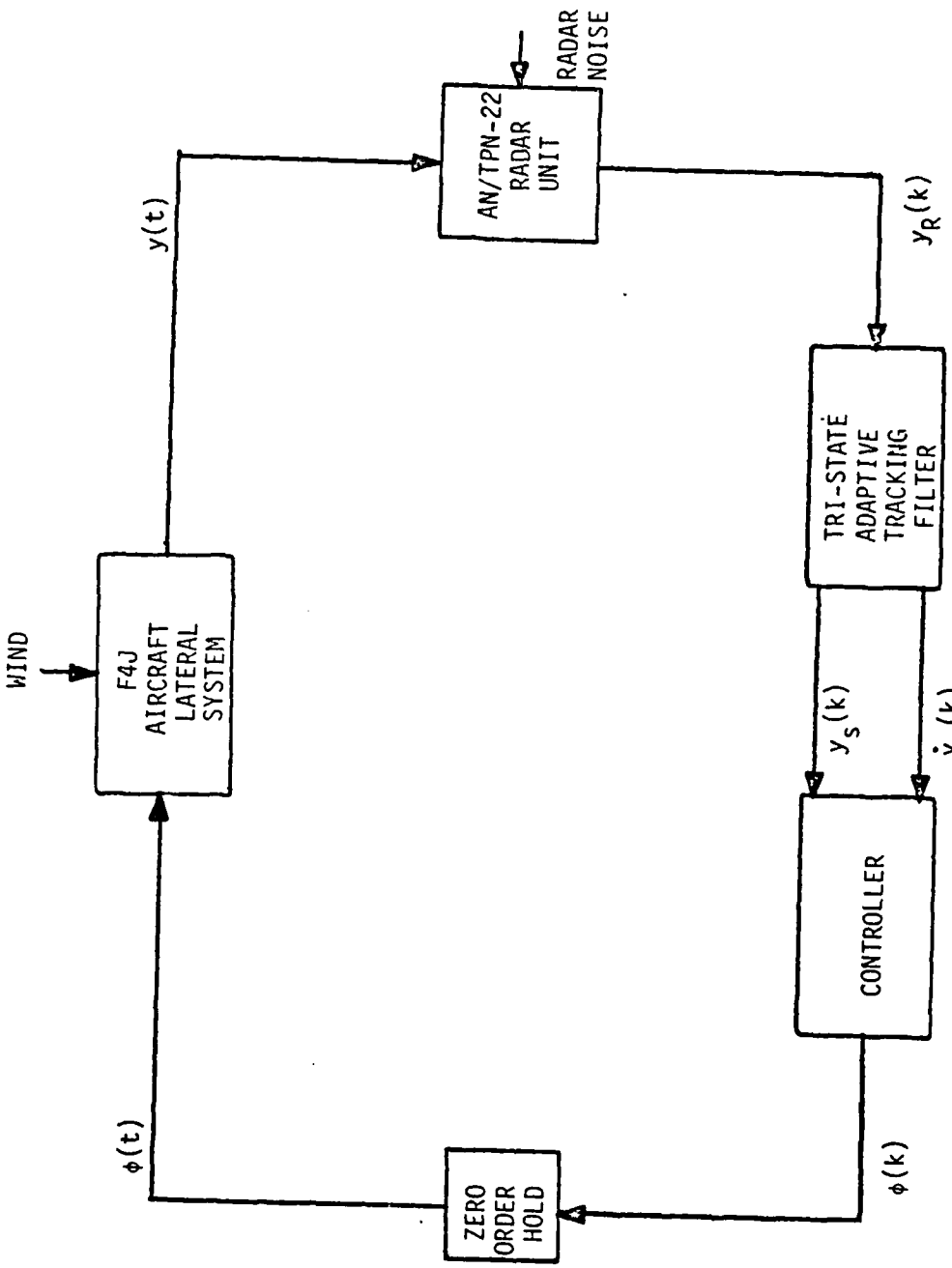

Figure 5.2. Block Diagram of the F4J Lateral Control System with the Tri-State Adaptive Tracking Filter in Operation.

TABLE 5-1

FILTER PARAMETERS

	ALPHA-BETA CONTROL SYSTEM	TRI-STATE ADAPTIVE CONTROL SYSTEM		
		ALPHA FILTER	ALPHA-BETA FILTER	ALPHA-BETA-GAMMA FILTER
α	0.51	0.15	0.51	0.46864
β	0.1746	--	0.1746	0.10136
γ	--	--	--	0.000684

control system were obtained from [17], and were found to provide the optimal noise smoothing performance for a given maneuver following capability. For this reason, the alpha-beta stage of the tri-state adaptive filter is identical to the filter used in the alpha-beta control system. The filter coefficients for the alpha and alpha-beta-gamma stages of the tri-state adaptive filter were determined experimentally by making repetitive simulation runs and selecting the coefficients which provided the best noise smoothing performance (alpha-filter) and the best maneuver following capability (alpha-beta-gamma filter).

Filter Frequency Response

A FORTRAN program from [19] was used to calculate the amplitude and phase responses of the alpha-beta filter and the three filters which make up the tri-state adaptive filter. These frequency responses are given in Figure 5-3 through Figure 5-6.

Control System Time Response with a Given Initial Condition

The initial condition time responses of the alpha-beta control system and the tri-state adaptive control system are given in Figure 5-7 and Figure 5-8.

The time responses of the two lateral control systems were obtained from simulation runs of the eighty seconds of the aircraft's flight prior to touchdown. This corresponds to an initial range of 17,632 feet. The aircraft is initially assumed to be offset laterally from the extended centerline of the runway by twenty feet. The lateral velocity of the aircraft is initially assumed to be zero while the

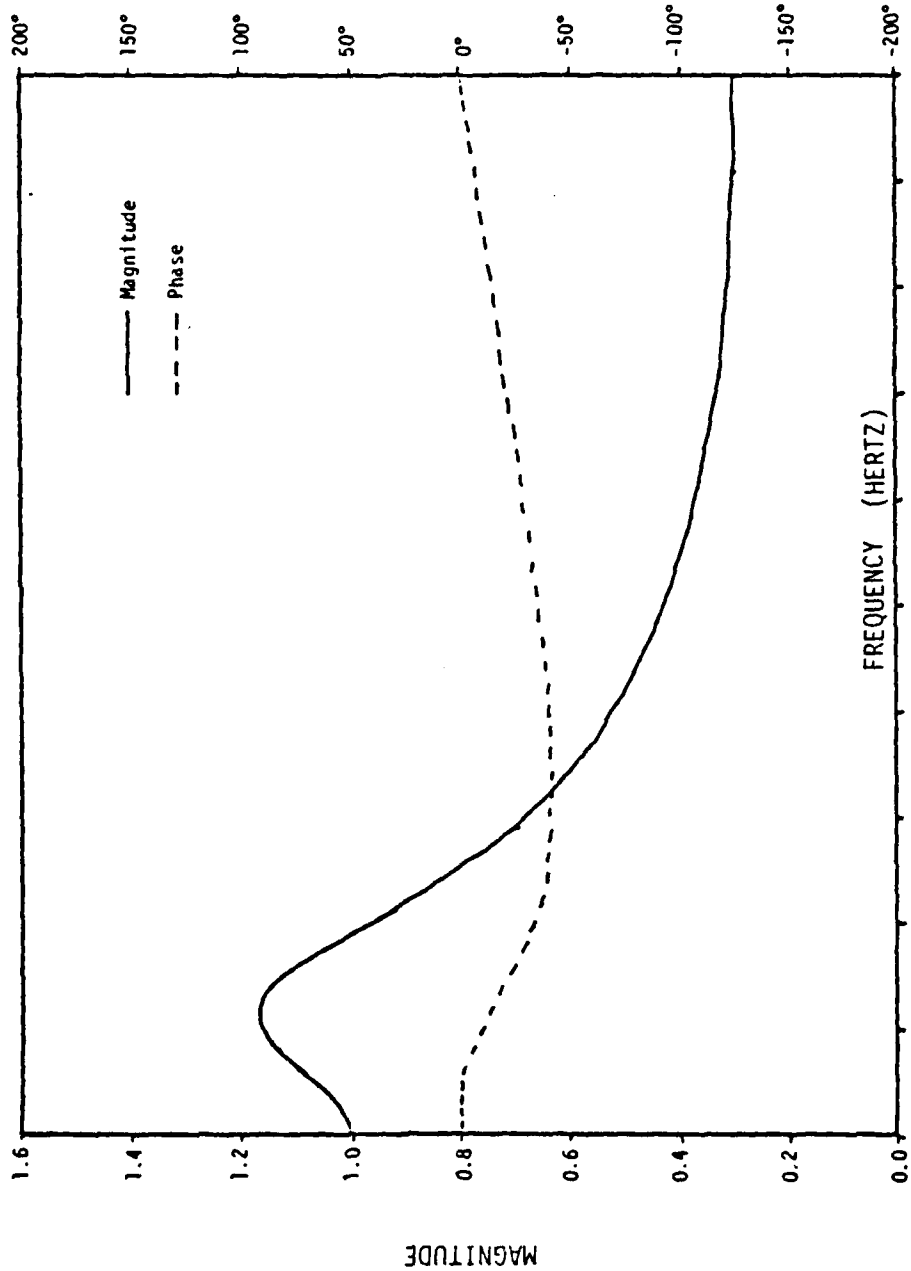

Figure 5.3. Frequency Response of the Alpha-Beta Filter used in the Alpha-Beta Control System.

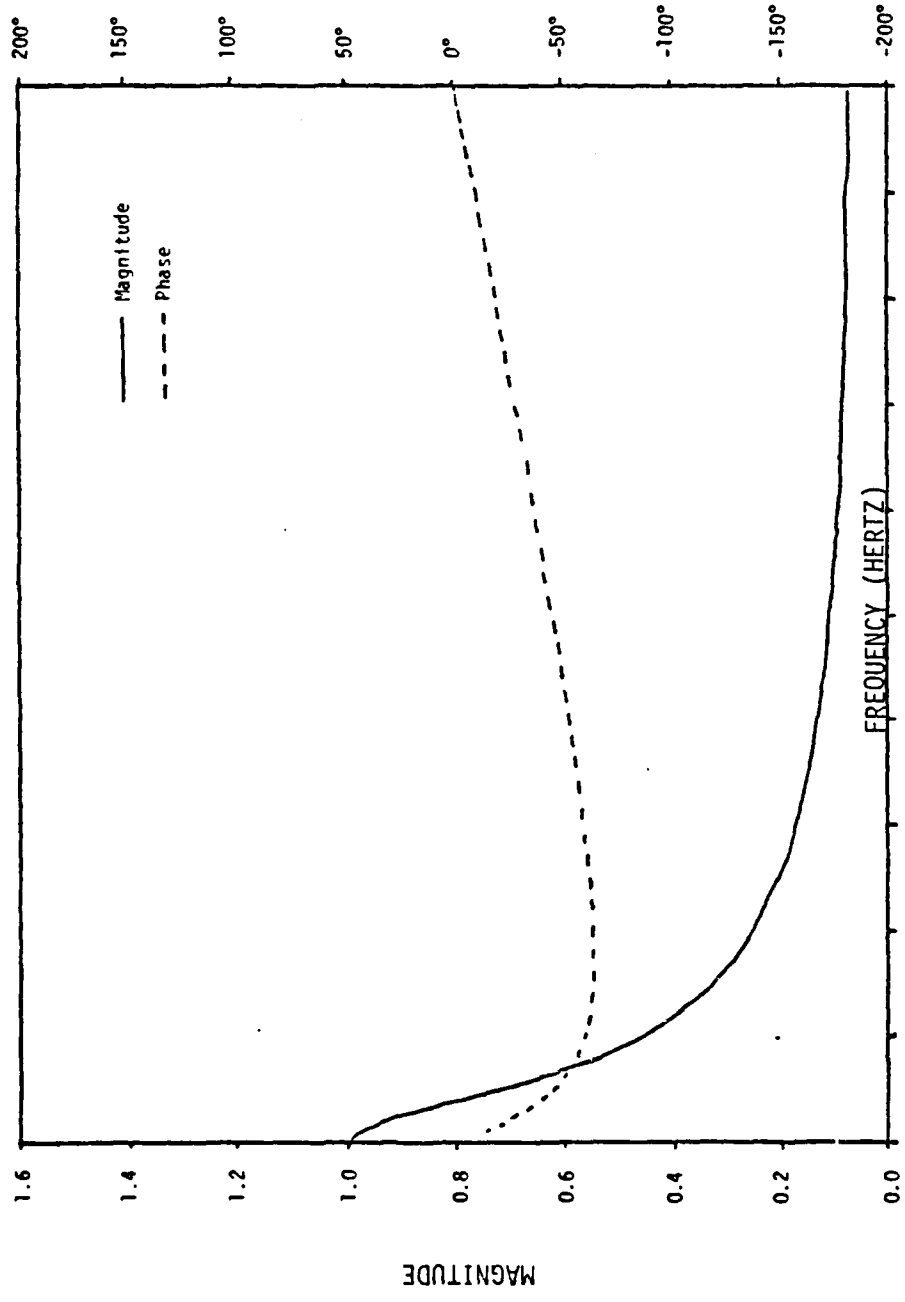

Figure 5.4. Frequency Response of the Alpha Filter used in the Tri-State Adaptive Control System.

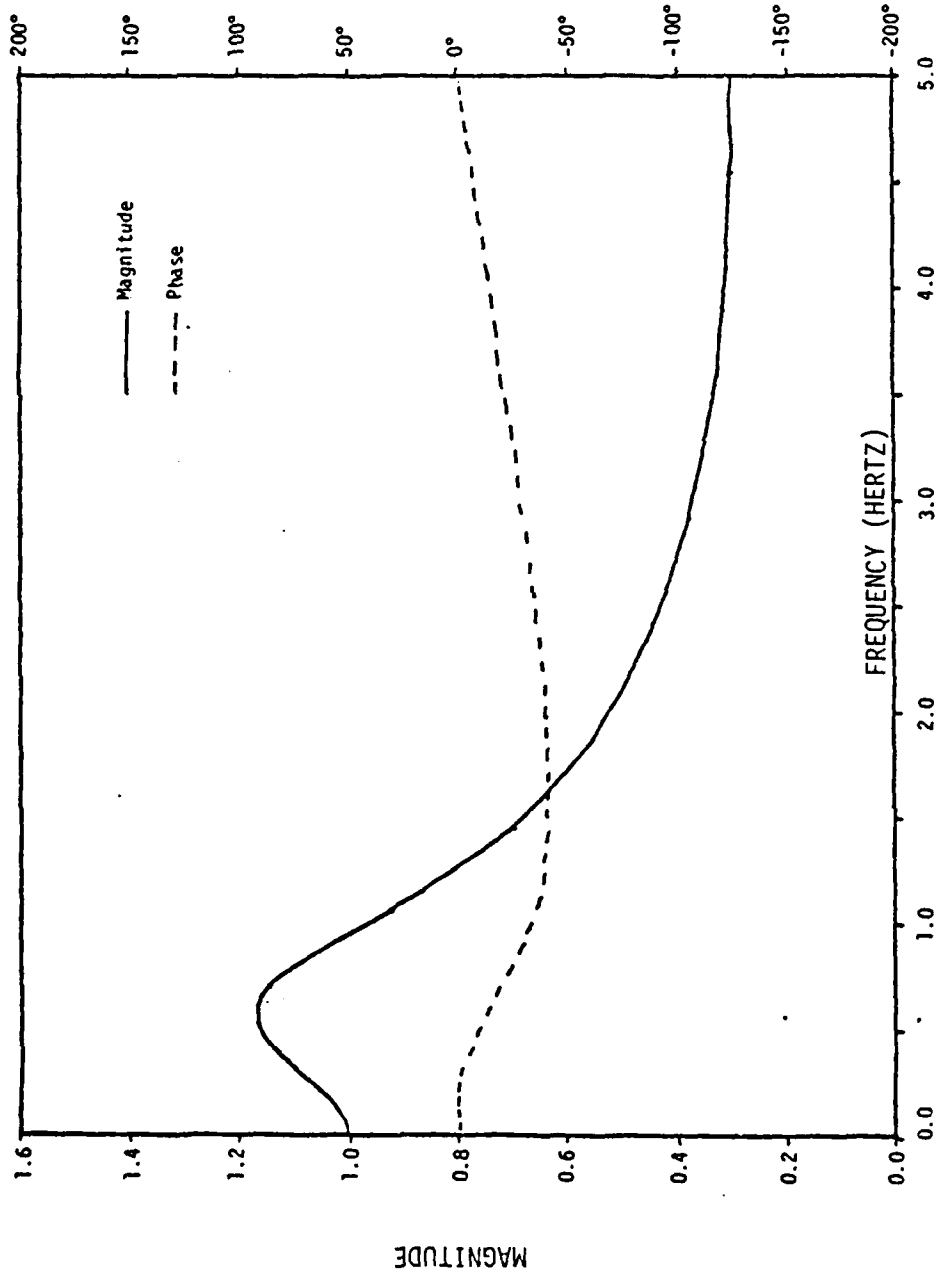

Figure 5.5. Frequency Response of the Alpha-Beta Filter used in the Tri-State Adaptive Control System.

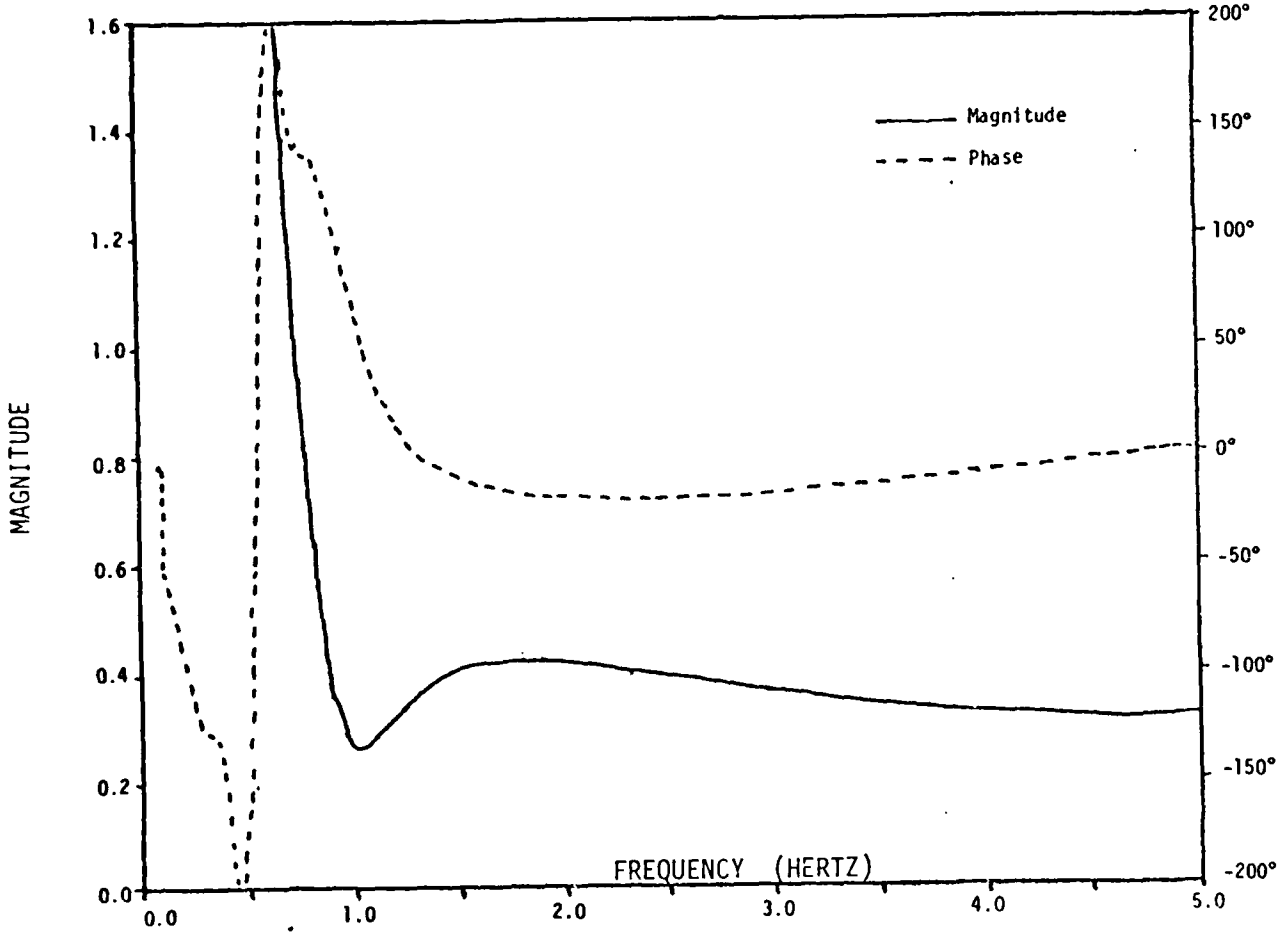

Figure 5.6. Frequency Response of the Alpha-Beta-Gamma Filter Used in the Tri-State Adaptive Tracking System.

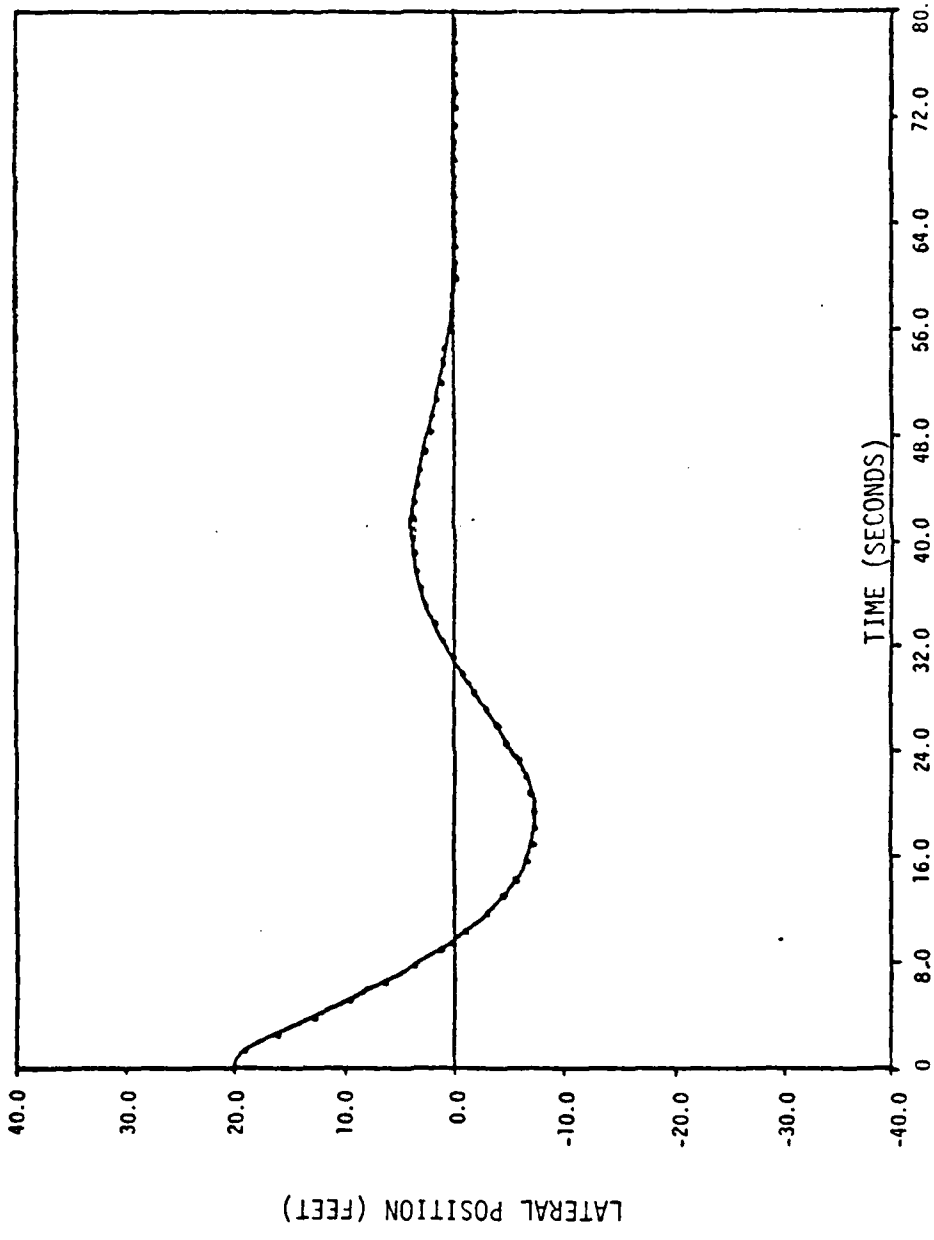

Figure 5.7. Initial Condition Time Response of the Alpha-Beta Control System.

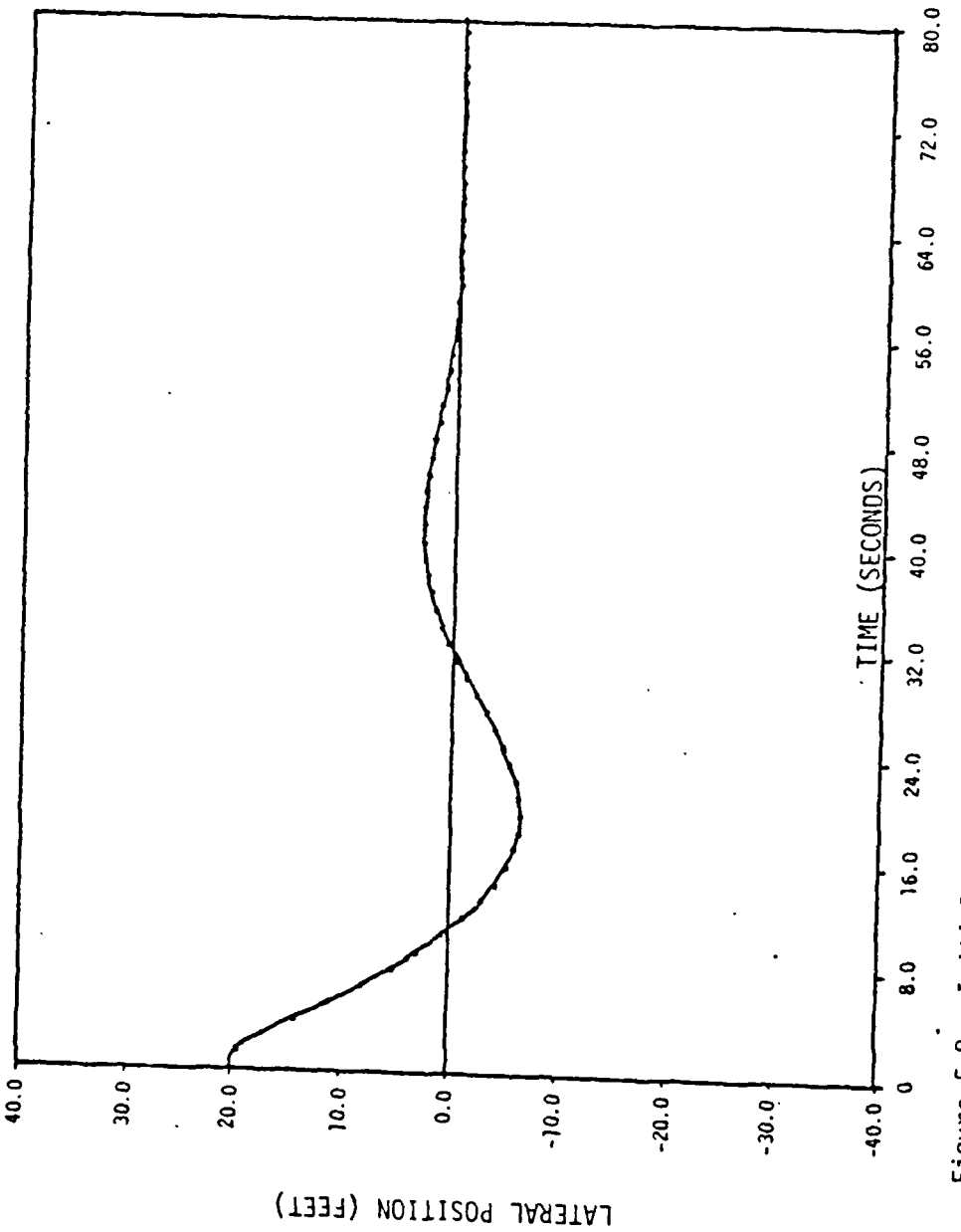

Figure 5.8. Initial Condition Time Response of the Tri-State Adaptive Control System.

forward velocity of the aircraft is assumed to be a constant 220.39 feet per second. For the time response simulations, the wind and noise disturbances were eliminated.

The time responses of the alpha-beta control system and the tri-state adaptive control system may be evaluated by comparing the transient response of each system and the ability of each system to guide the aircraft. The rise time and the time to peak provide a measure of the transient responses of the lateral control systems. The rise time, T_r, is defined as the time required for the aircraft to reach the extended centerline of the runway. The time to peak, Tp, is defined as the time required for the aircraft to reach its first peak. An idea of how well the lateral control systems guide the aircraft may be obtained by examining the percent overshoot and the time to settle for each system. The percent overshoot for the lateral control system is given by

$$P.O. = \frac{X_{peak}}{X_{IC}} \times 100\% \qquad (5\text{-}1)$$

where X_{peak} is the magnitude of the first peak position of the aircraft, and X_{IC} is the magnitude of the initial position of the aircraft. The time to settle is defined as the amount of time necessary for the control systems to settle the aircraft within 2% of its initial position of twenty feet. These time response performance measures for the alpha-beta control system and the tri-state adaptive control system are given in Table 5-2.

TABLE 5-2

TIME RESPONSE CHARACTERISTICS

	ALPHA-BETA FILTER CONTROL SYSTEM	TRI-STATE ADAPTIVE CONTROL SYSTEM
TIME TO RISE, T_r (seconds)	9.8	10.8
TIME TO PEAK, T_p (seconds)	18.3	19.6
TIME TO SETTLE, T_s (seconds)	56	56
PERCENT OF OVERSHOOT, P.O. (%)	36.75	32.3

The results given in Table 5-2 reveal that the alpha-beta control system has a faster response than the tri-state adaptive control system, but the tri-state adaptive control system does not overshoot as severely.

Tri-State Adaptive Control System Performance

The performance of the tri-state adaptive tracking filter may best be evaluated by comparing the results of a number of simulation runs of the tri-state adaptive control system with the results of similar runs of the alpha-beta control system. The characteristics of the system responses cannot be obtained from one simulation. To obtain an accurate statistical description, it is necessary to make many simulation runs and to statistically average the results.

Monte Carlo Simulation Runs

One method of obtaining accurate statistical descriptions of the two lateral control system responses is by making Monte Carlo runs. Each of the Monte Carlo runs that are to be presented is determined from twenty simulation runs. For each simulation run, the aircraft is initially assumed to be on the extended centerline of the runway at a starting range of 17,632 feet. Prior to the start of each simulation run, the aircraft is assumed to have zero lateral velocity, and a constant forward velocity of 220.39 feet per second. The forward velocity of 220.39 feet per second results in a flight time of eighty seconds to touchdown point. All lateral movements of the aircraft during the simulation runs are caused by wind turbulence or radar noise. The wind turbulence and radar noise for each of the twenty simulation runs have the same statistical parameters; however, the random number generators

in the wind turbulence and radar noise sources are started at different values thus generating different number sequences for each simulation run. It should be noted that each Monte Carlo run uses identical sets of random number sequences.

For the purpose of analyzing the two control system responses as a function of range, each simulation run is divided into four equal time bins, each having a duration of twenty seconds. This corresponds to four range bins, each having a length of 4408 feet.

Statistics are calculated to describe the system responses over the appropriate range bin for each simulation run. The statistics for each range bin are then averaged over the twenty simulation runs which make up the Monte Carlo run. The results, as a function of range, for the Monte Carlo runs with wind turbulence and radar noise included are given in Table 5-3. The statistics used to evaluate the alpha-beta control system and the tri-state adaptive control system are the mean square lateral position error off the extended centerline of the runway and the variance in position error off the extended centerline of the runway. A listing of percent improvement of the tri-state adaptive control system over the alpha-beta control system is included in the Tables. Percent improvement is defined as

$$\% \text{ Improvement} = \frac{(M_A - M_T)}{[(M_A + M_T)/2]} \times 100\% \qquad (5\text{-}2)$$

where M_A and M_T are the mean square error of position off the extended centerline of the runway for the alpha-beta control system and the tri-state adaptive control system, respectively.

TABLE 5-3

RESULTS OF MONTE CARLO RUNS
WITH WIND AND RADAR NOISE

BIN #	ALPHA-BETA FILTER CONTROL SYSTEM		TRI-STATE ADAPTIVE CONTROL SYSTEM		% IMPROVEMENT
	VARIANCE IN POSITION	M.S.E. POSITION	VARIANCE IN POSITION	M.S.E. POSITION	
1	21.5903778	46.4041748	10.060871	22.3553467	69.9
2	62.2022095	94.7764893	65.8923340	140.141174	-38.6
3	38.9550171	69.3792267	65.4622650	116.656082	-50.7
4	8.80756187	17.8845978	11.6634922	19.7320251	-9.8

Table 5-3 indicates that the tri-state adaptive control system does not perform as well as the alpha-beta control system when radar noise and wind turbulence is included in the simulation runs. Closer scrutiny of Table 5-3 reveals that the tri-state adaptive control system performs best only for bin 1 which corresponds to a range greater than 13,224 feet.

A possible reason for the inferior performance of the tri-state adaptive control system may lie in the switching process between the alpha and alpha-beta filter states of the tri-state adaptive filter. As pointed out in Chapter III, the alpha filter will provide excellent smoothing of position measurements so long as the lateral velocity of the aircraft is equal to zero. If the aircraft acquires a lateral velocity, then the alpha filter estimate will be in error. In order to determine if the aircraft is acquiring a lateral velocity, the variance in the smoothed position estimates of the alpha filter state must be calculated as given in equation (3-3). This variance in smoothed position is then compared to the variance threshold for the alpha filter given by equation (3-2). If the variance in the alpha filter's smoothed position estimates exceeds the threshold then the aircraft is assumed to have acquired a lateral velocity and the output of the alpha-beta filter should be selected. If, however, the variance in the alpha filter's smoothed position estimates does not increase rapidly enough, the tri-state adaptive filter will output the smoothed position estimate of the alpha filter, even though the aircraft has acquired a lateral velocity, and thus be in error.

TABLE 5-4

RESULTS OF MONTE CARLO RUNS
WITH WIND AND RADAR NOISE

	ALPHA-BETA FILTER CONTROL SYSTEM		TRI-STATE ADAPTIVE CONTROL SYSTEM		
BIN #	VARIANCE IN POSITION	M.S.E. POSITION	VARIANCE IN POSITION	M.S.E. POSITION	% IMPROVEMENT
1	21.5903378	46.4041748	16.8374481	32.8245697	34.3
2	62.2022095	94.7764893	41.3740845	82.5668945	13.8
3	38.9550171	69.3792267	33.0398560	61.7212372	11.7
4	8.80756187	17.8845978	9.87785721	19.7020874	-9.6

TABLE 5-5

RESULTS OF MONTE CARLO RUNS
WITH WIND ONLY

BIN #	ALPHA-BETA FILTER CONTROL SYSTEM		TRI-STATE ADAPTIVE CONTROL SYSTEM		% IMPROVEMENT
	VARIANCE IN POSITION	M.S.E. POSITION	VARIANCE IN POSITION	M.S.E. POSITION	
1	2.85398483	6.16137605	2.80738449	6.0294075	2.1
2	6.35484505	9.89277935	6.03726196	7.72684002	4.6
3	5.44185448	8.50222111	4.91503525	7.72684002	9.4
4	2.44774521	3.40685654	2.26694679	3.14779663	7.9

TABLE 5-6

RESULTS OF MONTE CARLO RUNS
WITH NOISE ONLY

BIN #	ALPHA-BETA FILTER CONTROL SYSTEM		TRI-STATE ADAPTIVE CONTROL SYSTEM		% IMPROVEMENT
	VARIANCE IN POSITION	M.S.E. POSITION	VARIANCE IN POSITION	M.S.E. POSITION	
1	3.70224380	7.88915062	12.5118027	29.1406250	-114.6
2	7.32055378	18.1728210	28.5565033	45.1800537	-85.3
3	5.61834717	10.7610340	14.9685907	31.2148437	-97.4
4	2.71902561	4.57846928	5.15683079	7.70898247	-50.9

simulation runs with identical wind and radar noise. One run uses the alpha-beta control system to guide the aircraft while the second run uses the tri-state adaptive control system. Figure 5-9 provides a comparison of the performance of the two control systems under the identical effects of wind and radar noise. The tri-state control system is seen to perform better than the alpha-beta control system, especially during the first fifty seconds of the simulation run.

The improvement in performance that the tri-state adaptive control system has over the alpha-beta control system is due to the tri-state adaptive filter's more accurate estimates of velocity. Shown in Figure 5-10 is a comparison of the actual aircraft lateral velocity to the alpha-beta filter estimates of velocity. A comparison of the actual aircraft lateral velocity to the tri-state adaptive filter estimates is shown in Figure 5-11. A tabular comparison of the mean square error in the two filter's velocity estimates is given in Table 5-7. The tri-state adaptive filter's ability to more accurately estimate the aircraft's lateral velocity is the key to the improvement in the performance of the tri-state adaptive control system over the alpha-beta control system presently used in the system.

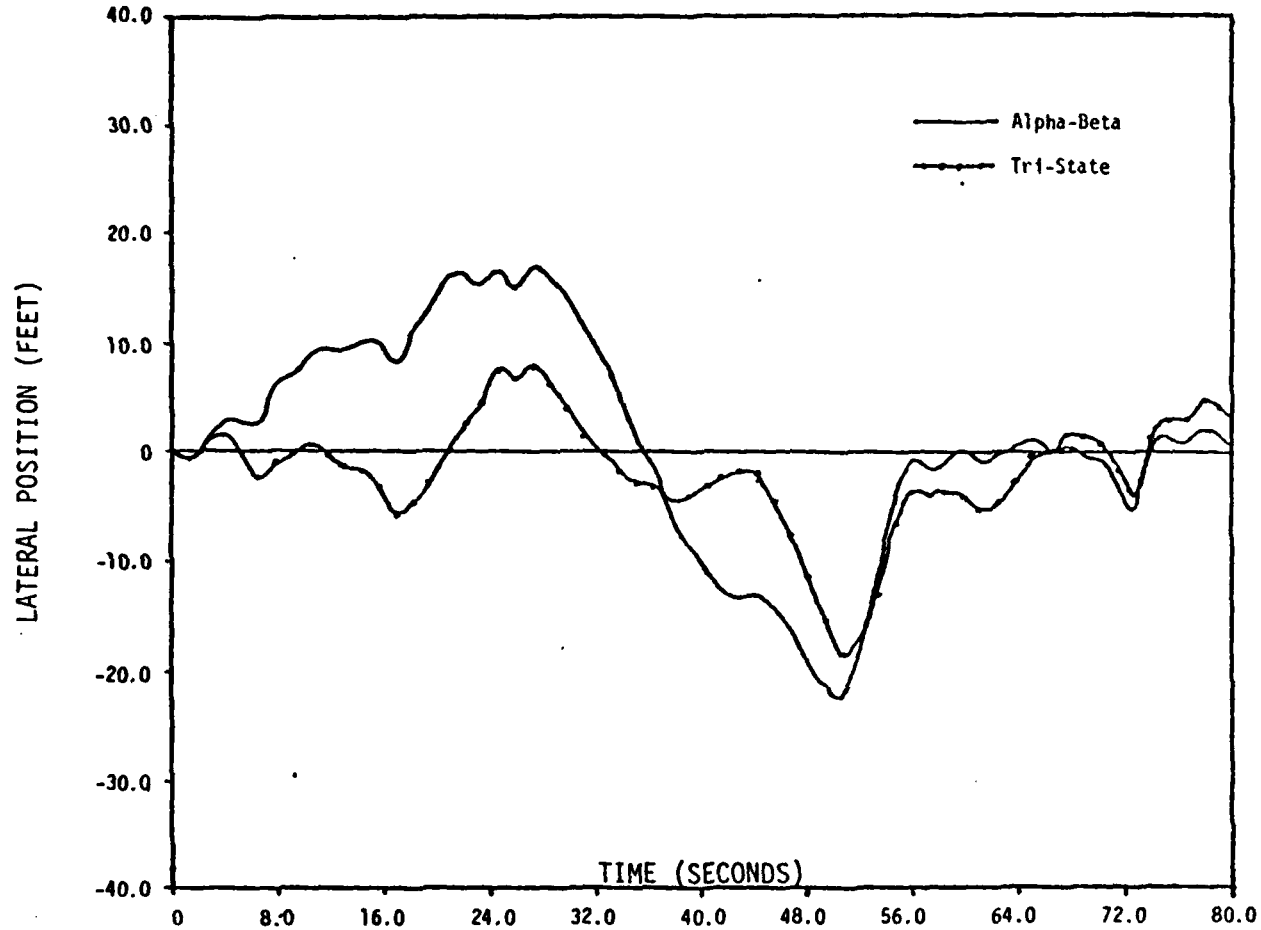

Figure 5.9. Comparison of the Tri-State Adaptive Control System Response to the Alpha-Beta Control System Response with Identical Wind and Radar Noise.

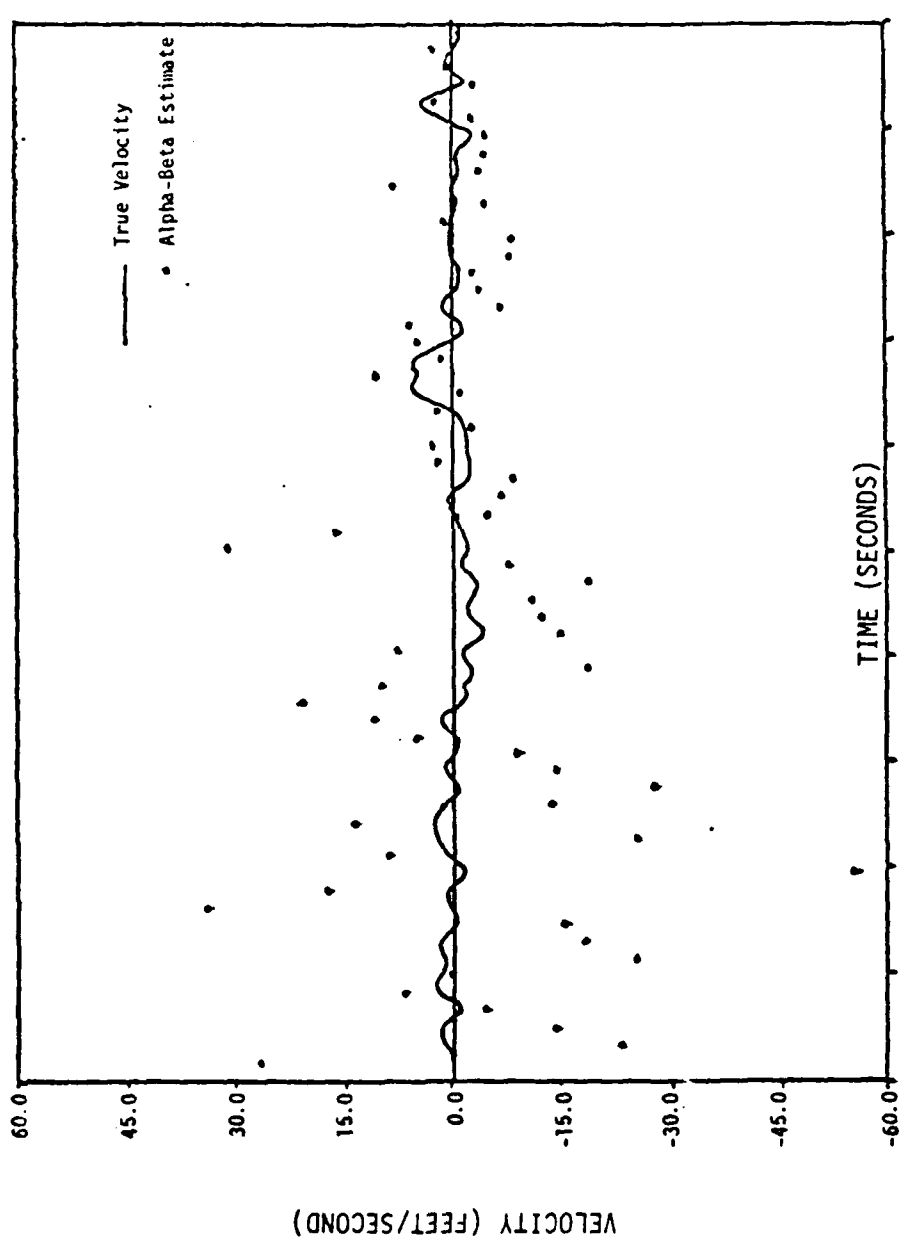

Figure 5.10. True Lateral Velocity of the Aircraft as Compared to the Alpha-Beta Filter Velocity Estimate.

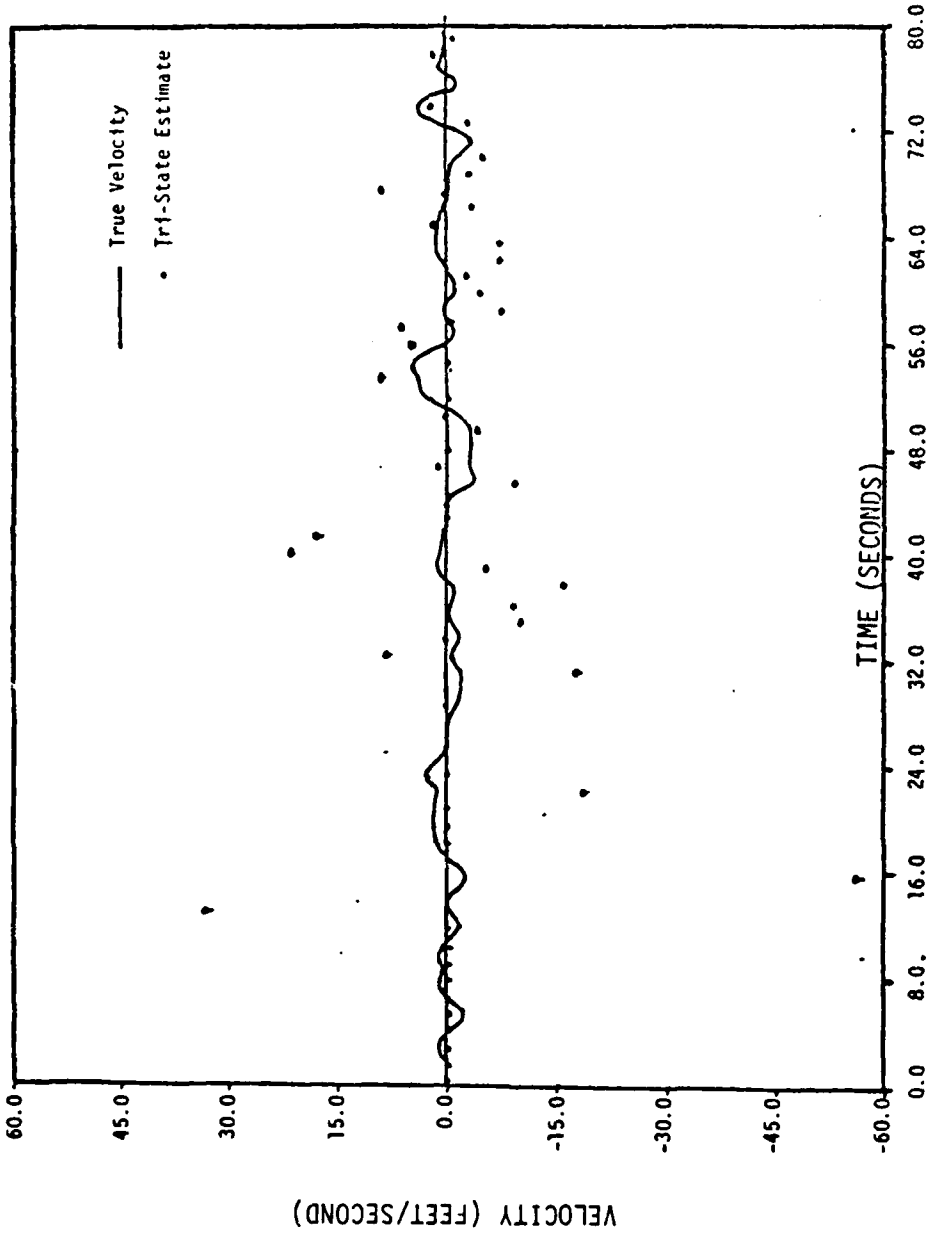

Figure 5.11. True Lateral Velocity of the Aircraft Compared to the Tri-State Adaptive Filter Velocity Estimate.

TABLE 5-7

MEAN SQUARE ERROR OF VELOCITY
ESTIMATES WITH WIND AND NOISE

BIN #	ALPHA-BETA FILTER VELOCITY ESTIMATE	TRI-STATE ADAPTIVE FILTER VELOCITY ESTIMATE	% IMPROVEMENT
1	564.058594	242.640625	79.7
2	291.140381	160.583984	57.8
3	121.441345	97.3016663	22.0
4	24.3543854	23.3751526	4.1

VI. CONCLUSIONS

Three digital tracking filters, each based upon a different aircraft dynamical model, were combined to form the tri-state adaptive tracking filter. The selection of the appropriate filter output was determined by the variance of the filters' smoothed position estimates. The tri-state adaptive filter was implemented in the simulation of the F4J lateral control system. The results given in Chapter V suggest that the performance of the F4J lateral control system may be improved through the use of a tri-state adaptive tracking filter. Since the F4J longitudinal control system is structurally identical to the lateral control system, the tri-state adaptive tracking filter may, in a similar manner, provide an improvement in the performance of the longitudinal control system.

The overall performance of the tri-state adaptive tracking filter may be enhanced by selecting the parameters of each of the three component filters in such a manner as to achieve a more complementary filter response. Another modification which might improve the performance of the tri-state adaptive filter is the adjustment of the variance thresholds of the alpha and alpha-beta filters. As was shown by the results of the F4J lateral control system simulation, the frequency response of the tri-state adaptive filter may be altered by the selection of the appropriate variance thresholds.

BIBLIOGRAPHY

[1] R. E. Kalman, "A New Approach to Linear Filtering and Prediction Problems," J. Basic Engineering, Transactions of ASME, Ser. D, Vol. 82, pp. 35-45, March 1960.

[2] R. G. Brown and R. F. Meyer, "The Fundamental Theorem of Exponential Smoothing," Operations Research, Vol. 9, 1961, pp. 673-687.

[3] T. R. Benedict and G. W. Bordner, "Synthesis of an Optimal Set of Radar Track-While-Scan Smoothing Equations," IRE Transactions on Automatic Control, Vol. AC-7, pp. 27-32, July 1962.

[4] H. R. Simpson, "Performance Measures and Optimization Condition for a Third Order Tracker," IEEE Transactions on Automatic Control, Vol. AC-8, pp. 182-183, April 1963.

[5] R. G. Brown, Smoothing Forecasting and Prediction of Discrete Time Series. Prentice Hall, Englewood Cliffs, NJ, 1963.

[6] A. C. Watts, "On Exponential Smoothing of Discrete Time Series," IEEE Transactions on Information Theory, September 1970, p. 630.

[7] J. R. Ragazzini and G. F. Franklin, Sampled Data Control Systems. McGraw-Hill Book Co., Inc., New York, NY, 1958.

[8] J. Sklansky, "Optimizing the Dynamic Parameters of a Track-While-Scan System," RCA Review, Vol. 18, pp. 163-185, June 1957.

[9] J. A. Cadzow, Discrete Time Systems. Prentice-Hall, Englewood Cliffs, NJ, 1973.

[10] E. I. Jury, Theory and Application of The Z-Transform Method. Robert E. Krieger Publishing Co., Huntingdon, NY, 1973.

[11] E. J. Routh, Dynamics of a System of Rigid Bodies. Macmillan, New York, NY, 1892.

[12] R. E. Wilcox, "The α-β-γ Tracking Filter in the Z-Domain," IEEE National Aerospace and Electronics Conference, 1979. pp. 1042-1046.

[13] Robert C. Weast, CRC Mathematical Handbook, Chemical Rubber Co., Cleveland, OH, 1966.

[14] R. A. Singer and K. W. Behnke, "Real Time Tracking Filter Evaluation and Selection for Tactical Applications," IEEE Transactions on Aerospace and Electronic Systems, Vol. AES-7, No. 1, pp. 100-110, January 1971.

[15] S. R. Neal, "Discussion on Parametric Relations for the α-β-γ Filter Predictor," IEEE Transactions on Automatic Control, pp. 315-317, June 1967.

[16] Charles L. Phillips, Edward R. Graf, and H. Troy Nagle, Jr., "Marine Air Traffic Control and Landing System Error and Stability Analysis," Vol. 1 and 2. Contract N00228-75-C-7080, Auburn University, AL, 1975.

[17] Edward R. Graf, Scott A. Starks, Charles L. Phillips, and Robert W. Simpson, "Marine Air Traffic Control and Landing System Control, Radar, and Software Analysis," Contract N00228-78-C-2233, Auburn University, Auburn University, AL, 1978.

[18] "MATCALS-AN/TPN-22 Mode I Final Report," ITT Gilfillan Technical Report, prepared for Naval Electronics Systems Command, Contract N00039-75-C-0021, August 1979.

[19] K. Steiglitz, An Introduction to Discrete Systems. John Wiley and Sons, Inc., New York, NY, 1974.

APPENDIX

```
      SUBROUTINE FILBNK (RADR)
      COMMON/RANG/RANGE
      COMMON/FILCON/SMP,SMV
      DIMENSION SP1(8), SP2(8), D1F1(8), D1F2(8)
      DATA SP1/8*0.0/,SP2/8*0.0/,D1F1/8*0.0/,D1F2/8*0.0/
C
C     CONVERT INPUT NOISE VARIANCE, VRP, FROM RADIANS TO FEET.
C
      VRP=4.225E-07*(RANGE**2)
C
C     SET L, THE LENGTH OF THE SHIFT REGISTERS.
C
      L=5
      L2=L-1
C
C     TT=SAMPLE INTERVAL=.1 SEC.
C     A1 IS THE POSITION SMOOTHING CONSTANT OF THE ALPHA FILTER.
C     A2 IS THE POSITION SMOOTHING CONSTANT OF THE ALPHA-BETA FILTER.
C     B2 IS THE VELOCITY SMOOTHING CONSTANT OF THE ALPHA-BETA FILTER.
C     A3 IS THE POSITION SMOOTHING CONSTANT OF THE ALPHA-BETA-GAMMA FILTER.
C     B3 IS THE VELOCITY SMOOTHING CONSTANT OF THE ALPHA-BETA-GAMMA FILTER.
C     G IS THE ACCELERATION SMOOTHING CONSTANT OF THE ALPHA-BETA-GAMMA FILTER.
C
C     RADR=RADAR MEASUREMENT OF AZIMUTH INPUT TO SUBROUTINE.
C     SP1(L)=L-LENGTH ARRAY CONTAINING THE LAST L-VALUES OF THE ALPHA
      FILTER'S SMOOTH POSITION ESTIMATES.
C     SP2(L)-L LENGTH ARRAY CONTAINING THE LAST L-VALUES OF THE ALPHA-BETA
      FILTER'S SMOOTH POSITION ESTIMATES.
C     SP3=ALPHA-BETA-GAMMA FILTER'S SMOOTH POSITION ESTIMATE.
C     SV1=ALPHA FILTER'S SMOOTH VELOCITY ESTIMATE
C     SV2=ALPHA-BETA FILTER'S SMOOTH VELOCITY ESTIMATE.
C     SV3=ALPHA-BETA-GAMMA FILTER'S SMOOTH VELOCITY ESTIMATE.
C     SA3=ALPHA-BETA-GAMMA FILTER'S SMOOTH ACCELERATION ESTIMATE.
C
      A1=0.15
      A2=0.51
      B2=(A2**2)/(2.0-A2)
      A3=0.46864
      B3=0.10136
      G=0.000684
C
C     CALCULATE THE VARIANCE THRESHOLDS FOR THE ALPHA FILTER AND THE ALPHA-
      BETA FILTER.
C     VOUT1=VARIANCE THRESHOLD OF THE ALPHA FILTER.
C     VOUT2=VARIANCE THRESHOLD OF THE ALPHA-BETA FILTER.
C
      VOUT1=(A1/2.0-A1)*VRP
      VOUT1=0.6*VOUT1
      VOUT2=((2.*(A2**2)+B2*(2.-3.*A2))/(A2*(4.-B2*A2)))*VRP
C
```

```
C  SHIFT SMOOTH POSITION ESTIMATES IN SHIFT REGISTERS
C
   DO 5  I=1, L2
   SP1(L+1-I) = SP1(L-I)
   SP2(L+1-I) = SP1(L-I)
5  CONTINUE
C  START FILTERS AFTER TWO MEASUREMENTS
   IF (T.GF.0.2) GO TO 10
C  INITIALIZE THE SMOOTHED VALUES OF POSITION, VELOCITY AND ACCELERATION
   SP1(1)=0
   SP2(1)=0
   SP3=0
   SV1=0
   SV2=0
   SA3=0
C  COMPUTE PREDICTED POSITIONS AND VELOCITIES FOR THE THREE FILTERS
10 PP1=SP1(1)
   PP2=SP2(1)+TT*SV2
   PP3=SP3+TT*SV3
   PV1=0
   PV2=SV2
   PV3=SP3+TT*SA3
C  COMPUTE THE SMOOTHED ESTIMATES OF POSITION, VELOCITY AND ACCELERATION
C  FOR THE THREE FILTERS
   SP1(1)=(1.-A1)*SP1+A1*SP1(1)
   SP2(1)=PP2+A2*(RADR-PP2)
   SP3=PP3+A3*(RADR-PP3)
   SV1=0
   SV2=PV2+(B2/TT)*(RADR-PP2)
   SV3=PV3+(B3/TT)*(RADR-PP3)
   SA3=SA3+C G/(TT**2))*(RADR-PP3)
C
C  CALCULATE THE MEAN OF THE ALPHA AND ALPHA-BETA FILTERS'
C  SMOOTHED POSITION.
C
   MSP1=0
   MSP2=0
   DO 20 I=1, L
   MSP1=MSP1+SP1(I)
   MSP2=MSP2+SP2(I)
20 CONTINUE
   MSP1=MSP1/L
   MSP2=MSP2/L
C
C  CALCULATE THE VARIANCE IN SMOOTHED POSITION OF THE ALPHA
C  AND ALPHA-BETA FILTERS.
C
   DO 30 I=1, L
   D1F1(I)=(SP1(I)-MSP1)**2
   D1F2(I)=(SP2(I)-MSP2)**2
30 CONTINUE
```

```
      VSP1=0
      VSP2=0
      DO 40 I=1, L
      VSP1=VSP1+DIF1(I)
      VSP2=VSP2+DIF2(I)
   40 CONTINUE
      VSP1=VSP1/L
      VSP2=VSP2/L
C
C     IF THE VARIANCE IN SMOOTHED POSITION OF THE ALPHA FILTER IS LESS THAN
      THE ALPHA FILTER'S VARIANCE THRESHOLD, THEN OUTPUT POSITION=SP1(1)
      AND O TPUT VELOCITY=0
C
C     IF (VSP1.GT.VOUT1) GO TO 50
      SMP=SP1(1)
      SMV=0
      RETURN
C
C     IF THE VARIANCE IN SMOOTHED POSITION OF THE ALPHA-BETA FILTER
C     IS LESS THAN THE ALPHA-BETA FILTER'S VARIANCE THRESHOLD, THEN OUTPUT
C     POSITION=SP2(1) AND OUTPUT VELOCITY=SV2.
C
   50 IF (VSP2.GT.VOUT2) GO TO 60
      SMP=SP2(1)
      SMV=SV2
      RETURN
C
C     IF THE SMOOTH POSITION ESTIMATES OF THE ALPHA FILTER AND THE ALPHA-
C     BETA FILTER ARE FOUND TO BE INACCURATE THEN OUTPUT POSITION=SP3 AND
C     OUTPUT VELOCITY=SV3.
C
   60 SMP=SP3
      SMV=SV3
      RETURN
      END
```

END

DATE
FILMED

3-82

DTIC